FORMATION AND FUNCTION OF COLLAGEN IV SULFILIMINE BONDS

By

Christopher Franklin Cummings

Dissertation

Submitted to the Faculty of the

Graduate School of Vanderbilt University

in partial fulfillment of the requirements

for the degree of

DOCTOR OF PHILOSOPHY

in

Biochemistry

May, 2013

Nashville, Tennessee

Approved:

Professor Billy G. Hudson

Professor Fred Guengerich

Professor Charles R. Sanders

Professor Kevin Strange

To my parents and grandparents, on whose shoulders I stand,

and

To my wife, Anna, for journeying with me hand-in-hand

Acknowledgements

A graduate education offers ample opportunity for professional and personal development, with growth coming from the hands of a multitude of instructors, colleagues, situations, resources, as well as close friends and family. My own graduate path is no exception, and I gratefully tip my hat to those mentioned below who have collectively shaped my internal qualities as a scientist and colleague, as a husband and father, and finally as a student and son.

Scientifically, I owe a great deal of appreciation to my mentor, Dr. Billy Hudson, who shouldered the lion's share of my training in research and critical thinking. Under his leadership, I learned the value of a question, the scientific rigor that underlies new discoveries, and the excellence that can emerge from a team of sharp minds. Within the Hudson lab, key individuals who contributed to my dissertation project were Drs. Gautam ("Jay") Bhave, Roberto Vanacore, Vadim Pedchenko, and Kyle Brown in addition to Ms. Parvin Todd and Mr. Mohammed Rafi. I also thank my dissertation committee, Drs. Fred Guengerich, Charles R. Sanders, and Kevin Strange who actively supervised my progress and lent their expert opinion to my forward direction. Finally, I am deeply appreciative for the input and guidance of Dr. Dean Ballard, who tracked with me from project conception to completion, offering much supportive critical review along the way.

My funding during graduate school was through a National Institute of Health (NIH) RO1 grant to Dr. Hudson (DK018381, "Studies on the Structure of Basement Membranes"), a T32 grant led by Dr. Jacek Hawiger (HL069765, "Immunobiology of Blood and Vascular Systems"), as well as support through the Vanderbilt Interdisciplinary Graduate Program during my first year. Additional resources of pivotal importance to my project included the VUMC Mass Spectrometry

Core and Molecular Biology Core, and close collaborations with work supported by the NIH 5R37-DK18381 Merit Award and 2P01-DK065123 Program Project grant, both led by Dr. Hudson.

My dissertation was supported by a core understanding of biology and chemistry provided by the Vanderbilt Interdisciplinary Graduate Program as well as my undergraduate training at California State University (CSU) Stanislaus. While an army of excellent individuals stand behind both institutions, all of whom are important to the success of their educational programs, my own development leans heavily on the efforts of Dr. Anthony ("Tony") Weil (Vanderbilt) for assisting in my adjustment to graduate school; Drs. Tina Iverson, Scott Heibert, Gerald Stubbs, Gregory Mundy, and Xiangli Yang for the brief periods that I rotated through their laboratories upon arriving at Vanderbilt; Drs. Chad Stessman, my undergraduate research mentor at CSU Stanislaus, and finally Drs. Nu-Y Stessman, Koni Stone, James Youngblom, and Horacio Ferriz, all at CSU Stanislaus, who each contributed heavily to my scientific acumen.

Though somewhat removed from my research presented herein, acknowledgement is indeed due to the numerous professionals from biotechnology, pharmaceutical, legal, financial, and healthcare industries for graciously providing career advice. Those conversations over coffee, breakfast, phone, and email were instrumental to my appreciation of the value of basic research and its role in advancing patient care. Your investment into my life has helped foster a genuine admiration for R&D.

My personal development during graduate school is largely a harvesting of the principles and values that were instilled in me through parents and grandparents. Implementation of those principles was no easy feat, and has been achieved only through the supportive love and understanding of my wife. Starting a family while we both pursued (and obtained) doctorates has truly been a joy. Finally and most importantly, I owe my life to my Lord and Savior Jesus Christ.

Preface

Many biology textbooks include some introductory statement that defines cells as the basic unit of life. This is indeed true, though perhaps overly simplified when considering human physiology. Cells require stimulation from the outside in order to remain active and even to avoid cell death in some cases. The term "outside-in signaling" has been coined to describe this extracellular influence on cell behavior. *In vivo*, these extracellular signaling events are often facilitated by the functional activity of solid matrices. Extracellular biology may thus be contextually described by its influence on cells and tissues, and the physiology of basement membranes are no exception.

Basement membranes are specialized matrices that underlie all epithelia throughout the human body, and form dense webs of proteins, glycoproteins, and signaling molecules. Somewhat analogous to the cement foundation of a brick-and-mortar building, basement membranes indeed provide physical and mechanical support for overlying cells, tissues, and organs. However, these matrices also play more advanced biologic roles in that they serve as anchors for cell binding and contain embedded signaling molecules to activate cell membrane receptors. Furthermore, the activity of basement membranes is not "one-size-fits-all" but rather, the composition and function of each matrix is tailored to the specific needs of the nearby tissues and organs. Basement membranes isolated from various tissues will display unique combinations of components and mechanical properties, presumably imparting organ-specific functional capabilities.

The role of basement membranes within biology is fundamental to conceptually understanding cell physiology, and is the intended vantage point from which to view this dissertation. The work focuses on the major component of basement membranes, networked

type IV collagen, and labors to unveil key biochemical events that surround its incorporation into and functioning within matrix. Central to these networks are covalent sulfilimine crosslinks that connect adjoining collagen IV protmers. These chemical bonds are virtually unknown in biomolecules outside collagen IV, being comprised of a double bond between sulfur and nitrogen (-S=N-). Elucidating the mechanism of bond formation is at the core of this dissertation, and provides a platform for discovering novel enzymatic and chemical events occurring within basement membranes. Unexpectedly, the physiology of collagen IV has been discovered, here shown, to be intimately associated with the functional biochemistry of halide ions, specifically bromide and chloride. After delineating the biochemistry surrounding sulfilimine bond formation, attention is given to presenting pathways by which these crosslinks may be damaged via environmental compounds, elevating the disease risk of some individuals.

The dissertation begins with an overview of the entire work in Chapter I, followed by more detailed background on the general biology and patho-physiology of collagen IV in Chapter II. The presentation of research efforts begins in Chapter III, presenting evidence that peroxidasin, a heme peroxidase enzyme located within basement membranes, is responsible for the formation of collagen IV sulfilimine bonds. Chapter IV explains the chemical mechanism by which peroxidasin forms sulfilimine bonds and reveals that the element bromine is essential to this process. Chapter V reveals that the non-covalent assembly of collagen IV networks requires the structural function of chloride, which is distinct from the role of bromide in sulfilimine bond formation. Finally, considering that mechanical strength is central to collagen IV physiology, Chapter VI contains evidence that sulfilimine bonds provide stability to collagen IV networks. This chapter concludes by identifying several environmental compounds that inhibit enzymatic formation of sulfilimine bonds, with potential disease rammifications. Based on this work,

Chapter VII suggests future studies that may be conducted in order to further uncover the functional biology of collagen IV sulfilimine bonds.

The scope of this work was designed to comprehensively address sulfilimine bond formation, and the feasibility of answering this level of questioning necessitated a team effort. Thus this work is reflective of collaborative efforts, conducted in parallel, as well as the free exchange of ideas and experimental data. Some of the results presented herein stem from these collaborative efforts, and credit is given where due to those colleagues who were deeply involved with these discoveries.

Considering the organ-specific functions of basement membranes, the sulfilimine chemistry of collagen IV provides a mechanism to modulate the mechanical properties of matrices. In sum, this work provides a biochemical foundation for appreciating the biology of basement membranes, thus contributing to the scientific understanding of cell-matrix interactions.

Table of Contents

List of Tables

Table Page

List of Figures

Chapter I

AN OVERVIEW: UNUSUAL BIOCHEMISTRY REVEALS INNOVATIVE HALOGEN BIOLOGY WITHIN BASEMENT MEMBRANES

Introduction

Basement membranes are fundamental tissue components, characterized by a biochemical profile that is unseen elsewhere in biology. Networked collagen IV is a critical element of these extracellular matrices, with network assembly proceeding through the formation of sulfilimine (-S=N-) crosslinks at the C-termini hexameric quaternary structures formed by adjoining collagen IV protomers. The discovery of these covalent bonds within collagen IV was the first identification of this type of bond within biomolecules, being published by members of the Hudson research group in a 2009 *Science* report (1). Interestingly, autoimmune research within the Hudson laboratory has suggested that the collagen IV sulfilimine crosslink may functionally influence the etiology of Goodpasture's autoimmune disease, as the reduced prevalence of crosslinks correlates with enhanced tissue binding of pathogenic autoantibodies (2,3). Prior to the initiation of this dissertation project, investigations aimed at identifying the mechanism of bond assembly revealed that bond assembly is inhibited by phloroglucinol, a general peroxidase inhibitor. This project was thus begun with these aims:

- Identify the putative crosslink-forming enzyme
- Describe the mechanism of bond formation in terms of the required cofactors and minimal substrate domain
- Identify any inhibitors of the crosslinking reaction

Finally, during the course of the project, a fourth aim was added:

- Delineate the mechanism of NC1 hexamer assembly

This work successfully accomplished all aims and more, starting with the discovery that bond formation occurs within basement membranes as the enzymatic product of peroxidasin, a heme peroxidase found in basement membranes with a previously unknown biologic function. The reaction mechanism utilizes hypohalous acids as chemical intermediates, defining a novel biosynthetic role for these reactive oxidants. It was discovered that bromide is required for the reaction, representing the first essential biologic function for the element Br in animals. Mechanistic studies in matrix demonstrated that peroxidasin (PXDN) forms sulfilimine bonds via its halogenation cycle, oxidizing bromide ions into hypobromous acid, which is the chemical catalyst of bond formation. In addition, chloride has emerged as the central determinant of NC1 hexamer assembly in humans, inducing the formation of the proper quaternary structure prior to the crosslinking activity of PXDN. Altogether, the reaction hinges on the sequential action of both halides. Functionally, the bonds were experimentally shown to reinforce the NC1 hexamer substrate. Thus, sulfilimine bonds are key structural elements of collagen IV networks, forming through the separate and coordinated activity of bromide and chloride ions. Finally, small molecule inhibitors of bond formation have been identified through a matrix-based assay of crosslinking activity. These compounds are used within industrial settings, suggesting that physiologic crosslinking activity can be influenced by environmental factors with possible implications for the etiology of Goodpasture's disease. This work advances the field of basement membrane biology by highlighting the unique extracellular enzymology and chemistry occurring within matrices.

Peroxidasin Forms Sulfilimine Bonds

The initial characterization of sulfilimine bond formation focused on determining whether catalysis occurs chemically or enzymatically. This project successfully purified crosslinking activity from

solid-state matrix through the study of PFHR9 cells, a murine epithelial cell line that generates abundant quantities of extracellular matrix containing the sulfilimine-crosslinked collagen IV. Preliminary work identified several small molecule inhibitors of dimer formation that effectively allowed the production of an uncrosslinked matrix, while dimer formation was observed to proceed within the matrix following removal of the inhibitors. To purify the crosslinking agent, solid matrix was isolated from cells and enzymatically digested with bacterial collagenase. Supernatant resulting from this digest was found to retain the crosslinking activity, solving the critical issue of activity solubilization. Ion exchange chromatography was used to separate matrix components, allowing the isolation of crosslinking activity within a defined eluant fraction, while mass spectrometric analysis identified the enzyme PXDN within the active fraction. As a parallel approach conducted separately within the Hudson laboratory, the enzyme was overexpressed in mammalian cell culture and shown to form sulfilimine bonds, thus providing direct evidence that PXDN is indeed the crosslinking enzyme. Underscoring the importance of sulfilimine bonds, loss-of-function mutations in the *Drosophila melanogaster* analogue of PXDN show disordered collagen IV networks and disrupted tissue morphology (4).

Analysis of crosslinking activity observed in collagenase digest supernatant leads to the conclusion that NC1 domains are a sufficiently minimal substrate for enzymatic crosslinking. Considering that bond formation *in vivo* occurs within a solid matrix, including abundant hetero-triple helical collagen domains, this data suggests that PXDN does not require additional binding sites outside the NC1 domain for crosslinking activity.

The Element Bromine is Required for Sulfilimine Bond Formation

Identification of Reaction Cofactors and the Catalytic Intermediate

A defining feature of heme peroxidases is the requirement of a peroxide cofactor, and as such, the addition of exogenous hydrogen peroxide enhances dimer formation within PFHR9 matrix.

Peroxidase mechanisms are known to consume halide ions as a possible catalytic pathway, resulting in the formation of hypohalous acid products. We asked whether PXDN uses halides to form sulfilimine bonds, subsequently observing that peroxide is insufficient to promote bond formation in the absence of halides while addition of either Br^- or Cl^- in the presence of peroxide rescued the reaction. PXDN thus requires an oxidant and a halide ion to form sulfilimine bonds.

Heme peroxidases are widely known sources of hypochlorous (HOCl) and hypobromous (HOBr) acids during immune responses, where the strong reactivity of the molecules destroys pathogens by causing oxidative damage. In contrast, the halide requirement for dimer formation suggests that PXDN uniquely harnesses this oxidizing reactivity as a mechanism for anabolic protein conjugation via sulfilimine bonds. Confirming this hypothesis was the discovery that hypohalous acids catalyze the formation of sulfilimine bonds when incubated with uncrosslinked NC1 hexamers. This delineates a biosynthetic function for hypohalous acids as catalytic intermediates of bond formation, critically import for the stability and functioning of tissues.

Role of Halides within the Enzymatic Reaction, and a Biologic Role for Bromide

Reflecting on the experimental demonstration that bond formation requires halides, matrix pellets were noticeably compacted in the low-ionic strength conditions that resulted from removal of endogenous matrix halides. The addition of either Br^- or Cl^- at 100 mM restored the crosslinking reaction, though this concentration of Br^- lies well outside its human serum concentrations of 10-60 μM. Furthermore, HOBr was demonstrated to be a much more efficient catalyst of *in vitro* crosslink formation than HOCl. Questioning the physiologic relevance of the experimental design, the matrix reaction was repeated in the presence of 100 mM potassium fluoride as an ionic control, an inert halide with respect to bond formation by PXDN. Under these conditions, bromide strongly promoted the

reaction at 10 µM and 100 µM establishing that the ion is sufficient at physiologic concentration to support bond formation.

Reagent grade chloride (>99.5% purity, Sigma-Aldrich) promoted dimer formation at 100 mM irrespective of ionic strength. This concentration was much higher than the 10 µM Br- needed for crosslinking, and considering that bromide may be present in the reagent grade chloride in small quantities, the next question raised was whether the bond formation attributed to chloride-based activity might have in fact been caused by the contaminating bromide. Through collaborative efforts, chloride salts were purified in house until only trace concentrations of bromide remained. Subsequent testing in matrix revealed that pure chloride does not support the reaction yet 5 µM supplemental bromide restores activity. Thus, bromide is required for the sulfilimine bond formation observed in culture and tissues.

In animals, bromide biology has been ambiguous prior to this discovery. The element is present in low concentrations and oxidized bromide is rapidly quenched by thiocyanate ions (5). Brominated peptides have been described *ex vivo*, but without functional significance (6-8). Within this context, the discovery that bromide ions are required during bond formation seems to elevate the element Br to the status of an essential element for animal biology.

Chloride is Required for Assembly of NC1 Hexamers

Chloride has long been known as an ionic resident within hexamers (9) but this present work unexpectedly revealed that these ions are fundamental to the assembly and stability of uncrosslinked hexamers. Dissociation of the quaternary structure was observed upon dialysis into halide-free buffer, while hexamers assembled following incubation in the appropriate halide concentrations, as monitored by gel filtration chromatography. The assembly reaction benefited from increasing concentrations of all halides, progressing furthest to completion near 100 mM halide. Chloride is the only halide present

near this concentration in serum, thus this suggests that chloride might be responsible for hexamer formation in organisms. To examine this a bit further, physiologic concentrations of bromide and iodide were added to dissociated NC1 domains without effect.

This demonstration of an assembly role for chloride ions is uncommon, being more often seen with calcium ions, which are also present within NC1 hexamers. Rigorous searching for an assembly role of Ca^{2+} within hexamers was unfruitful, and the issue was resolved by observing hexamer assembly in the presence of 1 mM EDTA upon addition of 100 mM Cl^-. Thus, chloride is essential for NC1 hexamer formation. When viewed together with the catalytic role of HOBr in sulfilimine crosslinking, the activities of halide ions are then seen as being fundamental to the formation of collagen IV networks and by inference, are critical components of basement membrane biology.

Sulfilimine Biology in Networks and Disease

Using hexamer dissociation as a diagnostic, halides were removed from PHFR9 hexamers with either reduced or enhanced crosslinks. Hexamer dissociation was inversely proportional to the degree of sulfilimine bonding where reduced crosslinking increased the amount of NC1 domains that dissociated, thus demonstrating that the bonds provide structural reinforcement to the hexamer. Disruption of this stabilizing function of sulfilimine bonds is a key etiologic feature of Goodpasture's disease (2). Central to the disease pathology are autoantibodies targeting the α3 chain of collagen IV, binding the NC1 domains of uncrosslinked hexamers (3). Disruptions to the crosslink or interference with bond formation are involved within the disease etiology by allowing pathogenic conformational changes within collagen IV (2).

Considering that damage to the process of sulfilimine bond formation may be predisposing toward Goodpasture's disease, a panel of compounds was assembled based on their structural similarity to a known inhibitor of PXDN. These compounds all possess industrial applications, thus providing a

route for environmental exposure. Using the matrix activity assay, experiments indicate that multiple benzene-based compounds are capable of inhibiting PXDN at micro-molar concentrations.

Summary

Addressing the secretion of collagen IV protomers and their deposition into nascent matrices, culminating in the final crosslinked state networked collagen IV, this work sheds light on key events in the formation of the basement membranes. Highlights include the delineation of a physiologic role for the extracellular heme peroxidase, PXDN, the unequivocal discovery that Br is an essential element within animal biology, the establishment of a biosynthetic function for HOBr, the demonstration that sulfilimine bonds structurally reinforce NC1 hexamers, the detailed characterization of the role of chloride ions in hexamer assembly, and the identification of environmental small molecule inhibitors of bond formation. The foundational understanding presented herein further advances the basic understanding of basement membrane biology.

Chapter II

COLLAGEN IV NETWORKS AND SULFILIMINE BONDS

Introduction: Basement Membrane & Collagen IV Biology

Biologic tissues and basement membranes are functionally symbiotic, beginning with the cellular synthesis and secretion of glycoproteins that become deposited into specialized matrices, in turn providing mechanical support for tissue growth, activation of cell surface receptors via matrix-embedded signaling molecules, and the anchoring of cytoskeletons to extracellular ligands (10). The dogmatic relationship between structure and biologic activity holds true for these specialized matrices, as networks of collagen IV provide a framework for the matrix super-structure that is required for the proper functioning of basement membranes (11-13). The assembly of these networks involves formation of covalent sulfilimine bonds, a biologically novel form of sulfur-nitrogen interactions that was unknown within tissues prior to its discovery in collagen IV. As the most abundant component of basement membranes, collagen IV embodies the essence of basement membranes through its own mechanical properties, growth factor binding, and integrin activation.

Collagen IV Structure & Function

Protomers, Hexamers, and Networks

Type IV collagen is composed of six homologous α chains (α1-6) that associate into heterotrimeric collagen IV protomers with specific chain combinations. Though differing in chain composition, all protomers share structural similarities of a lengthy triple-helical collagenous domain

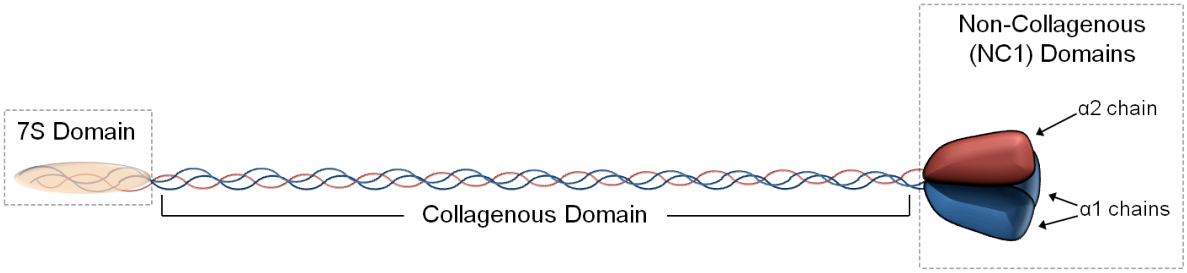

Figure 2.1: Domain Structure of Collagen IV α112 Protomer.

with the triplet peptide sequence of Gly-X-Y (14), and ends in a globular C-terminal region termed the non-collagenous 1 (NC) domain (Figure 2.1). The N-termini is composed of a helical domain termed the 7S domain, named for its sedimentation coefficient (15), which is involved in protomer-protomer interactions. Assembly of the heterotrimer initiates within the NC1 domains (16, 17), then followed by the left-handed helical winding of the collagenous domain to form the full-length protomer molecule.

Heterotrimers occur in the specific combinations of α1α1α2, α3α4α5, and α5α5α6 (3, 17), which is notable due to the lack of homotrimers as well as numerous alternative combinations that are absent. Protomer assembly is thus a selective process whereby chain sequence structure directs the specific interaction with partner chains. Kinetic analysis of the α1α1α2 heterotrimer assembly suggests that differential binding affinities between NC1 domains heavily influence the selectivity of chain inclusion within nascent protomers (17). Greater binding activity was observed for α1-α2 interactions than homodimeric binding of α1-α1 complexes, indicating that the α2 chain acts as a nucleus for protomer assembly. Crystallographic studies revealed a domain-swapping interface between the NC1 subunits within protomers (18, 17) where a β-hairpin motif is fit within a grooved docking site on the adjacent NC1 domain. Furthermore, while the six different α chains are highly similar in their amino acid sequences, regions of variability are present near the domain-swapping sites that impute specificity of chain selection during protomer assembly (17). Sequence alignments based on the α2 suggest that the α4 and 6 chains may initiate formation of their respective protomers (17).

Adjoining NC1 trimers connect via head-to-head interactions to form a hexameric quaternary structure from the six constituent α chain NC1 domains. Electrostatic interactions are present internally along the trimer-trimer interface and central to hexamer assembly with key residues being Arg^{77} and Glu^{176} that form ionic bonds between the two trimers (18, 17). Analysis of tissue isolates revealed additional covalent sulfilimine bonding connecting Met^{93} and Hyl^{211} residues from opposing trimers (1).

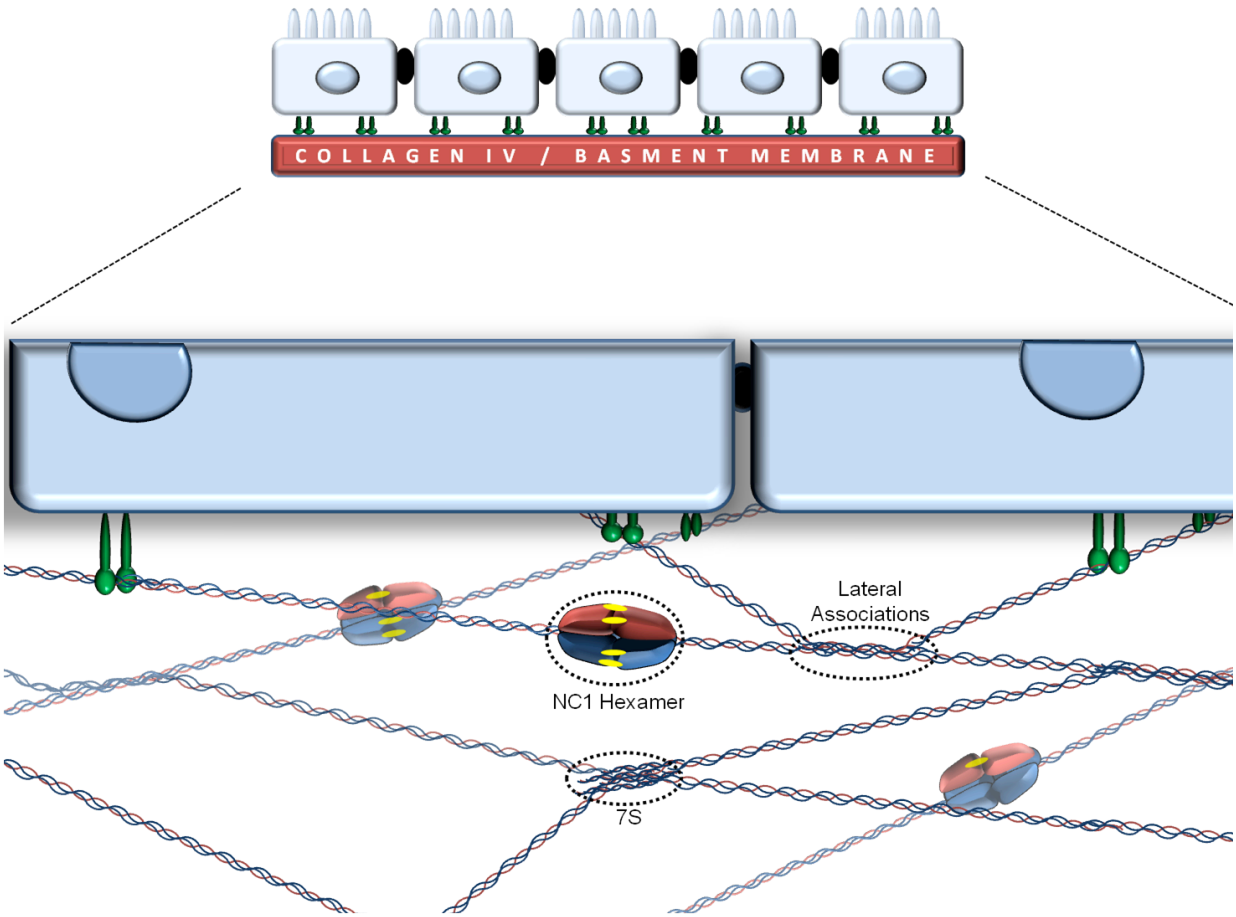

Figure 2.2: Model of Collagen IV Networks Underlying Epithelial Cell Layer. Protomer-protomer interactions forming C-terminal NC1 hexamers, N-terminal 7S dodecamers, and lateral associations are encircled. Cell-matrix interactions are facilitated by plasma membrane-bound integrins (green).

Finally, the trimer-trimer interface contains potassium, chloride, and calcium ions at ratios of one ion of K^+ and Cl^- per NC1 domain while a Ca^{2+} is bound to each α2 (9).

In addition to the establishment of NC1 hexamers, collagen IV networks assemble through extensive protomer-protomer interactions along the length of the heterotrimer. The N-terminal 7S domains of four independent protomers are covalently bound together, a dodecamer of α chains, allowing the protomer to be secured at either termini by covalent interactions (19). Noncovalent interactions form rapidly along the collagenous domains among protomers to complete the mesh-like structure (20) (Figure 2.2).

Collagen IV Functions

Genetic studies indicate the importance of collagen IV networks for basement membrane biology. Indeed, mutation of the ubiquitous collagen IV α112 network in mice (11) and nematodes (12) has been independently observed leading to the dual phenotypes of basement membrane instability and embryonic lethality. In humans, point mutations affecting glycine residues within the Gly-X-Y motif of collagen IV α1 have been shown to cause small vessel diseases affecting retinal and cerebral vasculature including hemorrhagic stroke (21, 22). Thus, it would appear that a primary function of collagen IV networks is to provide stability for basement membranes and the overlying tissues. This same feature appears to be important for the stability of neuromuscular junctions (23, 24), exemplified in embryonic flies lacking the highly-expressed α1 and α2 collagen IV chains that show ca. 70% loss of these synapses (24). Relatedly, removal of collagen IV from basement membranes via enzymatic digestion leads to disordered organ morphology (25).

It is strongly implied that the specific chain combinations result in distinct functional influences on tissues. Not all chains are expressed in a particular tissue at the same stage of development (26, 23), but are observed as networks composed of similar protomers. The α112 network is expressed

ubiquitously in humans, and the chains are the sole collagens in *Caenorhabditis elegans (C.elegans)* (27). The α345 network has more limited distribution, primarily in lung, testes, glomerulus, eye, and inner ear (3). Uniquely, the α556 protomer has not been observed as its own network *per se* but rather is expressed within specific α112 networks (28), likely as means of tailoring basement membrane function to the localized cellular requirements. This tissue-specific function of collagen IV networks is well visualized in Alport's syndrome, where genetic loss of the α345 protomer is phenotypically expressed only within the biodistribution of the network (3). Furthermore, differential temporal patterns of expression may be seen in murine motor nerve terminals where α112 networks are required for early organ development while α3-6 chains are central to its maintenance (23).

Beyond its mechanical role, collagen IV participates in the activation of cell surface receptors mainly by serving as an integrin ligand and through binding interactions with soluble growth factors. α1β1 and α2β1 integrins recognize and bind collagen IV (Figure 2.2), and interestingly, are functionally involved with promoting angiogenesis (29). *Drosophila melanogaster (D. melanogaster)* developmental analysis has revealed that collagen IV also binds the bone morphogenic protein (BMP) decapentaplegic (Dpp). BMP signaling is a regulator of embryonic development and tissue homeostasis, accomplishing much of its activity through the use of concentration gradients in tissues. Interactions with collagen IV networks provide an anchor for Dpp molecules and are likely a key component in establishing concentration gradients of the growth factor (30-32). Indeed, Dpp signaling across short distances is mediated by collagen IV while long range activity is independent due to solubility of the growth factor (31). In *D. melanogaster*, this short range signaling would appear to be critical for the role of Dpp in patterning of the dorsal ectoderm, maintaining germline stem cells (30), and renal tubule morphogenesis (33). BMP2 is the vertebrate orthologue of Dpp (31), while BMP4 demonstrably binds human collagen IV (30).

The interactions between cancers and the extracellular matrix have been long studied from the perspective of how biomechanical forces influence tumor growth, angiogenesis, and metastasis (34-37). These interactions are quite evident during the process of tumor extravasation from vasculature into metastatic sites via penetration of the underlying basement membrane (38). This process is not strictly pathologically associated as migration lymphocytes perform similar activity during normal homeostasis (38). Collagen IV itself has been shown to be essential for liver metastasis and comparatively scarce at some primary tumor sites (39), raising the possibility of its role as an attractant of migrating metastatic cells. Interestingly, the expression of α2 was also shown to correspond to increasing degrees of colorectal adenocarcinoma differentiation (28).

Collagen IV Sulfilimine Bonds

The sulfilimine covalent bonds found within NC1 hexamers of collagen IV networks are covalently stabilized by a unique double bond structure between juxtaposed methionine-93 (Met^{93}) and hydroxylysine-211 (Hyl^{211}) residues, termed a sulfilimine bond (Figure 2.3). Naturally occurring sulfilimine bonds were first identified in the collagen IV hexamers during the mass spectrometric analysis of collagen IV NC1 hexamers purified from placental basement membrane (1). Comprised of a double bond between sulfur and nitrogen atoms, these sulfilimine bonds are the only intermolecular covalent stabilizing forces at the C-termini of collagen IV protomers suggesting that their biologic role may be related to the stability and function of collagen IV networks.

Covalent crosslinking of NC1 domains via sulfilmine bonds creates a dimerized NC1 molecule that can be resolved from the monomeric subunits by SDS-PAGE. Indeed, densitometric analysis of dimer and monomer banding on SDS-PAGE provides a means of estimating the relative amount of bonds present within an NC1 population. Notably, the percentage of crosslinked dimers is not constant throughout an organism but is rather dependent on the particular tissue source. Placental and

glomerular basement membranes contain high amounts of sulfimine bonding while NC1 hexamers isolated from lense capsule contain minor amounts of crosslinking. Considering the mechanical influence of extracellular matrix on cellular behavior, it is possible that sulfilimine bonds act as a regulator of basement membrane function by tailoring the strength of the collagen IV network to the physiologic requirements of its overlying tissue.

Sulfilimine Chemistry

Sulfilimine bonds are classified as sulfur-nitrogen ylides with the general structure of:

$$R^1R^2\overset{+}{S}\text{-}\overset{-}{N}R^3 \leftrightarrow R^1R^2S{=}NR^3$$

with R being any carbon substituent. The zwitterionic compound likely resonates with the double bond form, providing the bond with a unique nature that is not easily categorized but has been well characterized (40-42). Empirical analysis of model sulfilimine-containing compounds strongly supports the argument that the chemical structure is more complex than simple σ-bonding. Yet the sulfilimine bond does not conform to the normal characteristics of double bonds, likely as a result of the electronegativity and atomic orbital properties of the constituent atoms.

The chemical structure of the collagen IV sulfilimine bond was confirmed through fragmentation of the crosslinked peptides where the cleavage process included the transfer of a β-proton from Met to the nitrogen on Lys, in a Cope-like elimination reaction (1). A lone electron pair on nitrogen is implicated in the nucleophilic attack of the proton, suggesting that the collagen IV sulfilimine crosslink is a double bond where the nitrogen is fully deprotonated. A contrasting structure for nitrogen is found in dehydromethionine, where X-ray studies displayed a protonated nitrogen with sp3 spectrometric data showing that the crosslinked peptides are two mass units less than the sum of the hybridization (43). The dehydromethionine thiol-nitro bond length is slightly longer (1.68Å) than that reported for other

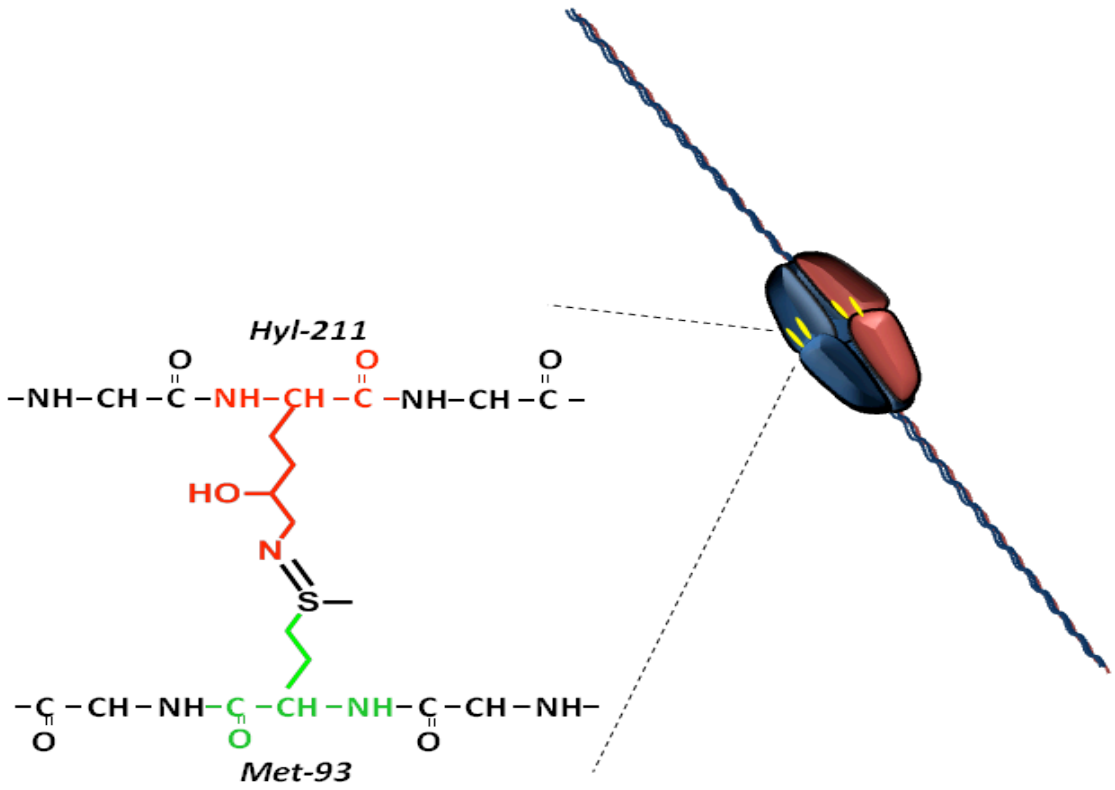

Figure 2.3: Sulfilimine Bonds (-S=N-) Covalently Join Collagen IV NC1 Hexamers.

sulfilimines (1.622Å-1.667Å) (41) yet still shorter than the combined radii of the two atoms (1.78Å). Although protonated and neutral, this form of nitrogen remains categorized as a sulfur-nitrogen ylide due to negative charge on the backbone carbonyl. A subsequent coordinated or sequential process of hydrogen loss from the nitrogen and protonation of the carbonyl, possibly via buffer hydrogen exchange, provides a means for resonance with the main sufilimine structures.

The atomic orbitals of sulfur lend partial explanation for the non-conforming multiple nature of sulfilmine bonds. In particular, owing to its elemental position within the period table, the π-orbitals of sulfur are energetically unsuitable for bonding. Rather, an overlap of *d* and π orbtials has been hypothesized as defining the bonding between sulfur and nitrogen, respectively (40). Much discussion within the publication record has been given to this second bond, on whether it is double or single (42, 44, 40). The simplest explanation may be that the component electrons are migratory with a preference for the nitrogen, conferring either a partial or full positive charge to the sulfur, and the balance being determined by the relative eletronegativity of the substituents on both sides.

Occurrence of Sulfilimine Chemistry in Biology

Various sulfilimine derivatives are known to have herbicidal and antimicrobial properties and may be used industrially as antioxidants for plastics, while pharmacologic effects include diuretic, natriuretic, hypotensive, antidepressant, central nervous system stimulant, and tumor inhibitor properties. (40).

Analogous bonds have been postulated to form via oxidative reactions during inflammatory responses. A representative structure is found in dehydromethionine, which is produced via halogen oxidation of methionine to yield a cyclic structure with the residue sulfur bonding to the backbone amide. The compound was first described by Lavine (45) using reagent molecular iodine, while subsequent work has expanded the list of catalysts to include hypochlorous acid (HOCl), hypobromous

acid (HOBr), hypoiodous acid (HOI), chloramines, and bromamines (46-48). Such reactive halides are generated by the halogenation cycle of mammalian heme peroxidases during neutrophil and eosinophil activation. *In vitro* stimulation of neutrophils resulted in the formation of dehydomethionine and methionine sulfoxide using model peptides containing an N-terminal Met (46).

Halogen-based formation of sulfilimines competes with the generation of numerous bond structures that differ in their degree of sulfur oxidation and nitrogen protonation. Methionine sulfoxide is the major product during dehydromethionine synthesis from HOCl (46), in addition to catalyzing the formation of intramolecular and intermolecular sulfenamide (RSNHR), sulfinamide (RSONHR), and sulfonamide (RSO_2NHR) bonds in peptides (47, 49). In a biologic context, the production of thiol-nitro bonds during immune responses may be deleterious considering that HOCl oxidation of low-density lipoprotein is associated with the progression of atherosclerosis. Indeed, the formation of thiol-nitro crosslinks has been hypothesized as participating in the disease mechanism (47).

Goodpasture's Disease & Sulfilimine Bonds

Alterations to the sulflimine bonds either through cleavage processes or inhibition of the bond formation may trigger pathophysiologic events such as the autoimmune Goodpasture's disease. Characterized in part by high titers of circulating autoantibodies targeting the collagen IV α3NC1 domain (50), patients typically experience renal and/or pulmonary symptoms due to the prominent role of the α3α4α5 collagen IV network within these basement membranes (3). *In vitro* binding studies between the autoantibodies and the α3α4α5 NC1 hexamer revealed that binding is enhanced in uncrosslinked hexamer populations or following dissociation of crosslinked hexamers via acid or denaturants (51, 52), suggesting that the disease aetiology may involve pathologic conformational changes within the collagen IV molecule. Further genetic associations (53, 54) and putative environmental triggers (55) have been suggested, which collectively imply the presence of a complex interaction among risk factors

(3). Increasingly, enlightening discoveries regarding the complex etiology, progression, and resolution of Goodpasture's disease has revealed much insight into the functional interfacing between basement membranes and immune homeostatis.

History of Goodpasture's Disease

In 1919, Dr. Earnest Goodpasture described a young patient with pulmonary hemmorage and glomerular nephropathy (56) who was presumed to be suffering from the widespread 1918 "Spanish Flu" influenza pandemic within the United States, yet the case was a bit distinct from influenza symptoms. Stanton and Tange later suggested that this combination of symptoms might represent a distinct pathology, respectfully proposing that the newly defined disease be named in honor of Dr. Goodpasture. (57). Following this, the characterization of Goodpasture's disease developed into its present day definition (3, 58, 59) involving the symptomatic triad of pulmonary hemmorage, crescentic glomerulonephritis, and pathologic autoantibodies against collagen IV α3NC1 (60). The organ-specific pathogenesis is due to the α3 chain of collagen IV being expressed within glomeuli and alveoli basement membranes (3). The key role of autoantibodies was confirmed by Lerner, Glassock, and Dixon in 1967 by transferring the disease into non-human primates via injection of antibodies from Goodpasture's patients (61).

Etiologic Factors: Genetic, Environmental, and Immunologic

The etiology of anti-GBM disease is poorly understood, likely comprising a dynamic balance of genetic and environmental factors, in addition to the condition of collagen IV networks and immune homeostasis of the patient. The genomic HLA-DRB1*1501 allele has been associated with Goodpasture's disease and particularly so among Asian populations (62). However, this allele has also been associated with other forms of autoimmunity (63, 64), indicating that Goodpasture's disease

should be considered a complex genetic trait. Interestingly, within a Chinese anti-GBM patient population the combination genotype of HLA-DRB1*1501-positive and HLA-DPB1*0401-null conferred more risk for anti-GBM disease than considering the DRB1 genotype in isolation (65). Functional evidence linking the HLA-DR15 allele with Goodpasture's disease was found by Phelps and coworkers (66) by noting the MHC presentation of α3NC1 peptides in lymphocytes exposed to recombinantly-expressed α3NC1 domains.

Goodpasture's disease also appears to be associated with increased copy numbers of the FCGR3A antibody receptor in patients (67) while copy number variation at the FcγRII locus in mice renders the animals susceptible to experimental induction of Goodpasture's disease (68). These observations are indeed interesting, raising questions regarding the phenotype verification and mechanistic characterization. Regardless of the answers, current genetic studies have demonstrated that Goodpasture's disease is a complex genetic trait.

Environmental factors have been hypothesized as causal disease triggers with particular emphasis placed on hydrocarbon exposure, though evidence to support this is anecdotal (55, 69) due to the limited patient population. Consequently, this severely restricts the formulation of any definitive conclusions. However, in light of the observations that sulfilimine bonds may protect NC1 hexamers from autoantibody attack, the question arises whether there may be some environmental agent that influences the disease etiology by interfering with bond formation or otherwise destabilizing the NC1 hexamer.

Particularly interesting are reports of circulating α3-reactive antibodies and T lymphocytes being identified in the serum of healthy individuals (71-73). This paradigm of non-pathogenic autoreactivity is not limited to Goodpasture's disease but has been observed targeting several self-antigens (72, 74-78). While generally hypothesized to be physiologically useful for immune homeostasis or housekeeping, "natural" autoantibodies differ from their pathogenic forms by Ig class and affinity (74). This pattern is

reflected in non-pathogenic Goodpasture's autoantibodies being constrained within the IgG2 and IgG4 subclasses while patients show an appearance of IgG1 and IgG3 autoantibodies (79, 71, 72). Interestingly, a rare case of Goodpasture's disease with normal renal function was characterized by IgG4 autoantibodies (80). With the frequent cross-talk between B and T lymphocytes, it should be unsurprising that α3-reactive T cells have also been reported in healthy individuals (73). Cultured peripheral blood mononuclear cells demonstrated a delayed proliferative response to autoantigen-derived peptides, suggesting that Goodpasture-type autoreactivity may be somehow suppressed or regulated in normal individuals.

The activation of auto-reactive T cells in Goodpasture's disease has been examined with respect to the activating peptides and the proteolytic processing pathway that is responsible for generation of the peptides (81). Investigations into the effect of cathepsin D and lysosomal extracts from B lymphocytes on recombinant α3NC1 demonstrated that the peptide sequences which elicit the strongest T cell response are cleaved through normal lysosomal degradation (82, 73).

Considering the etiologic significance of sulfilimime bonds in Goodpasture's disease, the crosslinking status of NC1 domains may bear influence on their proteolytic digestion and thereby alter its MHC presentation to lymphocytes. Alternatively, antibodies themselves are known to direct processing if they remain bound to antigen during proteolysis, potentially enhancing the presentation of otherwise cleaved epitopes, while simultaneously suppressing the presentation of other epitopes from the same antigen (83, 84). The presence of non-pathogenic α3-reactive natural antibodies seems to provide the necessary tools for accomplishing this, lacking only perturbation of the sulfilimine bond. Indeed, B cells have been implicated as activators of auto-reactive T cells in murine systemic lupus erythematosus (86-89) and type 1 diabetes (89-91). Further investigations into the molecular etiology of Goodpasture's Disease might very well shed light on novel pathways whereby self-tolerance is bypased as well as reestablished.

Summary

Collagen IV networks are fundamental elements of tissue development and physiology, with NC1 hexamers playing a central role in protomer assembly and network formation. Their significance is further underscored by the discovery of sulfilimine bonds as covalent constituents. Progressing deeper into the biology of collagen IV, the questions are thus raised of how the bonds form and what their function is within the hexamer. These issues have provided a springboard to advance the basic understanding of collagen IV network assembly and have built a framework to understand the pathologic outcomes associated with its disturbance.

Chapter III

PEROXIDASIN FORMS COLLAGEN IV SULFILMIINE BONDS IN BASEMENT MEMBRANES

Introduction

Collagen IV sulfilimine bonds represent a novel type of biochemistry, suggesting that the mechanism of formation may be equally unique. Severe phenotypes may occur in the absence of collagen IV networks (11-12), and the bond is the sole covalent reinforcement at the C-terminal junctions of adjoining collagen protomers. Thus, the agent responsible for bond formation might be expected to influence collagen IV network formation and, by inference, tissue stabilization. As an initial foray into the topic, the question was asked whether the bond forms via an enzymatic or chemical mechanism. Interestingly, extracellular lysyl oxidase activity may be used to demonstrate precedence for both pathways as the enzyme catalyzes formation of aldehyde groups which can then spontaneously react with the side-chain amine groups of lysine or hydroxylysine residues to form crosslinks (92). Analogously, it is here demonstrated that sulfilimine crosslinks are enzymatically formed by peroxidasin within basement membranes.

Results

PFHR9 Model Is Appropriate for Studying Collagen IV Network

Murine PFHR9 cells secrete an extracellular matrix rich in collagen IV (93, 94), which was thus explored as a potential model for network assembly. Cultured production of collagen IV initiates upon PFHR9 cells reaching confluency, accumulating into a thick matix when grown at confluency for extended periods of time. Thus, cells were maintained at confluency for approximately 7-10 days with

frequent media changes (<36 hours) to accommodate the aggregate metabolic activity, supplemented by ascorbic acid to facilitate post-translational hydroxylations. Briefly, matrix from culture plates was isolated by scraping and biochemically purified via detergent, high salt, and low salt washes. Observation of the NC1 domains is enabled by matrix digestion with bacterial collagenase which degrades collagenous domains yet leaves the globular NC1 domains intact.

Through the dedicated efforts of Hudson laboratory colleagues, PFHR9 NC1 was compared to tissue-isolated protein for hexamer assembly and presence of sulfilimine crosslinking. Collagen IV hexamers were thus analyzed by gel filtration (S200) chomatrography, and the cultured NC1 peak elution profile was similar to that of purified bPBM hexamer, suggesting that the cells produce properly assembled quaternary NC1 hexamer structures (Figure 3.1a). SDS-PAGE analysis of the hexamer separated the protein subunits into dimer and monomer bands (Figure 3.1a).

To ensure that PFHR9 collagen IV networks were crosslinked with sulfilimine bonds, NC1 hexamer isolated from cell culture was subjected to enzymatic digestion with trypsin and the resulting peptide fragments were analyzed by mass spectrometry. Through similar protocols used in the original identification of sulfilimine bonds from bovine PBM (1), sulfilimine crosslinks were also identified in PHFR9 NC1 domains between Met^{93} and Hyl^{211} residues (Figure 3.1b). With PFHR9 cells now collaboratively established as a system to properly address sulfilimine bond formation, individual efforts were here launched as a parallel strategy for identifying the crosslinking catalyst.

Inhibition of Sulfilimine Bond Formation in Basement Membranes

In an effort to identify pharmacologic modulators of sulfilimine bond formation, several small molecule inhibitors of heme peroxidase enzymes were found to also block the crosslinking reaction by Dr. Bhave (4). Included within this inhibitor panel was phloroglucinol (PHG), a phenol derivative of benzene. Also found to unexpectedly inhibit the reaction was high concentrations of potassium iodide,

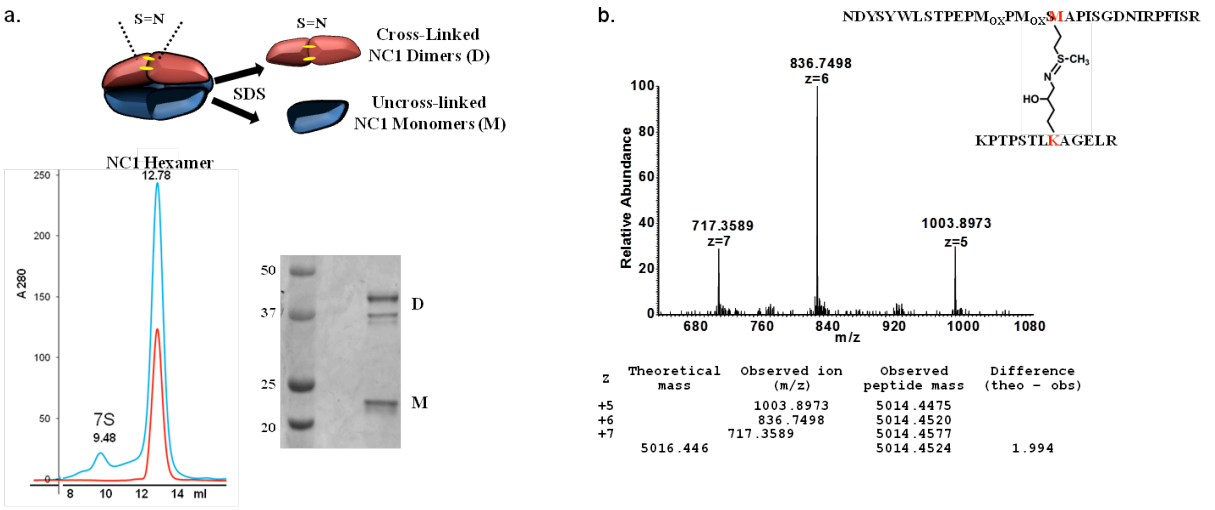

Figure 3.1: PFHR9 Cells Produce Collagen IV Matrix with Sulfilimine Crosslinks. (a) Collagen IV hexamers contain sulfilimine bonds that join individual NC1 domains (**a**, cartoon). To assess the structural integrity collagen IV NC1 domains were isolated from PFHR9 matrix and compared to tissue analogues by gel filtration chromatography (S200, GE Healthcare) (**a**). Cell-derived NC1 material (blue trace) eluted overtop NC1 hexamers that were isolated from placental basement membrane (red trace). Using non-reducing SDS-PAGE analysis with 12% gels, PFHR9 hexamers separated into NC1 dimers and monomer (**a**, inset). (**b**) Mass spectrometry revealed the presence of sulfilimine crosslinks within NC1 hexamers produced in PHFR9 culture. Additional protocol details are contained in the Methods section. Performed in collaboration with G. Bhave, R. Vanacore, and M. Rafi.

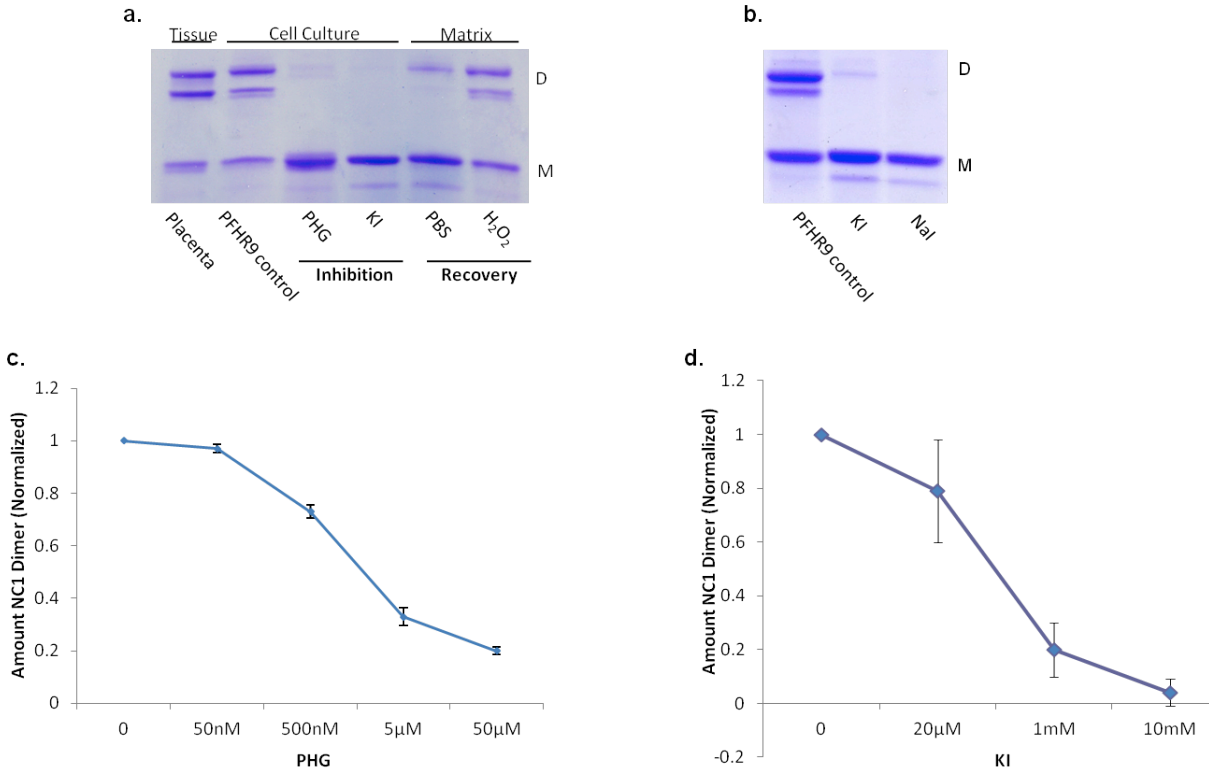

Figure 3.2: Inhibition and Controlled Formation of NC1 Dimers in Matrix. (**a**) Dimer formation was inhibited in PFHR9 cell culture by treatment with either 50 µM phloroglucinol (PHG) or 10 mM KI. Using KI-treated matrix, dimer formation was allowed to recover in matrix by washing away the inhibitor and incubating matrix pellets at 37˚C with or without H_2O_2. (**b**) To demonstrate that inhibition with KI occurs through halide ions, PFHR9 cells were grown in the presence of 10 mM NaI which inhibited dimer formation similar to KI treatment. (**c-d**) Inhibition of dimer formation is dependent on the concentration of PHG (**c**) and KI (**d**), as quantified through densitometric analysis in ImageJ and Excel. Additional protocol details are contained in the Methods section.

which is surprising considering the catalytic formation of dehydromethionine by oxidized iodide.

Inhibition from PHG and KI treatments was initially characterized by an analysis of the effective concentration of both compounds. PHG treatment resulted in ca. 50% inhibition near 1 µM of the compound, notably similar to the published concentration of 0.5 µM PHG used for comparible inhibition of the peroxidasin enzyme (Figure 3.2c) (95). Potassium iodide also inhibited dimer formation at low millimolar concentrations (Figure 3.2d) with similar inhibition achieved via sodium iodide (Figure 3.2b), confirming that the effect stems from halide activity. Iodide inhibition of dimer formation resembles the clinically described "Wolff-Chaikoff effect" where the organification of iodide in thyroid tissues is temporarily blocked via excessive iodide and overcome by down-regulation of iodide transport mechanisms (96).

Peroxide-Enhanced Recovery of Bond Formation in Matrix

Inhibition of bond formation in matrix was found to be reversible following the removal of the inhibitor during biochemical matrix purification and subsequent incubation of matrix at 37°C for an extended period of time (Figure 3.2a). Thus, crosslinking activity was effectively demonstrated within isolated matrix. Protocol limitations indeed allowed the possibility for cell membrane remnants to contaminate matrix preparations, introducing the possibility that crosslinking is either intracellular or plasma membrane-associated. Since the majority of isolated components were extracellularly derived, this concern was placed secondary to the hypothesis that crosslinking is catalyzed by a matrix protein.

The ability of peroxidase inhibitors to block dimer formation suggests that an extracellular heme peroxidase might catalyze the reaction, and we thus tested this hypothesis by adding hydrogen peroxide to uncrosslinked matrix. Indeed, the addition of exogenous hydrogen peroxide caused an increase of dimer formation in matrix, and this effect was blocked in the presence of catalase (Figure 3.3). To confirm that the observed H_2O_2 effect was not simply due to non-specific crosslinking, the "recovered"

dimer banding was examined by high-resolution mass spectrometry to determine if the sulfilmine bond was indeed formed. Sample material was prepared by reacting uncrosslinked matrix with H_2O_2, followed by isolation of the NC1 domains via digestion with bacterial collagenase. The digest supernatant was resolved under non-reducing SDS-PAGE conditions in 7.5% gels, visualized by colloidal Coomassie stain, and the dimer bands were excised and digested with trypsin. As a control, uncrosslinked matrix not treated with H_2O_2 was also digested, the NC1 domains were separated on 7.5% SDS gels, and the residual dimer banding was excised and trypsinized. Following treatment with trypsin, peptide fragments were eluted from gel slices and analyzed with liquid chromatography fourier transform mass spectrometry (LC-FTMS) using an LTQ Orbitrap mass spectrometer (Thermo Fischer Scientific; San Jose, CA). The mass of sulfilmine-crosslinked tryptic peptides is equal to two protons less than the sum of the uncrosslinked peptides (1). LC-FTMS spectra revealed peaks corresponding to +5, +6, and +7 positively-charged ions, which were undetected in the control sample, and the average mass of these ions was 2 amu less the theoretical sum of the uncrosslinked peptides (Figure 3.4). This data suggests that H_2O_2 indeed promotes sulfilimine bond formation in matrix.

KI and PHG were compared for their ability to reversibly inhibit the reaction. Uncrosslinked matrix was incubated with either 10 mM KI or 200 μM PHG in the presence of H_2O_2. Following the incubation, matrix samples were examined for their ability to form dimers. Robust crosslinking was observed in KI-treated samples while no detectible crosslinking was seen in PHG-treated samples (Figure 3.5). Thus, KI is a reversible inhibitor of bond formation while PHG may potentially damage the reaction. Due to these differential properties, KI treatment was utilized for examining bond formation *in vitro* while the strength of PHG inhibition provided great value as a negative control for the reactions.

Solubilization & Purification of Active PXDN *From Matrix via Collagenase Digestion*

Hypothesizing that bond formation is an enzymatically-catalyzed reaction, attention was

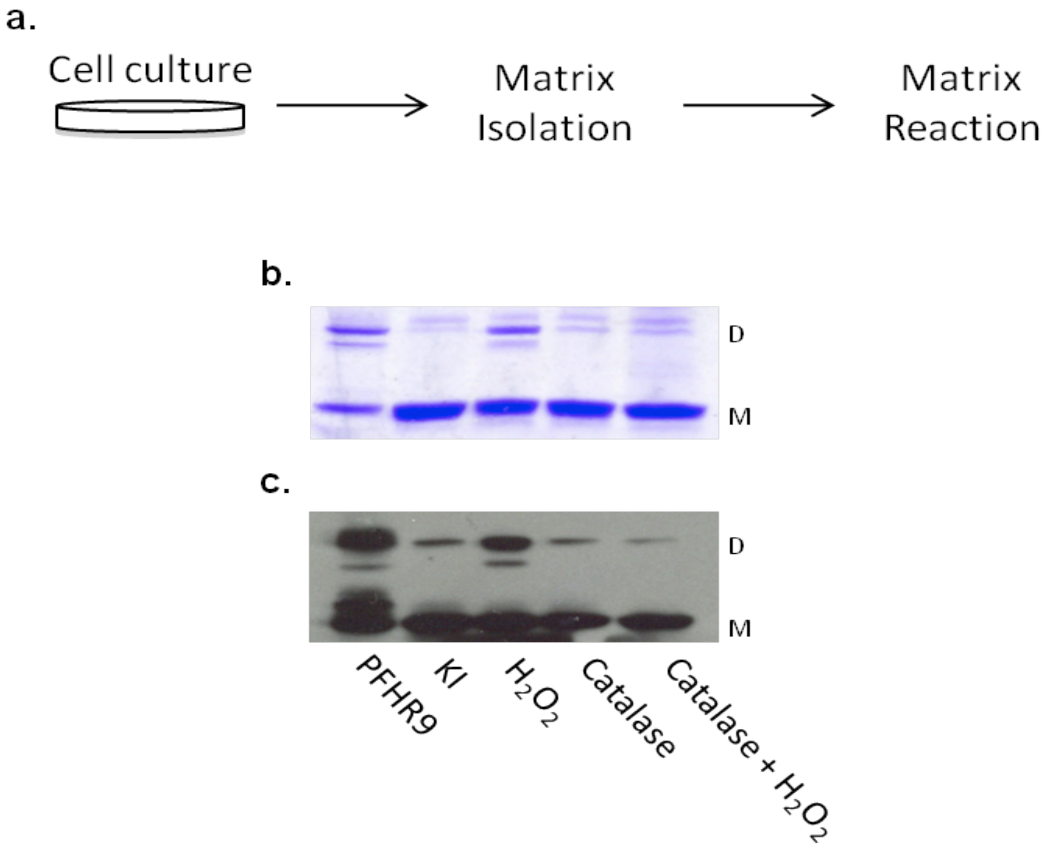

Figure 3.3: Peroxide is Required for Bond Formation. (**a**) Purification schematic outlines the process of demonstrating *in vitro* bond formation within matrix. (**b**) Exogenous hydrogen peroxide (3 mM) was added to matrix pellets in the presence and absence of bovine catalase enzyme, and reacted overnight at 37˚C in 1x TBS. The effect of exogenous H_2O_2 on crosslinking was blocked by the enzyme. Samples were analyzed by 12% SDS-PAGE gels under non-reducing conditions and visualized by Coomassie staining. (**c**) Western blotting using the H22 anti-NC1 antibody confirmed the peroxide-dependent formation of NC1 dimers. Additional protocol details are contained in the Methods section.

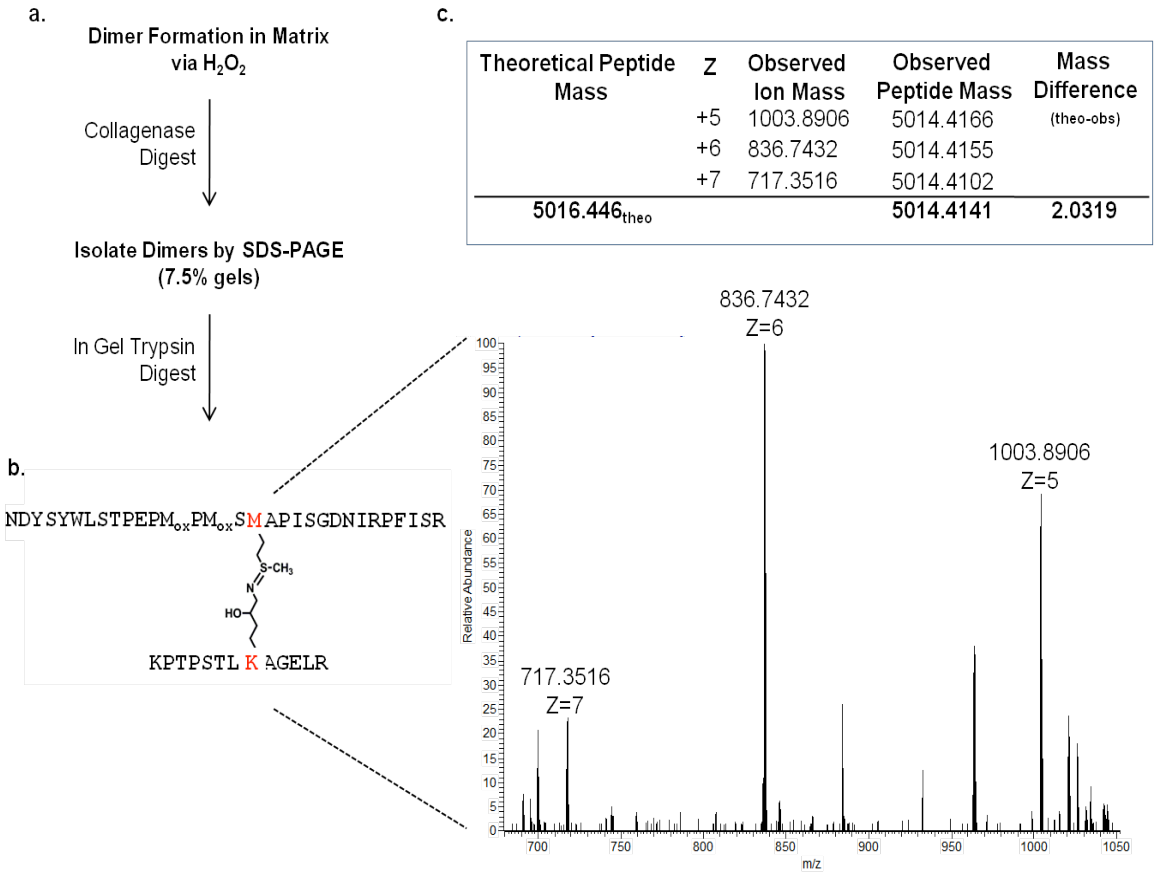

Theoretical Peptide Mass	Z	Observed Ion Mass	Observed Peptide Mass	Mass Difference (theo-obs)
	+5	1003.8906	5014.4166	
	+6	836.7432	5014.4155	
	+7	717.3516	5014.4102	
5016.446$_{theo}$			**5014.4141**	**2.0319**

Figure 3.4: H_2O_2-Enhanced Dimer Formation Leads to Catalysis of Sulfilimine Bonds. (**a**) Protocol schematic for isolating sulfilimine-containing NC1 peptides. NC1 dimers formed through an H_2O_2-based reaction in matrix were excised from an SDS-PAGE gel slice. (**b**) The isolated dimers were treated with trypsin via an in-gel enzymatic digest to generate the predicted crosslinking-containing peptide sequence. (**c**) Peptides were eluted from the gel slice and analyzed by Fourier Transform mass spectrometry at the VUMC Mass Spectrometry Core facility using an LTQ Orbitrap instrument (Thermo Fischer Scientific). Mass spectra revealed loss of two mass units as a signature of the sulfilimine bond which contains two protons less than the sum of the uncrosslinked peptides (**c**). Additional protocol details are contained in the Methods section. Performed in collaboration with R. Vanacore.

devoted to solubilizing crosslinking activity from matrix and identifying the responsible enzyme. Bacterial collagenase effectively releases NC1 domains into solution, and was therefore tested as a means of additionally solubilizing the crosslinking activity. Supernatant from collagenase digests were incubated at 37°C with and without hydrogen peroxide, followed by analysis by SDS-PAGE. Indeed, dimer formation occurred in the presence of H_2O_2 only. The peroxidase enhancer cetyl trimethylammonium bromide (CTAB) (95) was added, leading to the strikingly robust dimer formation that was blocked in the presence of PHG (Figure 3.6).

In sum, soluble crosslinking activity was dependent on hydrogen peroxide and responsive to the treatment by either peroxidase enhancers or inhibitors, together suggesting that sulfilimine bonds form through the enzymatic activity of a matrix-located peroxidase. One such candidate is peroxidasin (PXDN), a heme peroxidase located with basement membranes lacking any well-established biologic function yet sensitive to PHG treatment (95).

A particularly notable point was that collagenase treatment rendered a suitable substrate for catalysis, with the NC1 domain being effectively severed from the remainder of the collagen IV protomer. Considering that the *in vivo* reaction proceeds with the globular NC1 attached to the helical collagenous domain, and in the absence of additional insight regarding any putative protein-protein interactions between enzyme and substrate, the demonstration of soluble crosslinking indicates that the NC1 domain is a sufficient substrate for catalysis.

In an effort to purify the putative crosslinking enzyme, collagenase digest supernatant was resolved by anion exchange chromatography using a MonoQ column. In low ionic strength conditions, the NC1 domain is non-binding, found in the flow through fractions, thus presenting a potential means of initially separating substrate from the active component. Supernatant was passed over the column in 20 mM Tris-HCl (pH 7.5) with NC1 domains being collected in the flow-through fraction while bound proteins were eluted in a 1 M NaCl gradient (Figure 3.7a-b). The eluting peaks were screened by

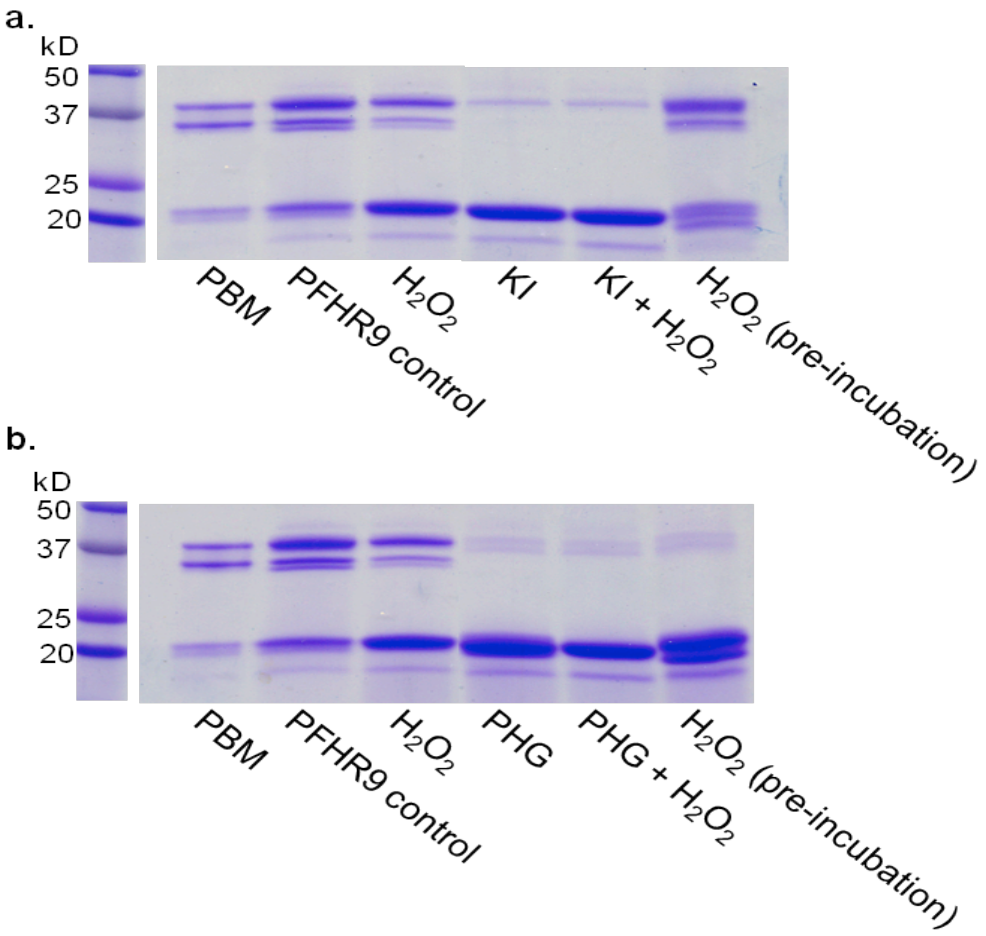

Figure 3.5: KI Treatment Reversibly Inhibits Bond Formation and PHG Damages the Reaction. Uncrosslinked matrix was pre-incubated with either 10 mM KI or 200 µM PHG in PBS with H_2O_2 at 4˚C for 1 day prior to reaction. Samples were then reacted in the above conditions overnight at 37˚C, using 200 µM PHG and 2.9 mM H_2O_2. (**a-b**) SDS-PAGE analysis using 12% gels in non-reducing conditions revealed that KI acted as a reversible inhibitor of dimer formation (**a**) while pre-incubation with PHG damaged the recovery of dimer formation (**b**). Additional protocol details are contained in the Methods section.

combining flow-through fractions with peak fractions in the presence of H_2O_2, and subsequent SDS-PAGE analysis for detecting any crosslinking activity. By this means, an approximately 75kD isolated protein displayed activity that was H_2O_2-dependent and CTAB-enhanced (Figure 3.7c-d). Curiously, the activity was not sensitive to PHG treatment. Additional purification efforts were hampered by gel filtration or by protein concentration, presumably due to protein dilution in the former techniques and insolubility in the latter.

Since the isolated active fraction was reasonably pure as seen by Sypro Ruby staining (Figure 3.7, panel c), the major 75 kD band was excised from the gel, digested with trypsin, and the resultant peptide fragments were analyzed by mass spectrometry on a linear LTQ ion trap mass spectrometer for identification of the constituent protein(s). PXDN was the most abundant protein by number of observed peptides, though other proteins were co-purified (Table 3.1). This signified the initial activity-based evidence suggesting that PXDN forms collagen IV sulfilimine bonds in basement membranes.

A conflict resulted in attempting to harmonize the approximately 500 kD homotrimeric molecular weight of PXDN with the observed ~75 kD prominent banding in the active fraction. One possible explanation is that the enzyme underwent a proteolytic cleavage event, possibly during the collagenase digestion, which removed the trimerization domain and shortened the enzyme. Considering that the purified fraction was not sensitive to PHG, this scenario suggests that the inhibitor binding site was removed during the proteolysis.

Verification Through Parallel Studies of Exogenous PXDN *Expression*

To verify the role of PXDN in catalyzing sufilimine bond formation, a top-down approach was conducted in parallel to the biochemical purification of PXDN from matrix. This alternative strategy included searching for PXDN within PFHR9 matrix, heterologous overexpression of the enzyme in culture, and *in vitro* crosslinking experiments using purified PXDN and NC1 hexamers. Dr. Guatam Bhave

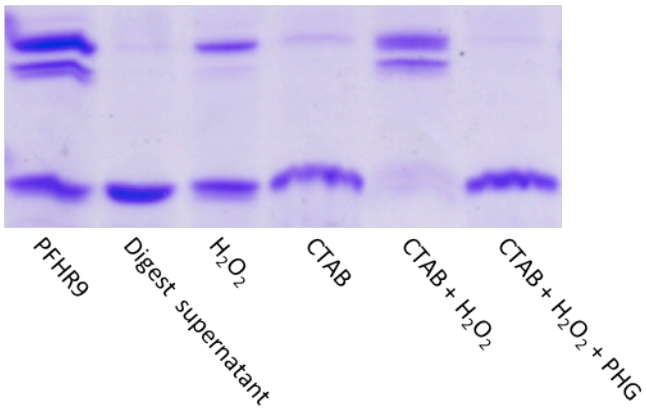

Figure 3.6: Enzymatic Crosslinking Activity is Solubilized from Matrix via Collagenase Treatment. Uncrosslinked matrix samples were digested overnight with bacterial collagenase enzyme at 37˚C in the presence of KI. Digest supernatant was subsequently dialyzed to remove residual KI, and tested for enzymatic crosslinking by reacting the matrix pellet with 1 mM H_2O_2 and/or 0.05% CTAB (w/v) in 1x PBS at 37˚C overnight. Samples were analyzed by SDS-PAGE using 12% gels and non-reducing conditions before visualization with Coomassie staining. Additional protocol details are contained in the Methods section.

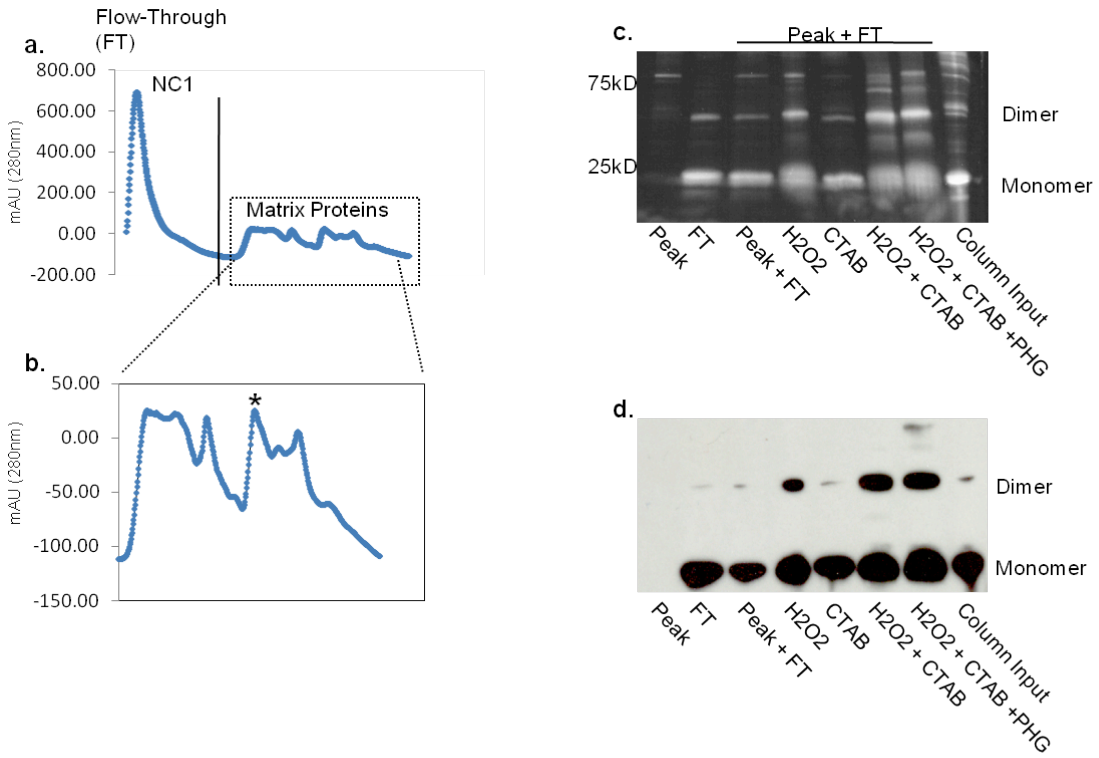

Figure 3.7: Purification of Crosslinking Activity from Matrix. (**a**) Supernatant from collagenase digest was separated by ion exchance (MonoQ) in low ionic strength buffer (20mM Tris-HCl, pH 7.4), monitored by A_{280} absorbance, with NC1 domains eluting in the flow-through fractions. (**b**) Column-bound material was eluted with a 1 M NaCl gradient, with an A_{280} peak retaining crosslinking activity (asterisk) evidenced in panels **c** and **d**. (**c-d**) Isolated peaks were mixed with flow-through fractions (containing uncrosslinked NC1 domains) in the presence of 1 mM H_2O_2 and/or 0.05% CTAB (w/v) in 1x TBS and reacted at 37˚C for 48 hours. SDS-Page analysis of the reaction revealed preservation of crosslinking activity in one fraction, as visualized with Sypro Ruby staining (**c**) and western blotting using the H22 anti-α22 NC1 antibody (**d**). Additional protocol details are contained in the Methods section.

Protein	Coverage	Number of Peptides	Description
B2RX13_MOUSE	13	17	Peroxidasin homolog (Drosophila)
B1B0C7_MOUSE	12	16	Perlecan (Heparan sulfate proteoglycan 2)
Q3UNG0_MOUSE	15	9	Putative uncharacterized protein
LAMC1_MOUSE	7	7	Laminin subunit gamma-1
Cntm_P13645	29	6	Unknown
LAMA1_MOUSE	3	6	Laminin subunit alpha-1
LOXL2_MOUSE	18	5	Lysyl oxidase homolog 2
CO4A1_MOUSE	4	4	Collagen IV alpha-1
B2RQQ8_MOUSE	3	3	Collagen IV alpha-2
PLOD2_MOUSE	13	1	Procollagen-lysine,2-oxoglutarate 5-dioxygenase 2
TPA_MOUSE	5	1	Tissue-type plasminogen activator
A2A4H7_MOUSE	3	1	Junction plakoglobin

Table 3.1: Mass Spectrometry Identifies PXDN as Co-purifying from Matrix with Crosslinking Activity. The ion exchange fraction possessing crosslinking activity was separated by 12% reducing SDS-PAGE where the major band was excised from the gel, digested with trypsin, and the peptide analyzed by mass spectrometry to identify the protein components. Mass spectrometry analysis was conducted on an LTQ ion trap instrument (Thermo Fischer Scientific) in the VUMC Mass Spectrometry Core facility. Peroxidasin, a heme peroxidasin within basement membranes, was the most abundant protein according to the number of peptides identified. Second most abundant was perlecan, a heparin sulfate proteoglycan. Additional protocol details are contained in the Methods section.

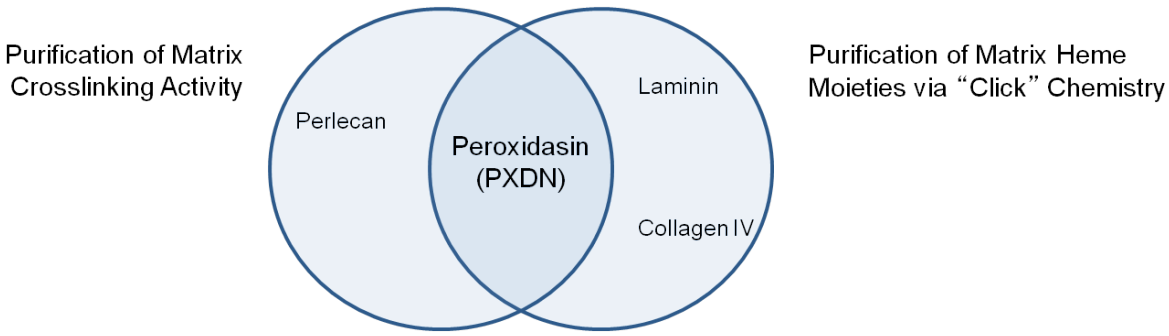

Figure 3.8: Parallel Strategies Implicate Peroxidasin as Responsible for Forming Sulflimine Bonds in Matrix. Two strategies implicated peroxidasin as forming sulfilimine crosslinks within matrix. Using a "bottom-up" approach, crosslinking activity was purified from matrix using a combination of enzymatic digestion of the matrix, ion chromatography, and mass spectrometry. A more targeted strategy was also conducted based on the hypothesis that a matrix heme peroxidase catalyzed the reaction. This approach was performed by G. Bhave and colleagues, utilizing azide-based "click chemistry" to biotinylate heme moieties within the matrix. Following purification with strepavidin, mass spectrometry analysis identified peroxidasin as the primary component, with collagen IV and laminin likely being co-purified due to their abundance in the PFHR9 matrix. Additional protocol details are contained in the Methods section.

and colleagues led these efforts in collaboration with the previously described purification of crosslinking activity from matrix.

During initial investigations, shotgun mass spectrometry was performed on matrix samples and indicated that PXDN is indeed expressed within the PFHR9 system. Adding to the evidence, "click chemistry" was employed involving the biotinylation of heme moieties through an azide-based reaction to allow purification with streptavidin (4). Reducing SDS-PAGE analysis of the samples revealed a prominent high molecular weight band (>250 kD). This band was excised from the gel, digested with trypsin, and the peptide fragments analyzed by mass spectrometry. This analysis identified PXDN as well as laminin and collagen IV likely as an off-target effect due to their high abundance within the PFHR9 matrix (Figure 3.8). This confirmed that PXDN is within matrix, setting the stage for more definitive evidence for its role in sulfilimine bond formation. Now focusing on PXDN, the human gene sequence was overexpressed in HEK293 cells grown on uncrosslinked PFHR9 matrix. Secretion and deposition of the enzyme into the underlying matrix resulted in crosslink formation that was inhibited by PHG treatment (Figure 3.9).

Secreted PXDN was collected from culture media, prior to its deposition within matrix, and purified via ammonium sulfate precipitation and sucrose gradient centrifugation. This yielded a single high molecular weight band when visualized by coomassie stain reducing gels, which further reacted with anti-PXDN antibodies (Figure 3.10a). When incubated with uncrosslinked NC1 hexamer in the presence of H_2O_2, dimer formation readily occurred (Figure 3.10b), definitively establishing PXDN as the enzyme responsible for crosslinking collagen IV.

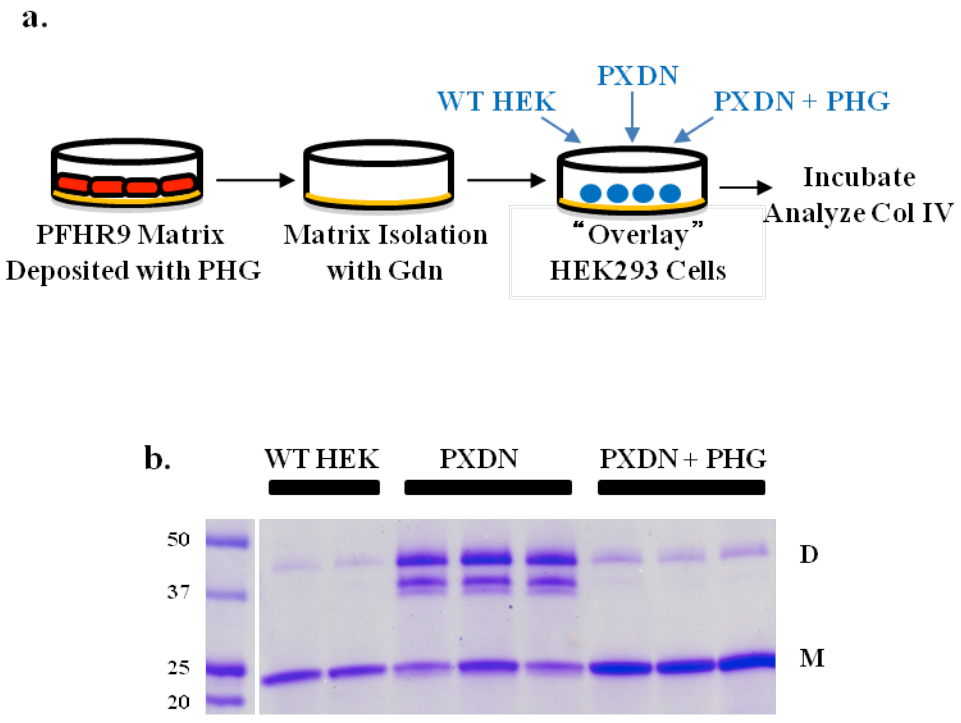

Figure 3.9: Exogenously Expressed PXDN Forms NC1 Sulfilimine Bonds *In Vitro*. Human *PXDN* (coding sequence provided by Dr. Miklos Geizst, Semmelweis University, Budapest, Hungary) was transiently expressed in mammalian cells grown on uncrosslinked PFHR9 matrices. Following induction of PXDN expression and deposition into the underlying matrix, collagen IV hexamers were isolated and shown by SDS-PAGE analysis, using 12% gels under non-reducing conditions, to have undergone dimer formation by PXDN. Additional protocol details are contained in the Methods section. Performed in collaboration with M. Rafi, R. Vanacore, and G. Bhave.

Discussion

Collagen IV sulfilimine bonds form extracellularly through the enzymatic activity of PXDN, a basement membrane heme peroxidase. Nearly twenty years elapsed between the initial discovery of PXDN (95) and the unveiling of its role in sulfilimine bond formation (4). Furthermore, PFHR9 cells had been extensively used for collagen IV research more than a decade prior to the original identification of PXDN (93, 94). Arguably, the discovery of sulfilimine bonds within collagen IV provided the impetus to revive the time-honored literature and demonstrate the function of PXDN in cell culture. Additional support for the role of PXDN in sulfilimine bond formation has since been shown in animal models, via loss-of-function *Pxn-/-* mutations in *D. melanogaster* organisms that are embryonic lethal at the third instar larval stage (4). Analysis of the mutant flies prior to the third instar stage revealed disordered collagen IV networks and disrupted tissue morphology, indicating that the enzyme performs a critical function within biology.

Structure-Function Analysis of PXDN

The enzyme was initially described in *D. melanogaster* hemocytes (95), later followed by scattered associations with seemingly unrelated biologic processes before conclusive functional evidence revealed its role in collagen IV crosslinking. Nomenclature was similarly uncoordinated and *ad hoc* as the enzyme assumed the alternative names of ”Vascular Peroxidase 1” (97) and “MG50” (98) due to its independent identification in vascular extracellular matrices and association with human melanoma, respectively.

PXDN is a large protein with an interesting array of functional domains (Figure 3.10). Monomers contain ~1500 aa with an approximate mass of 150 kD, increasing to 170 kD with N-linked sugars (95, 99). In basement membranes, the enzyme presumably exists as a homotrimer of approximately 500 kD, as evidenced by electron micrographs of *Drosophila* PXDN produced and isolated in culture

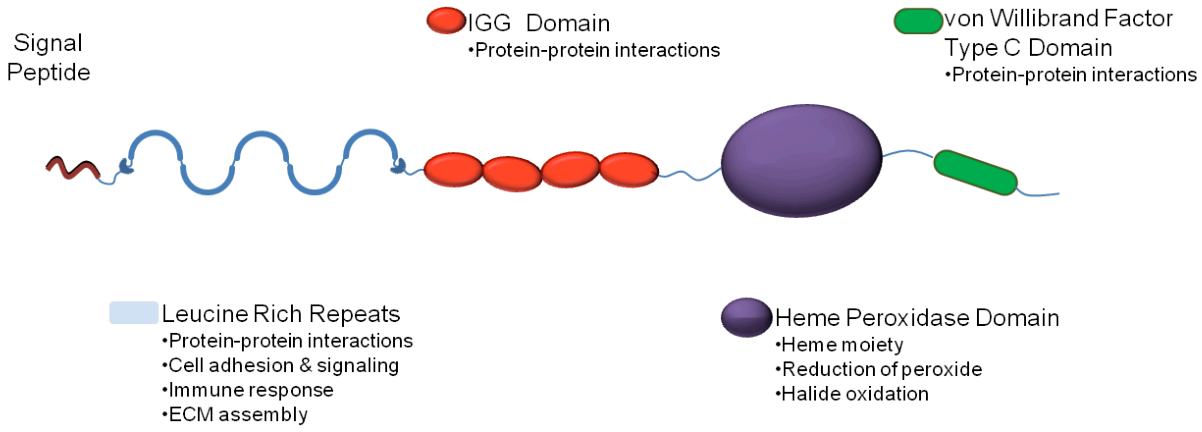

Figure 3.10: Schematic Diagram of PXDN Domain Structure

conditions (94), while the enzyme reportedly circulates in plasma as monomers (101). As a secreted protein, the domain structure is N-terminally capped by a signal peptide, followed by four leucine rich repeats, four immunoglobulin domains, a peroxidase catalytic domain, and finally a Von Willebrand factor C type domain at the C-terminus (95, 97).

PXDN has two isoforms in humans, sharing 63% genomic sequence identity (100). Further complexities arise from a possible splice variant distinguished from PXDN2 by only five amino acid residues (99). PXDN2 has alternatively been termed VPO2 (97), cardiac peroxidase, and peroxidasin-like (99).

Studies in *C. elegans* suggest the two isoforms of peroxidasin, termed PXN-1 and PXN-2 in worms, are non-redundant and possibly antagonistic toward each other (102). *Pxn-2* loss-of-function mutants display similar embryonic lethality as worms lacking either collagen IV chain. In contrast, *pxn-1* mutants displayed no developmental phenotype, and no defects were observed in the double mutant *pxn-1; pxn-2*. Consequently, overexpression of PXN-1 on a *pxn-2* mutant background exacerbated the PXN-2 mutant phenotype yet the elevated protein levels were not apparently harmful to wild type worms. In mammals, no functional differences are known for the two PXDN proteins, though the issue is not without merit given the evidence from nematodes.

The complex domain structure of PXDN distinguishes it among mammalian peroxidases. All have a common heme peroxidase domain, though the additional motifs garnishing the catalytic region of PXDN are not found on other mammalian heme peroxidases. Leucine-rich repeats, IgG domains, and *von Willebrand* factor type C are all known to be useful facilitators of protein-protein interactions (103-105), although their specific roles within PXDN activity is unknown.

PXDN Functional Associations

While much of PXDN still remains shrouded, delineating its role in collagen IV network

stabilization has provided some rationale for understanding its diverse associations. Genetic mutation of either the enzyme or collagen IV has yielded strikingly similar phenotypes. In *C. elegans*, mutation of either peroxidasin 2 or collagen IV caused paralytic embryonic lethality due to unstable basement membranes and muscle-epidural attachment complications (102, 12), hinting at the critical nature of the sulfilimine bond within extracellular physiology. Indeed, *Drosophila* organisms with a hypomorphic *peroxidasin* allele displayed a molecular phenotype of collagen IV networks possessing limited sulfilimine crosslinking as well as a morphologic disruption of the basement membrane and the overlying tissue architecture (4).

A report of several families with congenital corneal opacity described separate genomic mutations in the *PXDN* locus, which were predicted to independently disrupt the catalytic site via truncation of the protein or site mutation in the amino acid sequence (106). While the pathologic mechanism of action was not determined, it is interesting to note that plausible etiologies of this phenotype include structural defects within the lens (107) potentially due to the absence of sulfilimine biochemistry, or alterations within the metabolism of reactive oxidative species due to lowered consumption of hydrogen peroxide by catalytically inactive PXDN mutants as suggested by Khan and colleagues (106).

While detailed questions remain, PXDN has a distinct neurologic function. The protein has been observed in the developing neural tube of *Xenopus tropicalis* (108) and the ventral nerve cord of *Drosophila* (109), and its mRNA expression occurs throughout the central and peripheral nervous systems in mice (110). Further, PXN-2 loss-of-function mutations in *C. elegans* displayed abnormal axon growth (102), although it is unclear whether the phenotype is due to direct PXN-neuron interactions or via basement membrane disruptions that develop in the absence of enzymatic activity.

PXDN has been associated with multiple cancers through *in vitro* studies and genomic screens (111, 113, 99). Gene expression profiling from tumor samples have demonstrated transcriptional

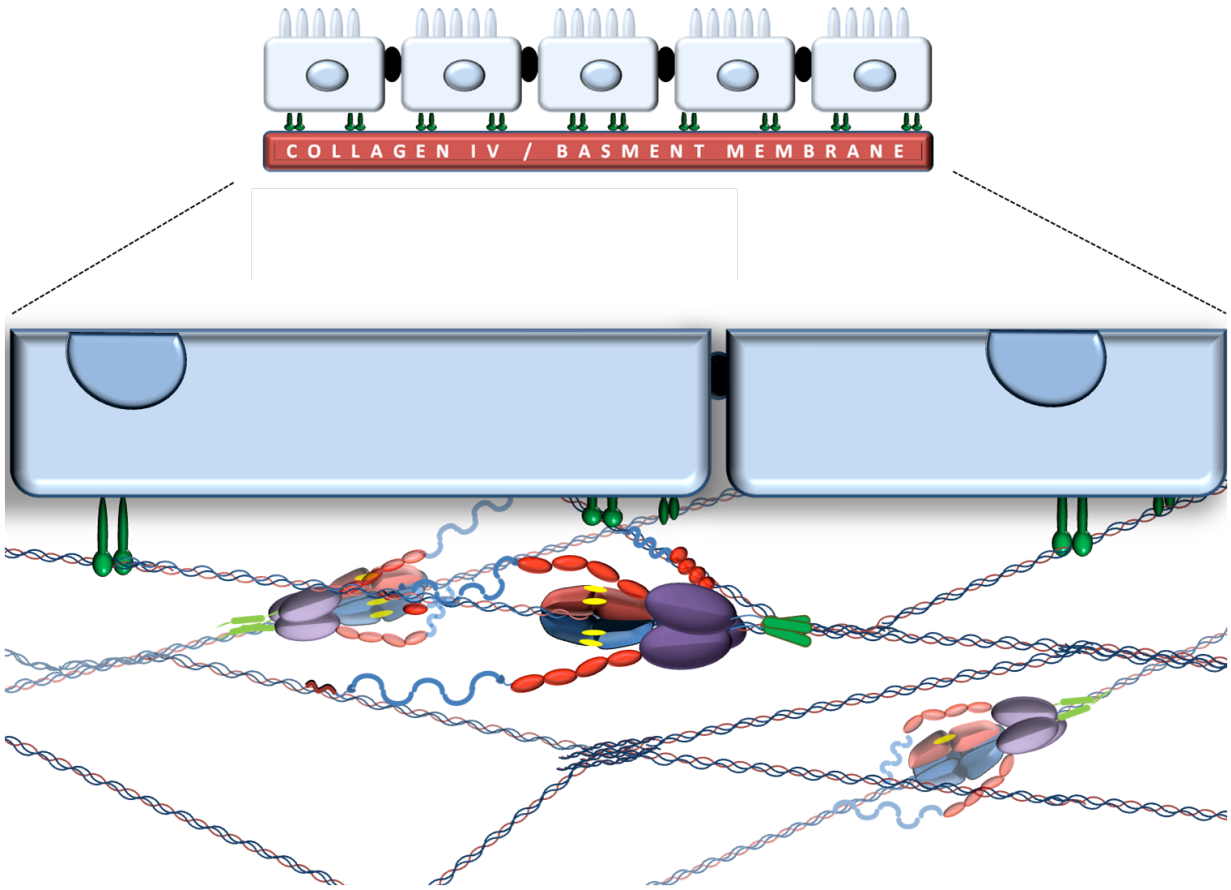

Figure 3.11: Working Model of PXDN Formation of Collagen IV Sulfilimine Bonds in Matrix

up-regulation of the enzyme in several cancer types including breast, melanoma, bladder, uterus, and pancreas (113). PXDN expressed sequence is non-mutated in these cancers (112), indicating that its normal function of sulfilmine formation may be commandeered to promote cancerous processes.

Cell culture studies with vascular endothelium suggest that PXDN may act as a downstream signaling element in the angiotensin-II cell signaling pathway (114). Evidence has also been submitted that the enzyme may produce hypochlorous acid in response to oxidative stress, leading to p38 MAPK-induced cellular apoptosis (115, 116). An apoptotic function for PXDN is further indicated by its transcriptional up-regulation in response to p53 activity (117).

Conclusion

PXDN is a novel peroxidase functioning within basement membranes (Figure 11). The large molecular weight and homo-trimeric assembly indicated that PXDN is a massive matrix component, on par with other core constituents such as collagen IV and laminin. Its peroxide-based mechanism uniquely postures PXDN as an oxidant generator within basement membranes, although this catalytic potential is harnessed toward collagen IV sulfilimine bond formation with additional putative functions. Canonically, mammalian heme peroxidases are strongly associated with immune functions and it is plausible that PXDN may possess alternative biological functions that utilize its potential for driving oxidative destruction. Identifying the enzymatic source of collagen IV sulfilimine bonds has raised fresh questions regarding the biology of basement membranes and the role of oxidative chemistry in tissue formation.

Methods

Materials & Cell Culture

Chloride salts were purchased from Thermo Fisher Scientific (Whaltham, MA), cell culture reagents from CellGro (Manassas, VA), and all other chemicals from Sigma-Aldrich (St. Louis, MO). PFHR9 cells were grown in complete DMEM media (Product Number: 15-013-CV, CellGro, Manassas, VA) supplemented with 5% FBS (Sigma-Aldrich, St. Louis, MO), L-glutamine, penicillin, and streptomycin. Cells were maintained at 37˚C with 10% CO_2.

Collagen IV Production, and Inhibition of Bond Formation in Cell Culture

For matrix production, cells were plated at high density and maintained at confluency for 5-8 days in the presence of 50µg/ml ascorbic acid, with media changes every 24-36 hours. Crosslinking was inhibited by supplementing the culture conditions with either 1 or 10 mM of KI or 50 µM of phloroglucinol (PHG). Inhibitor and ascorbic acid treatments were initiated upon confluency.

Isolation of Collagen IV Matrix & NC1 Domains

Cultured matrix was washed in 1x PBS before being scraped in a lysis buffer containing 10mM Tris-HCl (pH 7.5), 1mM ethylenediaminetetraacetic acid (EDTA), 1% (w/v) sodium deoxycholate, 0.4 mM phenylmethanesulfonyl fluoride (PMSF), 1 µg/ml aprotinin and 1 µg/ml leupeptin. Matrix was sonicated to sheer genomic DNA, 1 ml aliquots were placed into 1.5 ml eppendorf tubes on ice, and centrifuged at 14000 rpm for 20 minutes at 5˚C. The pellet material was washed in a high salt buffer containing 50 mM Tris-HCl (pH 7.5) and 1M NaCl before centrifugation at 14000 rpm for 10 minutes at 5˚C. The insoluble material was washed in low salt buffer consisting of 10 mM Tris-HCl (pH 7.5), and stored at 4˚C until use.

Isolation of NC1 domains from collagen IV matrix was accomplished by treating the matrix with bacterial collagenase enzyme (Worthington Biochemical Corporation, Lakewood, NJ) at 37°C in 10 mM

Tris-HCl (pH 7.5), 10 mM $CaCl_2$, 10 mM KI, 0.4 mM PMSF, 1 µg/ml aprotinin and 1 µg/ml leupeptin. Collagenase enzyme was stored in the above buffer at -20°C until use, in 1 mg/ml aliquots, and thawed prior to use. Matrix was digested overnight with 0.167 µg/ml enzyme in 60 µl, typically by adding 10 µl of 1 mg/ml enzyme solution to 50 µl of buffer. As collagenase treatment effectively solubilized NC1 domains as well as crosslinking activity, the supernatant was obtained following digestion and used directly for SDS-PAGE and crosslinking purification.

For further purification of NC1 hexamers, collagenase digest supernatant was dialyzed into 50 mM Tris-HCl (pH 7.5) before being passed over a DEAE-Cellulose column. The flow-through material was collected and passed over a Superdex™ 200 10/300GL gel filtration column (GE Healthcare Life Sciences; Piscataway, NJ) in 1x TBS, using an ÄKTA Purifier P-900 (GE Healthcare Life Sciences; Piscataway, NJ). Expectedly, elution of the NC1 hexamers produced a peak in the A_{280} profile near 13 ml. Hexamer fractions were pooled and concentrated to ca. 1 mg/ml, (extinction coefficient: 1.6 ≈ 1 mg/ml NC1 domains).

SDS-PAGE and Western Blotting of Proteins

SDS-PAGE analysis of NC1 domains was performed by sampling the digest supernatant directly. Equal volumes of supernatant and 2x loading buffer (0.125 M Tris-HCl [pH 6.8], 4% SDS, 20% glycerol, and bromophenol blue) were boiled for 5 minutes before separation of the samples on 12% non-reducing tris/glycine gels (Bio-Rad Laboratories, Inc: Hercules, CA). Running buffer was made from 10x Tris/Glycine/SDS buffer (Bio-Rad Laboratories, Inc; Hercules, CA). Proteins were visualized by staining with 0.1% of Coomassie Blue R250 stain (National Diagnostics, Charlotte, NC) in 50% methanol and 10% acetic acid, followed by destaining in 5% methanol with 10% acetic acid. For enhanced protein detection, Sypro® Ruby Protein Gel Stain (Molecular Probes, Eugene, OR) was used according to manufacturer's protocol with slight modifications. Briefly, following electrophoresis, gels were

transferred to a dark container with foil covering and washed twice in 100 ml solutions of 50% methanol and 7% acetic acid, with each wash lasting over 1 hour with rocking at room temperature. Gels were subsequently stained overnight in ca. 50 ml/gel of Sypro® Ruby stain, with rocking at 4˚C. Stain was re-used for up to 3 or 4 gels without unacceptable losses in the staining intensity. Stained gels were transferred to fresh containers and foil coverings, so as to reduce background "spotting" of gels, and washed twice in 100ml solutions of 10% methanol and 7% acetic acid, for approximately 30 minutes per wash. Gels were subsequently washed extensively in ddH_2O before imaging.

Western blot detection of NC1 domains used H22 antibodies (Shigei Medical Research Institute, Okayama, Japan), which recognizes the α2 NC1 domain. Briefly, samples were resolved on non-reducing 12% Tris/Glycine gels and transferred to Immoblion FT for 2 hours at 80 V and 4˚C, in Tris/Glycine buffer with 20% methanol. Blots were subsequently blocked for 30 minutes in 5% non-fat powdered milk (Product: 170-6406, Bio-Rad Laboratories, Inc, Hercules, CA) in 1x PBS with 0.4% Tween® 20 (0.4% PBST). For the primary detection of α2 NC1, H22 was incubated with the transfer membrane for 1 hour at room temperature with rocking in 0.4% PBST. Antibodies were used one time, without reuse, at a 1:1000 dilution from a 30 μg/ml antibody stock. Following the primary antibody binding, the membrane was extensively washed overnight in 0.4% PBST at 4˚C. Primary antibody was then labeled with horseradish peroxidase-conjugated anti-rat antibodies, for 1 hour at room temperature in 0.4% PBST with rocking. After this, membrane was washed extensively in 0.4% PBST before detection of the secondary antibody with Super Signal West Pico Chemiluminescent Signal (Thermo Fischer Scientific, Rockford, IL).

Imagining and Quantification of NC1 Domains

Gels images were captured using a Molecular Imager® ChemiDoc™ XRS+ with Image Lab™ TM software (Bio-Rad Laboratories, Inc, Hercules, CA) and alternatively with an HP Scanjet 5590. Images

were processed using ImageJ software (version 1.43u, National Institutes of Health, Bethesda, MD), which was also used for all densitometry analysis. Data was plotted using Excel (Microsoft Office 2007).

Bond Formation within Matrix

Uncrosslinked collagen IV pellets were incubated at 37°C for up to 48 hours in 1x PBS, and reactions were initiated by the addition of 1 - 3 mM H_2O_2. For the experiments presented in Chapter III, peroxide concentrations were calculated by converting the 30% (w/w) concentration of stock H_2O_2 (Product: H1009-100ML, Sigma-Aldrich, St. Louis, MO) into molar units. Reactions were halted by freezing at -20°C, where they were stored until further analysis. Samples were analyzed by digestion with bacterial collagenase to solubilize the NC1, and run on 12% non-reducing SDS-PAGE gels. All Coomassie staining used R250 stain, except for gel-purifed samples prepared for mass spectrometry which were stained with Bio-Safe colloidal Coomassie blue G-250 (BioRad Laboratories; Hercules, CA).

Mass Spectrometry of Sulfilimine Bond Formation

Verification of sulfilimine bond formation was obtained with mass spectrometry using protocols modified from the literature (4). Briefly, NC1 hexamers in solution were reduced in boiling 4 M guanidine-HCl with 25 mM DTT (200 mM Tris-HCl, pH 7.5), alkylated with iodoacetamide, ethanol precipitated, resuspended in fresh ammonium bicarbonate, and digested with trypsin (sequencing grade enzyme, Promega; Madison, WI). Peptide fragments of ca. 5000 Da were isolated on a Superdex peptide column (GE Healthcare Life Sciences; Piscataway, NJ) Pooled fractions were placed in 0.1% formic acid through a process of drying and resuspension before separation on a C18 reverse phase column (20 cm, Jupiter, 3 µm, 300 Å, Phenomenex) using an acetonitrile elution gradient. Chromatography was conducted on an Eksigent NanoLC Ultra HLPC with autosampler, and eluted samples were analyzed on LTW Orbitrap XL or Velos mass spectrometers (Thermo Fisher Scientific; San

Jose, CA) with nano-electrospray ionization. Both data dependent as well as targeted methodologies were utilized, depending on the abundance of sulfilmine bonds within the sample. LC-MS was conducted at the Vanderbilt Mass Spectrometry Core.

Sulfilimine bonds were alternatively identified by mass spectrometry of dimers isolated from SDS-PAGE gel slices. Following electrophoresis using 7.5% gels in non-reducing conditions, gels were stained in Bio-Safe colloidal Coomassie Blue G-250 Stain (BioRad Laboratories; Hercules, CA), destained with ddH_2O, and dimers were identified and excised. Gel slices were submitted in 1.5 ml eppendorf tubes to the Vanderbilt Mass Spectrometry Core where they underwent trypsin digestion, elution of the peptides, and mass spectrometry analysis on an LTQ Orbitrap instrument.

Mass spectra were manually analyzed with Xcalibur software (Thermo Fischer Scientific), GPMAW ver. 8.00sr1 (Lighthouse Data; Denmark), and Excel. GPMAW was used to calculate the mono-isotopic mass of sulfilimine-containing peptides, calculated as the sum of trypically digested peptide sequences surrounding Met^{93} and Hyl^{211} minus two hydrogen atoms (1). Typical observed modifications included oxidation of nearby methionine residues, adding ca. 16 amu to the expected ion masses.

Purification of Crosslinking Activity

Uncrosslinked PFHR9 matrix was digested with bacterial collagenase (37°C, overnight) with potassium iodide (10 mM) to prevent premature crosslinking. Protein concentration steps damaged crosslinking activity, so minimal digestion volumes were utilized to ensure sufficiently concentrated activity for subsequent purification steps. Samples were reacted at 37° prior to SDS-PAGE analysis.

Digestion supernatant was dialyzed into 20mM Tris-HCl (pH 7.5) to remove residual iodide, before loading on Mono-Q column. Flow-through fractions contained collagen IV NC1 domains and were reserved for later use. Bound proteins were eluted via a 1M NaCl salt gradient and monitored by A_{280} spectra. The eluting fractions were assayed for activity by combining with aliquots of uncrosslinked

NC1 domains in the flow-through and incubating at 37°C, with SDS-PAGE monitoring for dimer formation. Fractions demonstrating activity were resolved under non-reducing conditions in a 12% SDS-PAGE gel, the gel was stained with Bio-Safe colloidal Coomassie Blue G-250 Stain (BioRad Labortories, Inc.), and the major protein band (~75 kD) was excised for further analysis at the Vanderbilt Mass Spectrometry Core. Gel slices were treted with trypsin for digestion of the contained proteins, and the resulting peptide fragments were eluted from the gel for analysis by mass spectrometry using a linear LTQ ion trap instrument.

Identification of PXDN by Mass Spectrometry using "Click Chemistry"

The identification of PXDN via "click chemistry" utilized an azide-biotin labeling of matrix heme moieties and is explained in detail elsewhere (4). Briefly, PFHR9 matrix was reacted at 37˚C for 1 hour with up to 10 mM azide and 1 mM H_2O_2 in 1x PBS. Following this reaction, the reagents were washed out in 1x PBS and the matrix solubilized in 1x PBS with 2% SDS. This material was biotinylated through a 1 hour reaction (37˚C) with 100 µM Tris[(1-benzyl-1H-1,2,3-triazol-4-yl)methyl]amine (Anaspec; Fremont, CA), 1 mM Tris(2-carboxyethyl)phosphine hydrochloride (ThermoFisher Pierce; Rockford, IL), 1 mM cupric sulfate, and 100 µM biotin alkyne. Reaction products were precipitated and washed in acetone, re-solubilized in 1x PBS with 2% SDS, and captured by streptavidin-agarose beads (GE Healthcare Life Sciences, Piscataway, NJ). Samples were reduced with 50 mM DTT by boiling in SDS-PAGE sample buffer, electrophoresed, and the prominent band (>250 kD) was excised for in-gel trypsin digest and mass spectrometric analysis. In-gel digestion and mass spectrometry was conducted by the Vanderbilt Mass Spectrometry Core, using a linear LTQ ion trap instrument for analysis.

Overlay Crosslinking Assay in Cell Culture

PFHR9 cultured with inhibited collagen IV networks were stripped of intact cells through a series of biochemical washes that lysed cell membranes with only minimal damage to the underlying matrix. Cell media was first removed, then cells were washed briefly on plate with hypotonic buffer (10 mM Tris-HCl [pH 7.4], 0.1 mM $CaCl_2$, and 0.1% bovine serum albumin [wt/v]), followed by aspiration of the buffer and the cells then incubated for 10 minutes in fresh hypotonic buffer. Plates were next underwent two successive 5 minute washes in hypotonic buffer supplemented with 1% triton-X 100 detergent (v/v), followed by two 1 minute washes in hypotonic buffer with 0.1% sodium deoxycholate (wt/v). Detergents were removed by several rinses in 1x PBS. Microscopic analysis of the resultant samples revealed decellularized matrices on the bottom of the plate, with small rounded attachments representing residual patches of plasma membranes. The decellularized matrices were subsequently treated briefly with guanidine to destroy any residual endogenous enzymatic crosslinking activity. Human cells were stably transfected to express PXDN proteins, and were plated overtop this matrix in order to deposit active, exogenous enzyme into the matrix. NC1 hexamers from the PFHR9 matrix were then isolated via biochemical treatments and collagenase digestion as above, and assessed for crosslinking by SDS-PAGE. All overlay assays were performed by G. Bhave and colleagues.

Chapter IV

THE ELEMENT BROMINE IS REQUIRED FOR ENZYMATIC CATALYSIS OF SULFILIMINE BONDS

Introduction

The historical chemistry of sulfilimine bonds includes the 1943 discovery by Lavine that iodine catalyzes the formation of dehydromethione (45). The product of this reaction is characterized by a unique covalent crosslink between the backbone amine and the thioester group, highly analogous in structure to collagen IV sulfilimine bonds with differences being mostly limited to protonation status. Unknowingly, this relationship between halides and sulfilimine chemistry foreshadowed the mechanism by which peroxidasin (PXDN) catalyzes collagen sulfilimine bond formation *in vivo*.

Mammalian heme peroxidases utilize two general catalytic mechanisms that both require initial activation via a two-electron oxidation reaction with hydrogen peroxide. At the heme moiety, the reaction with peroxide induces oxidation from the native Fe^{3+} to an $Fe^{4+\bullet}$=O state, denoted as the Compound I enzymatic state (118). From here, the catalytic pathways separate into the single-step halogenation cycle, involving a two-electron oxidation of halide ions into their hypohalous acid derivatives, and the peroxidase cycle, which is composed of two single-electron reductions of the Compound I heme, yielding radical byproducts (Figure 4.1).

In this study, the solid-state enzymology of PXDN activity was monitored in matrix by assessing the crosslinking status of collagenase-solubilized NC1 domains. Despite the limitations imposed by insoluble matrix, enzymatic activity is indeed amenable to characterizing the cofactors that are required for bond formation, here resulting in an empirical understanding of the reaction mechanism. This work defines bromide as a required reaction cofactor, previously unrecognized as an essential element in

mammalian physiology, and reveals a biosynthetic function for HOBr as the intermediate of collagen IV sulfilimine bond formation.

Results

Characterizing Bond Formation in Matrix With H_2O_2

The responsiveness of the reaction to peroxide concentrations was determined in uncrosslinked matrix. Dimer formation was enhanced up to 1 mM H_2O_2 (Figure 4.2), which is interesting in light of the suggested alternative catalase function for PXDN in lens basement membrane (107). To avoid peroxide limitations on the reaction, 1 mM H_2O_2 was therefore used for all matrix experiments. At this concentration, the time scale of PXDN crosslinking was assessed in matrix with 1x PBS and 1 mM H_2O_2. Dimer intensity increased within minutes, and continued being enriched out to 24 hours (Figure 4.3). Notable differences between the upper and lower dimer banding were detected, and will be discussed below.

Comparative reactions in Tris versus phosphate buffered saline solutions showed that the reaction progressed equally well when 1 mM H_2O_2 was supplemented into either condition. Differences were detected though in the absence of peroxide, with background dimer formation progressing significantly better in PBS than in the Tris-based system. This effect was lessened at 10 μM H_2O_2, and was not significantly different at higher peroxide concentrations. The reaction is apparently responsive to certain buffer components, and the masking of the effect in the presence of exogenous peroxide suggests that the buffer may provide an oxidant source for the enzyme. Despite the background dimer formation in PBS, phosphate buffers are more compatible for studying heme peroxidases due to the potential for enzymatic products to be quenched by amine groups in Tris bufferThe enzymology of PXDN was therefore characterized in phosphate with 1 mM H_2O_2.

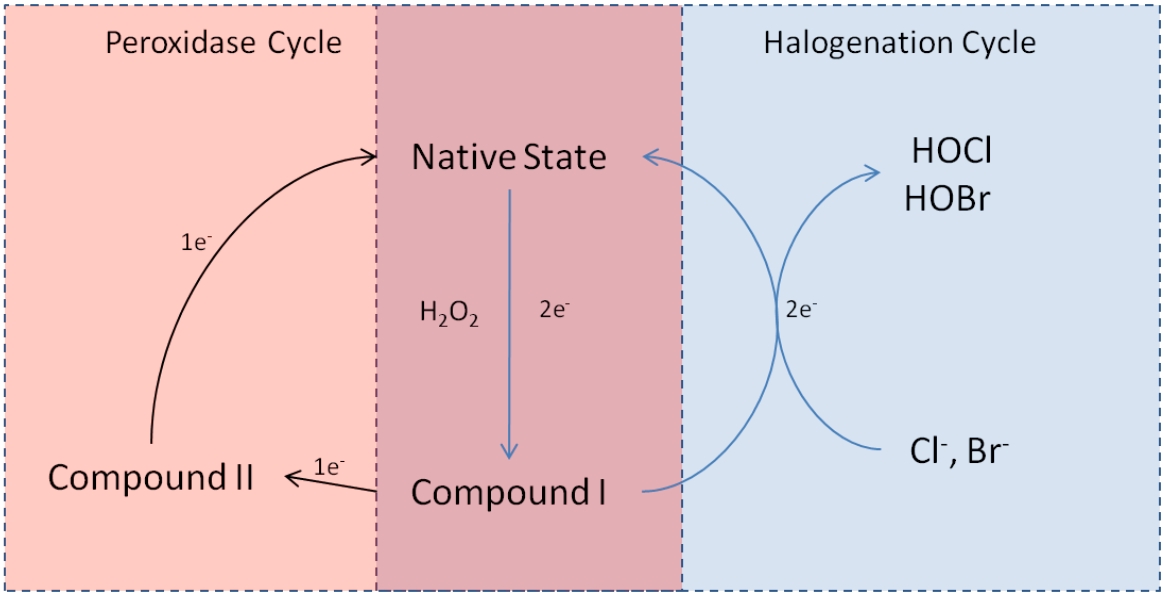

Figure 4.1: General Mechanism of Heme Peroxidases

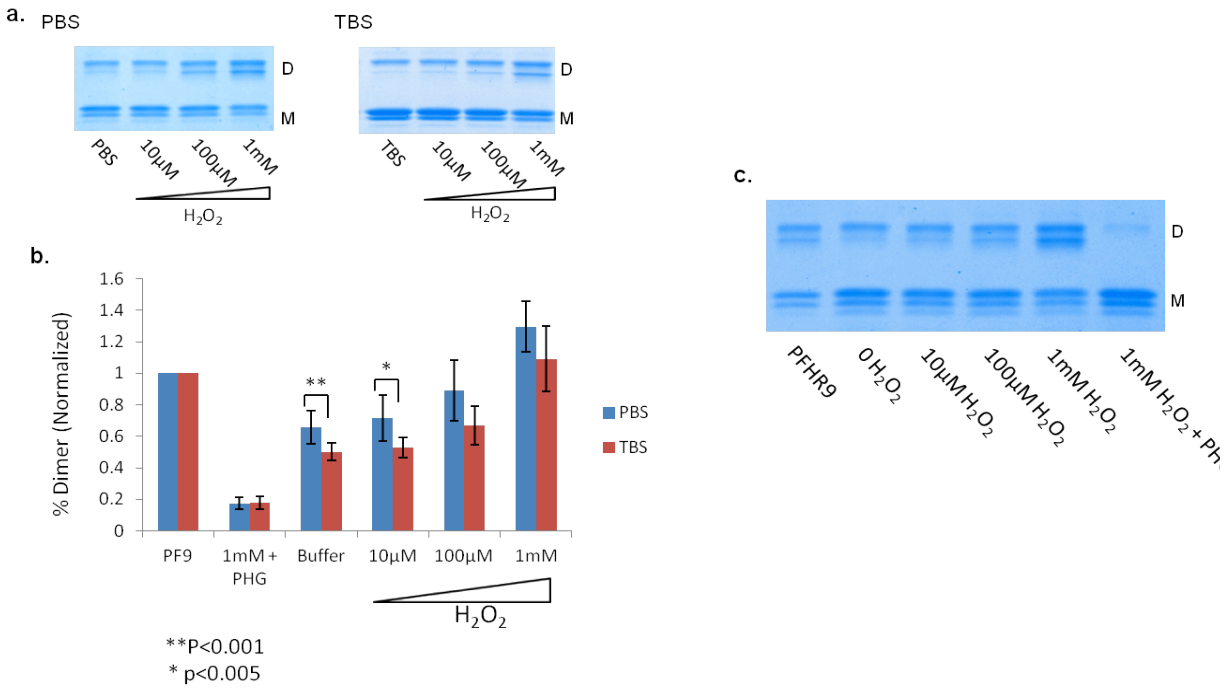

Figure 4.2: Characterizing Hydrogen Peroxide Enhancement of Matrix Crosslinking. (**a**) Up to 1 mM Hydrogen peroxide was titrated into uncrosslinked matrix samples in either 1x PBS or 1x TBS and reacted at 37˚C for 12.5 hours prior to freezing at -20˚C. Crosslinking was evaluated by SDS-PAGE using 12% gels under non-reducing conditions and visualized with Coomassie staining. (**b**) Following SDS-PAGE, densitometry analysis was conducted with IMAGEJ software and quantified in Excel. (**c**) Peroxide-enhanced crosslinking was inhibited by 200 µM PHG treatment, confirming that the reaction occurs through an enzymatic mechanism. Concentrations indicated represent final peroxide concentration. Additional protocol details are contained in the Methods section.

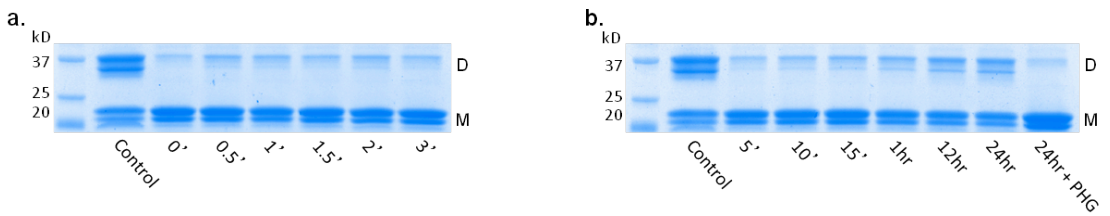

Figure 4.3: Time Course of Dimer Formation in Matrix. Uncrosslinked matrix samples were reacted in 1x PBS at 37°C for up to 24 hours. Reaction was initiated by addition of 1 mM H_2O_2. (**a**) Minimal dimer formation occurred within the first 3 minutes. (**b**) Appreciable amounts of dimer formed within 1 hour while dimer formation progressed out to 24 hours in the absence of PHG. NC1 domains were solubilized with collagenase and analyzed by SDS-PAGE using 12% gels under non-reducing conditions. Additional protocol details are contained in the Methods section.

PXDN-Bond Formation is Halide Dependent

Since general peroxidase mechanisms include a catalytic pathway that is halide-dependent, halide and thiocyanate ("pseudohalide") ions were screened in PFHR9 cell culture for their effect on sulfilimine bond formation (Figure 4.4a). Expectedly, potassium iodide inhibited bond formation at 1 mM, as did treatment with sodium iodide confirming the role of halides in this phenomenon. Thiocyanate also completely inhibited bond formation by 100 μM. In contrast, exogenous bromide enhanced the reaction at comparable concentrations, with 1 mM KBr increasing the dimer population as a proportion of the total NC1 by 52%. The reaction in culture was not significantly responsive to chloride, possibly due to interference by media chloride concentrations (115 mM), while exogenous fluoride sufficiently disrupted the metabolic activity of PHFR9 cells to prevent analysis.

Enhancement of dimer formation with bromide is notable, particularly in light of the inhibitory effects of iodide and thiocyanate, suggesting the enzymatic reaction may proceed via the halogenation cycle of PXDN which would require halide and peroxide cofactors. To directly address the putative halide requirment, matrix pellets were extensively washed in 10 mM phosphate buffer (pH 7.4), and the pellets then incubated at 37˚C in the same buffer with supplemental 1 mM H_2O_2. Surprisingly, H_2O_2 was insufficient to support PXDN catalysis of dimer formation. Crosslinking activity was restored by titration of 100mM of the potassium salts of either bromide or chloride (Figure 4.5). Thus, sulfilimine bond formation via PXDN requires two cofactors: a peroxide molecule as well as a halide ion.

Physiologic Bromide Concentrations are Sufficient Halide Source

SDS-PAGE analysis of NC1 dimers revealed discrete upper and lower crosslinked bands. Bromide enhancement of bond formation in cell culture caused a disproportional increase within the lower band

(Figure 4.6c), while lesser I^- and SCN^- concentrations were required to inhibit formation of the lower band as compared to the upper band (Figure 4.6e-f). Questioning the chemical distinction between the two bands, the reaction time course revealed that their order of appearance followed a consistent pattern with upper NC1 dimers emerging prior to the secondary appearance of lower dimer band (Figure 4.3). This suggests a hierarchical process of dimer formation as defined by initial and advanced stages of PXDN crosslinking activity, with the final reaction equilibrium being vulnerable to the presence of halide cofactors or inhibitors. Indeed among the halides, strengthening of the lower dimer band appears to be a unique mark of bromide activity. Considering the possibility of two sulfilimine crosslinks per dimer, it seems reasonable that the upper bands may contain singly-crosslinked dimers while the lower bands possess two sulfilimine bonds per dimer (Figure 4.6b).

Prior demonstration of PXDN crosslinking in matrix required 100mM of either bromide or chloride, which are inside the physiologic range of chloride yet more than 1000-fold above *in vivo* bromide concentrations. These experiments were carried out in low ionic strength conditions and matrix samples resultantly experienced noticeable compaction during halide removal, possibly adversely influencing bond formation via structural disturbances to the matrix. Thus, we repeated the reaction in 100 mM potassium fluoride to control ionic strength, yet was inert to bond formation even in the presence of 1 mM H_2O_2 (Figure 4.7). Under these conditions, bromide robustly catalyzed bond formation at 10 μM while chloride remained inactive until 100 mM, indicating that the physiologic concentration of bromide is sufficient for PXDN formation of sulfilimine bonds. Ensuring that the enhanced activity of bromide was solely via the ionic control, matrix reactions were run with sodium gluconate as an ionic control showing similar activity in physiologic bromide concentrations (Figure 4.8).

Viewing the spectrum of halogens, the effects of iodide were examined again in light of the possibility that PXDN activity may depend on the concentration of iodide. The analogous Wolf-Chaikoff

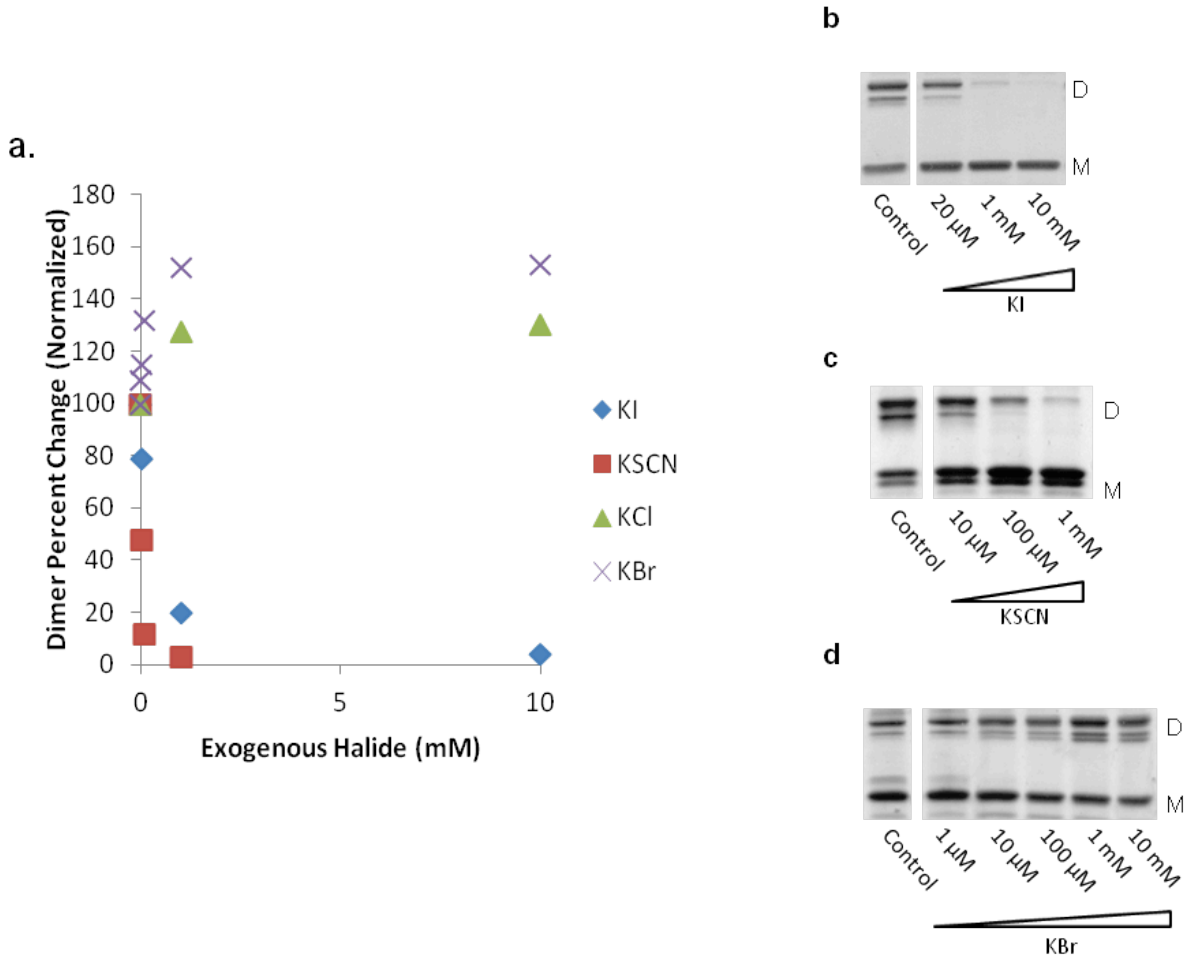

Figure 4.4: Bromide Enhances Collagen IV Sulfilimine Bond Formation in Culture. (**a**) Dimer analysis of PFHR9 matrix grown for 5-8 days in the presence of potassium halide salts and 50µg/ml ascorbic acid. NC1 domains were solubilized by collagenase, resolved by SDS-PAGE using 12% gels under non-reducing conditions, and analyzed via densitometry measurements with ImageJ software and Excel. (**b-d**) SDS-PAGE analysis revealed dimer inhibition by KI (**b**) and KSCN (**c**), while dimer enhancement was observed with KBr treatment (**d**). Additional protocol details are contained in the Methods section.

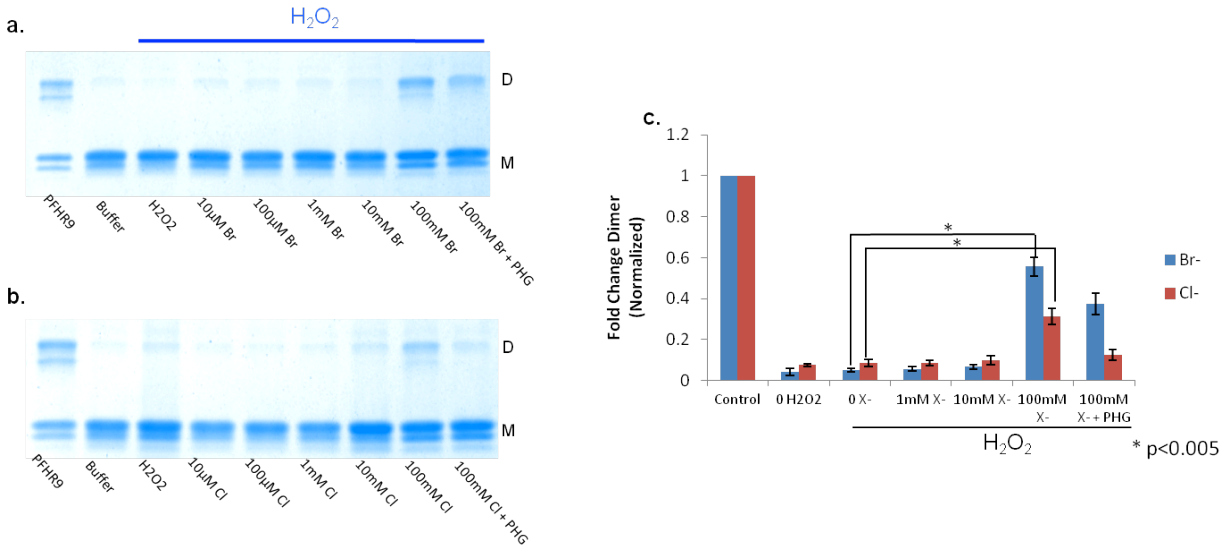

Figure 4.5: Enzymatic Dimer Formation Requires Halides. (**a-b**) To test whether halides are required for bond formation, uncrosslinked matrix was washed extensively into 10 mM phosphate buffer (pH 7.4) to remove endogenous halides from the matrix. Samples were then reacted with 1 mM H_2O_2 and increasing amounts of potassium bromide (**a**) and chloride (**b**) salts at 37°C for 1 hour. Samples were prepared for analysis by overnight digestion with collagenase, and ratios of NC1 dimers and monomers were observed by SDS-PAGE using 12% gels under non-reducing conditions with Coomassie staining. Peroxide was insufficient to sustain dimer formation in the absence of halides, while dimer formation occurred when either halide was present at 100 mM. (**c**) Densitometric analysis of gels was conducted using ImageJ software and graphed in Excel. Additional protocol details are contained in the Methods section.

phenomenon is induced by high plasma concentrations of iodide that lead to the temporary inhibition of iodide organification within thyroid tissues, though lower anion concentrations are not inhibitory (119). As such it was reasoned that PXDN might be incapable of oxidizing iodide at high micromolar and millimolar concentrations. The enzyme is indeed apparently capable of iodinating proteins *in vitro* (94). To confirm that iodide was not acting as a reaction cofactor at physiologic concentrations, the halide was added to uncrosslinked matrix samples from 1 nM to 100 µM in the presence of hydrogen peroxide, but the enzymatic reaction was unresponsive (Figure 4.7c-d).

PXDN is Selective for Bromide

To determine the relative importance between bromide and chloride, a series of dual halide experiments was designed where one of the halides was maintained at constant levels in the phosphate buffer followed by titration of the alternative halide into the reaction. In the presence of 1 mM H_2O_2 and 100 mM Cl^-, 10 µM bromide was sufficient to robustly enhance the reaction (Figure 4.9). In contrast, when bromide was maintained in the buffer at either 100 mM or 100 µM, additional chloride did not enhance the reaction even when added to a 100-fold greater concentration than bromide (100 µM Br^- plus 100 mM Cl^-). Particularly interesting, the lower dimer band was enriched during bromide titration and was coordinated with losses in both the upper dimer and monomer bands. These dual halide experiments suggest that PXDN is selective for bromide during matrix-based bond formation.

Enzymatic Formation of Collagen IV Sulfilimine Bonds Requires Bromide

During the course of experiments, ion chromatography inductively coupled plasma mass

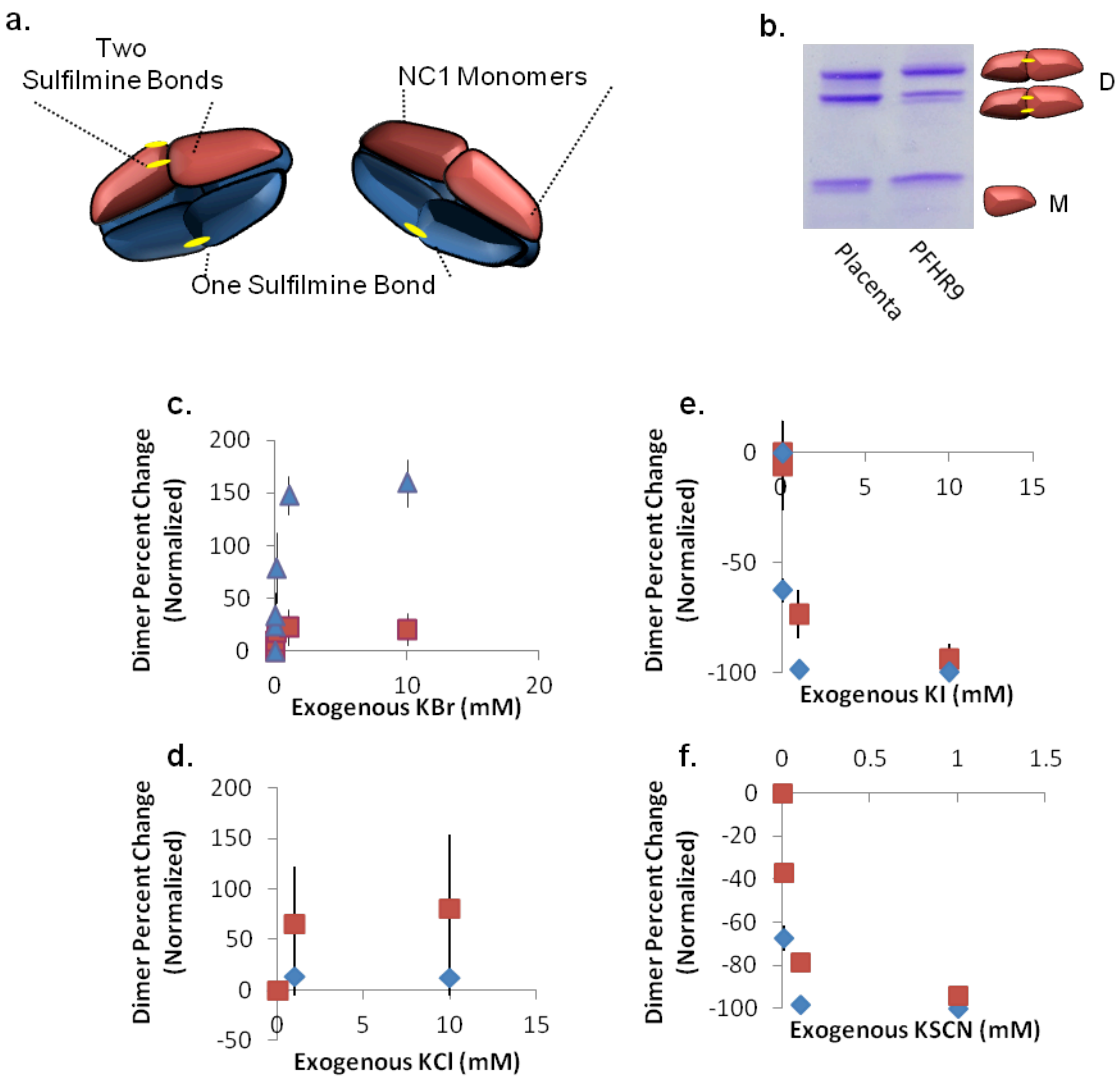

Figure 4.6: Halides Influence Collagen IV Sulfilimine Bond Formation in Culture. (**a**) Schmatic of NC1 hexamers showing monomer subunits, dimers with one sulfilmine bonds, and dimers with two sulfilimine bonds. (**b**) SDS-PAGE analysis of NC1 domains from bovine tissue PBM and PFHR9 cell matrix, solubilized by collagenase digest, displaying similar dimer and monomer banding. (**c-f**) Dimer analysis of PFHR9 matrix grown in the presence of potassium halide salts, showing lower dimer (blue diamonds) and upper dimers (red squares). NC1 domains were solubilized by collagenase, resolved by non-reducing SDS-PAGE using 12% gels, and densitometry analyzed with ImageJ software and Excel. Analysis of halide effects on upper (red) vs. lower (blue) dimer subunits in response to treatment with KBr (**c**), KCl (**d**), KI (**e**), and KSCN (**f**). Additional protocol details are contained in the Methods section.

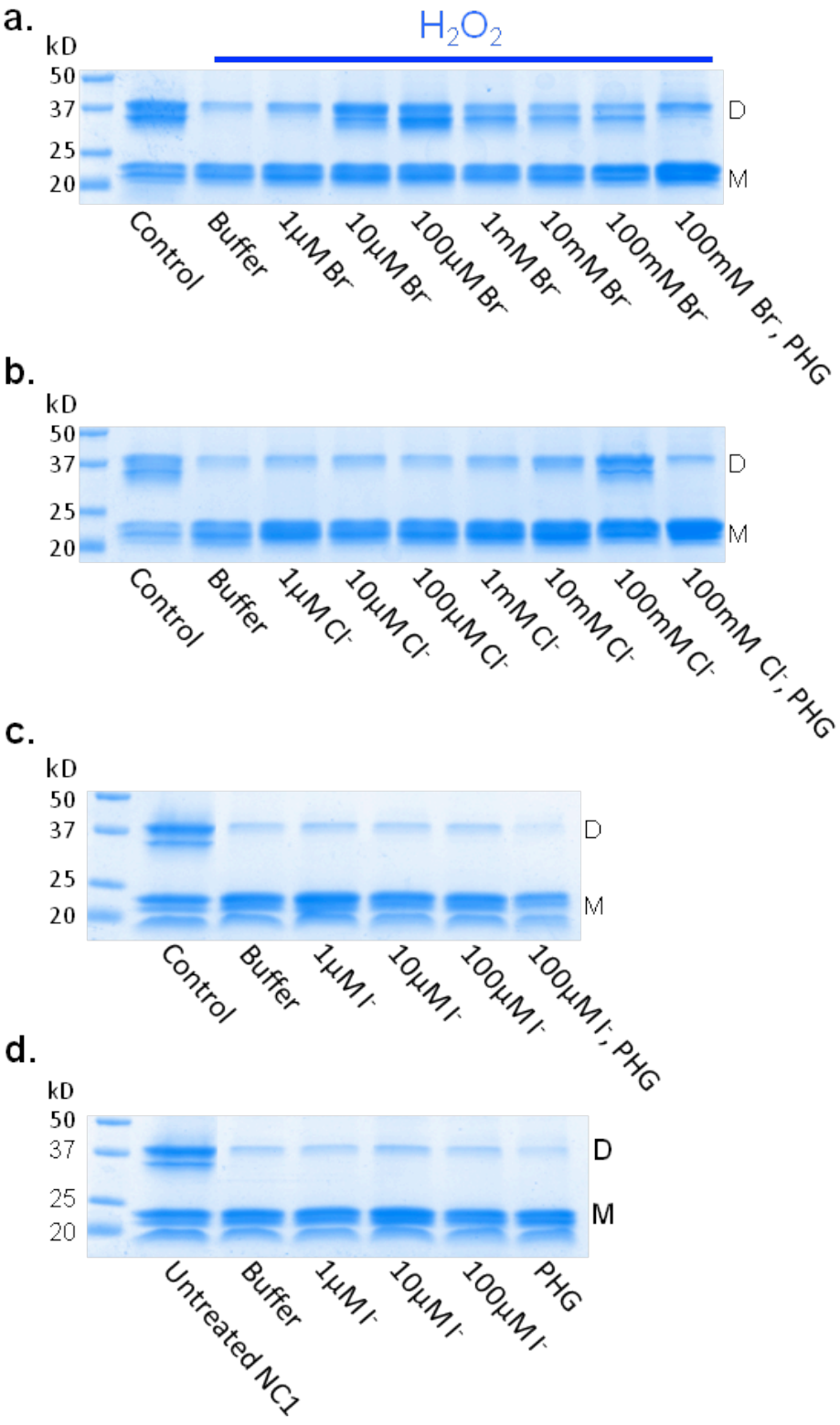
a.
H_2O_2
kD
50
37
25
20
D
M
Control
Buffer
1μM Br^-
10μM Br^-
100μM Br^-
1mM Br^-
10mM Br^-
100mM Br^-
100mM Br^-, PHG
b.
kD
50
37
25
20
D
M
Control
Buffer
1μM Cl^-
10μM Cl^-
100μM Cl^-
1mM Cl^-
10mM Cl^-
100mM Cl^-
100mM Cl^-, PHG
c.
kD
50
37
25
20
D
M
Control
Buffer
1μM I^-
10μM I^-
100μM I^-
100μM I^-, PHG
d.
kD
50
37
25
20
D
M
Untreated NC1
Buffer
1μM I^-
10μM I^-
100μM I^-
PHG

Figure 4.7 (opposite): Physiologic Bromide Concentrations are Sufficient for Sulfilimine Bond Formation by PXDN. Uncroslinked PFHR9 matrix was extensively washed into 10 mM phosphate buffer (pH 7.4) that was supplemented with 100 mM KF to maintain ionic strength. One hour reactions at 37˚C were initiated by addition of H_2O_2 to 1 mM and stopped by freezing at -20˚C. (**a-b**) Titration of KBr (**a**) or KCl (**b**) resulted in dimer formation near the human serum concentration of each. (**c-d**) KI (**c-d**) did not faciliate crosslinking at nano- (**c**) and micro-molar concentrations (**d**). Samples were digested with collagenase at 37˚C overnight and visualized by SDS-PAGE using 12% gels under non-reducing conditions with Coomassie staining. Additional protocol details are contained in the Methods section.

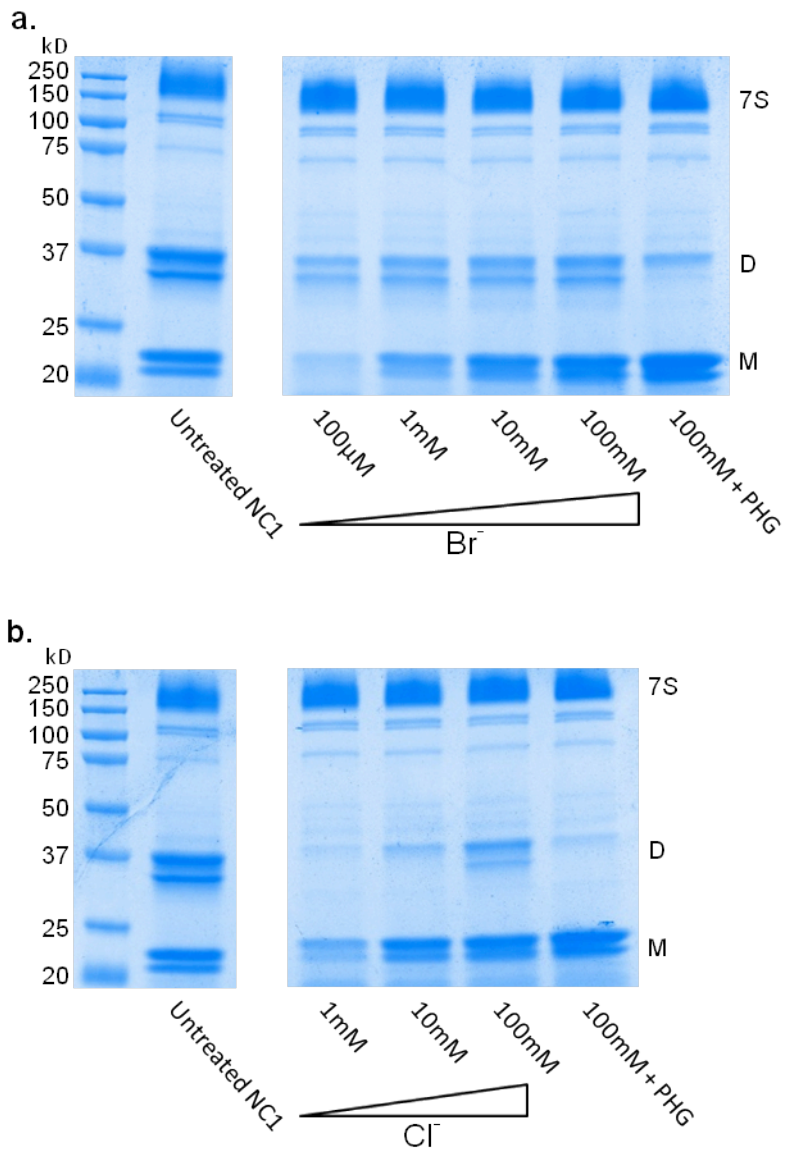

Figure 4.8: Role for Ionic Strength in Bromide-Dependent Bond Formation. Uncrosslinked matrix samples were washed extensively into 10 mM phosphate buffer (pH 7.4) containing 140 mM sodium gluconate for ionic control. Crosslinking reactions were initiated by adding H_2O_2 to 1 mM along with increasing concentrations of potassium bromide (**a**) and chloride (**b**), and incubated for 1 hour at 37˚C before placing at -20˚C. Samples were digested with collagenase at 37˚C overnight, and visualized by SDS-PAGE using 12% gels under non-reducing conditions with Coomassie staining. Additional protocol details are contained in the Methods section.

spectrometry (IC-ICP-MS) was used to assess the purity of our chloride reagents with respect to the presence of any contaminating bromide. Concern about background Br concentrations arose from the apparent ability of bromide and chloride to promote bond formation at 10 µM and 100 mM, respectively. The difference in effective concentrations is similar to the 0.01% bromide contamination within reagent potassium chloride salt, as stated in the lot analysis (Lot No. 035662, Product P217-500, Fischer Scientific). Thus, the possibility was raised whether the apparent chloride-based crosslinking was caused by bromide contamination. Indeed, upon IC-ICP-MS analysis Br^- was found to be present at 5.91 µM Br^- per 100 mM KCl and 2.35 µM per 100 mM NaCl (Table 4.1), naturally raising the question of whether crosslinking observed in matrix in experiments containing 100 mM Cl^- was due to the small amount of bromide present. To address the issue with confidence, the preferential volatilization of HCl over HBr was utilized to isolate hydrochlorous acid by gas diffusion, and HCl was subsequently captured through a condensation reaction with NaOH (Figure 4.10a) (120). This methodology generated recrystallized potassium chloride salt with Br^-:Cl^- ratios approaching 10^{-7} (<11.4 nM Br^- per 100 mM KCl or 100 mM NaCl). This purified chloride then assayed within the matrix reaction in the presence of hydrogen peroxide. Purified KCl did not support dimer formation to levels comparable with untreated controls, and similar results were also obtained using purified NaCl (Figure 4.10b-c). Crosslink formation was restored upon addition of 5 µM Br^-, to either the potassium- or sodium-based reactions, demonstrating that bromide is an essential component of enzymatic bond formation.

Iodine & Dehydromethionine Indicate Chemical Synthesis of Collagen IV Sulfilmine Bonds

Lavine's synthesis of dehydromethionine via molecular iodine was seminal for sulfilimine chemistry, opening the door for much productivity and many yet-unanswered questions. Molecular iodine, however, is relatively unstable in aqueous solutions, requiring an excess iodide anion that

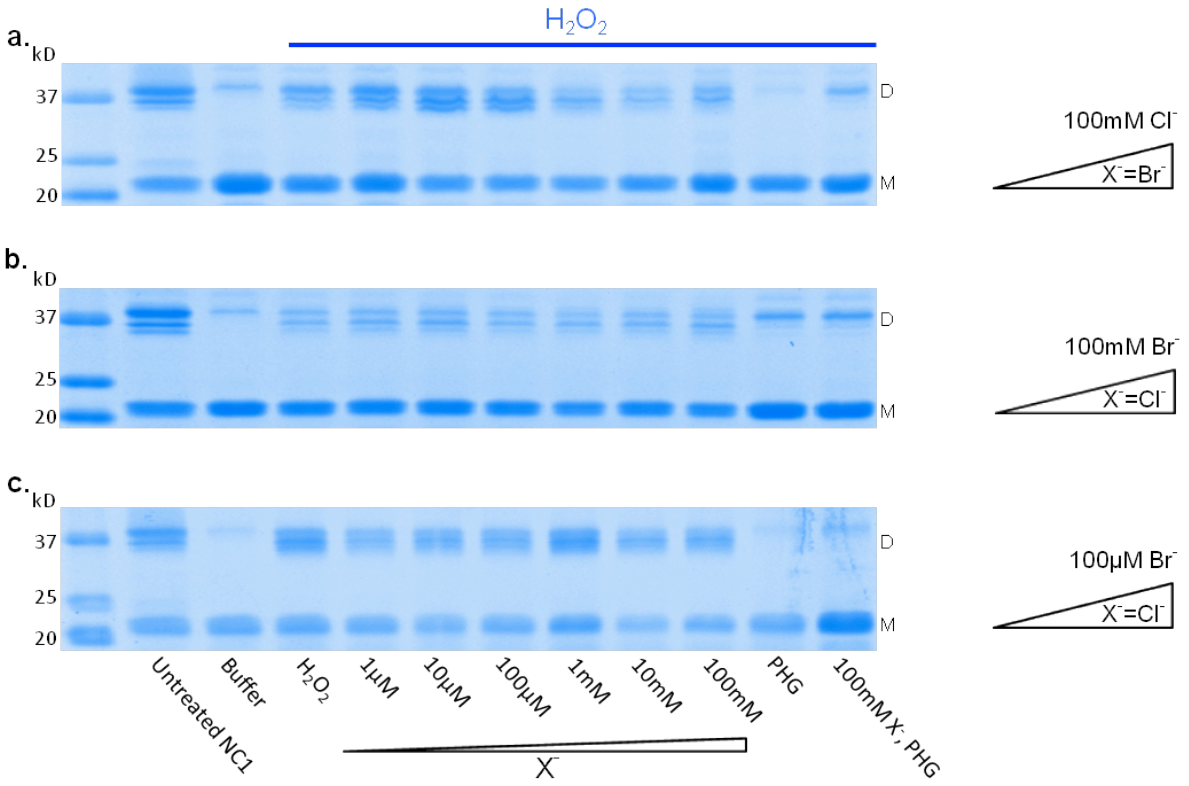

Figure 4.9: Enzymatic Bond Formation is Selective for Bromide. Uncrosslinked matrix samples were isolated and washed extensively into 10 mM phosphate buffer (pH 7.4) containing 100 mM KCl (**a**), 100mM KBr (**b**), or 100 µM KBr and 100 mM KF for ionic control (**c**). Preference for bromide was demonstrated by enhanced crosslinking occurring upon titration of KBr into the samples with 100 mM KCl (**a**) but minimal effect on the reaction when KCl was titrated into reactions containing either 100 mM KBr (**b**) or 100 µM KBr (**c**). Samples were digested with collagenase at 37˚C overnight, and visualized by SDS-PAGE using 12% gels under non-reducing conditions with Coomassie staining. Additional protocol details are contained in the Methods section.

Sample	Bromide	
	µg/L	nM
1xPBS	521	6520
1xTBS	510	6380
10mM KBr	$1.1x10^6$	$13.77x10^6$
100mM KCl (reagent grade)	472	5907
100mM NaCl (reagent grade)	188	2353
10mM Phosphate buffer (pH 7.4)	<4.6	<57.57
H_2O (Millipore)	<4.6	<57.57
100mM KI	5.32	66.6
100mM KSCN	67.3	84.2
100mM KF	5.60	70.1
100mM KCl (pure)	<0.91	<11.4
100mM NaCl (pure)	<0.91	<11.4

Table 4.1: Determination of Bromide Contamination in Reaction Buffers. Reagent grade chloride salts are significant sources of bromide, as determined through ion chromatography inductively coupled plasma mass spectrometry by Applied Speciation and Consulting, LLC. (Bothell, WA). Reagent grade KCl and NaCl were both assayed at 10 mM concentrations, and the results were used to calculate the bromide contamination. Additional protocol details are contained in the Methods section. Performed in collaboration with G. Bhave.

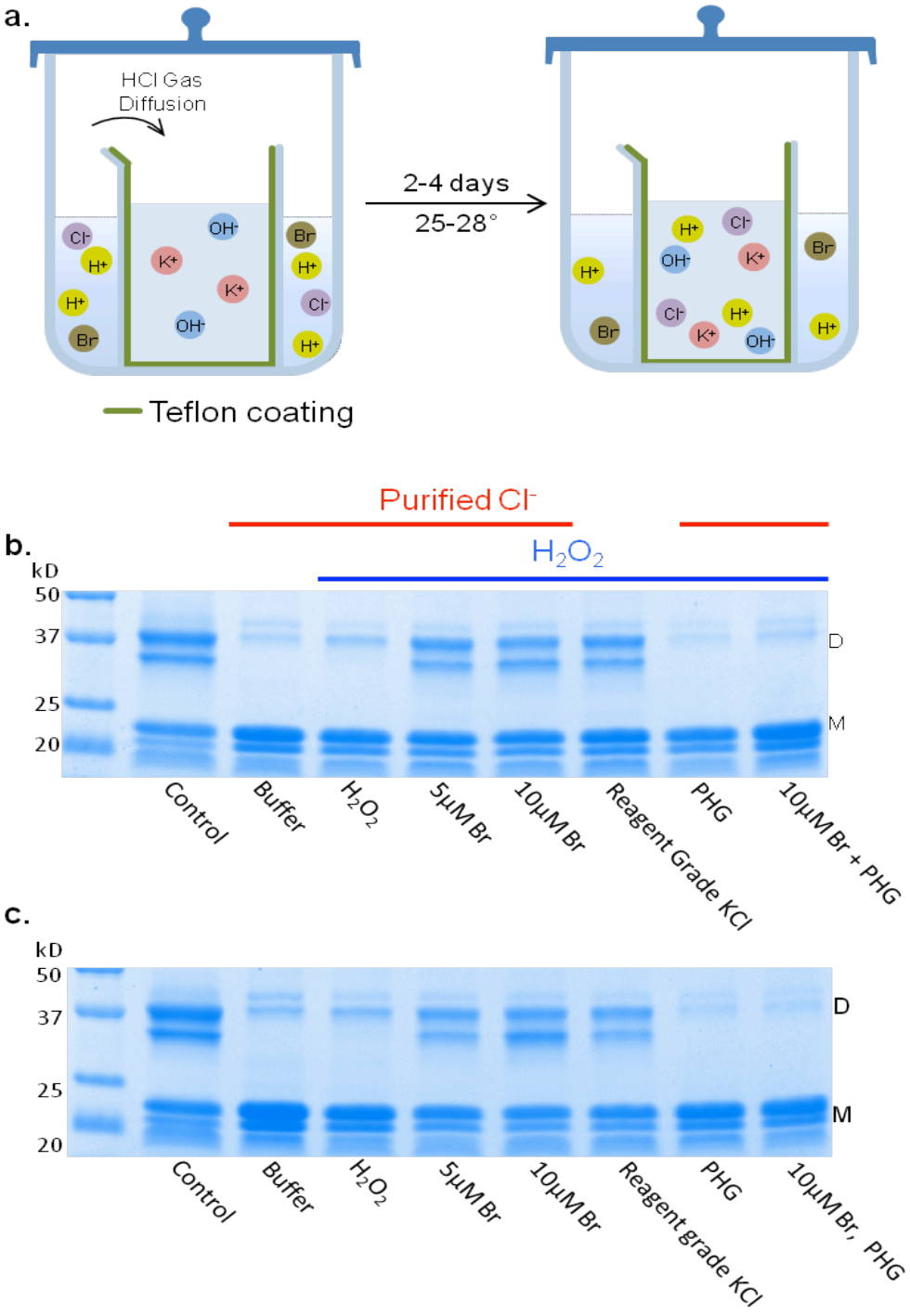
a.
HCl Gas Diffusion
2-4 days
25-28°
Teflon coating
b.
Purified Cl-
H2O2
kD
50
37
25
20
D
M
Control
Buffer
H2O2
5μM Br
10μM Br
Reagent Grade KCl
PHG
10μM Br + PHG
c.
kD
50
37
25
20
D
M
Control
Buffer
H2O2
5μM Br
10μM Br
Reagent grade KCl
PHG
10μM Br, PHG

Figure 4.10 (opposite): Bromide is Required for Sulfilimine Bond Formation by PXDN. (**a**) Purification of chloride salt was based on the preferential volatilization of HCl over HBr. Thus, reagent grade HCl with contaminating HBr was placed into a customized, sealed chamber (Adams & Chittenden Scientific Glass, Berkeley, CA) that separated the acid from a solution of 50% potassium hydroxide (w/w). Selective diffusion of molecular HCl was allowed to occur between 25-28˚C until the inner caustic solution was neutralized. This chloride-containing liquid was concentrated by boiling, followed by drying under vacuum filtration. The final salt was assessed for pH and residual bromide contamination (Applied Speciation and Consulting, LLC, Bothel, WA) prior to testing within the matrix enzymatic assay. (**b**) In the presence of 1 mM H_2O_2, samples were assayed in highly pure potassium chloride, highly pure chloride plus supplemental Br^-, and unrefined chloride. Robust crosslinking only occurring in samples containing either supplemental or contaminating Br^-. (**c**) Similar results were also obtained using purified sodium chloride. Reaction buffers contained 10 mM phosphate buffer (pH 7.4), 100 mM pure Cl^-, in addition to 1 mM H_2O_2 and 200 µM PHG where appropriate. Samples were digested with collagenase at 37˚C overnight, and visualized by SDS-PAGE using 12% gels under non-reducing conditions with Coomassie staining. Additional protocol details are contained in the Methods section. Performed in collaboration with A.S. McCall and G. Bhave.

combines with I_2 to yield the soluble compound I_3^-. The complexity of this solution is further increased by the competing hydrolytic reaction of iodine to form HOI (Figure 4.11a). Confirmation that catalysis occurs via HOI was obtained by formation of the reagent through a transhalogenation reaction with hypochlorite at high pH, its immediate incubation with methionine, and identification of the dehydromethionine product via liquid chromatography MS^2 (46).

Due to the analogous covalent strucures underlying dehydromethionine and collagen sulfilimine bonds, the potential for chemically catalyzing NC1 dimer formation was explored using similar complex solutions of molecular iodine. At 1 mM iodine, monomeric NC1 domains were crosslinked into dimers as observed by SDS-PAGE (Figure 4.11b). Dimer formation was examined using NC1 hexamers obtained from cell culture as well as from tissue. Furthermore, using collagenase digest supernatant, dimers formed in the presence of PHG, catalase, or EDTA, indicating that the reaction is purely chemical rather than enzyme-mediated. The effect was not observed with either 1 mM IO_3^- or IO_4^-.

Biosynthetic Role of HOBr in Sulfilimine Bond Formation

During the *in vivo* formation of collagen sulfilimine bonds by PXDN, the enzymatic usage of bromide implies that HOBr may be a critical reaction intermediate. To test the hypothesis that PXDN utilizes this oxidant to biosynthesize collagen sulfilimine bonds, *in vitro* crosslinking experiments were conducted by reacting hypohaous acids with uncrosslinked NC1 hexamers in isolation. A panel of hypohalous acids as well as hypothiocyanous acid, which is widely available biologically (121), was thus examined. Hypohalous derivates of bromide (HOBr), chloride (HOCl), iodide (HOI), and thiocyanate (HOSCN) were added to 5 μM of purified uncrosslinked NC1 hexamers. HOBr efficiently formed dimers even at parity with NC1 concentrations, while 50 μM HOCl or HOI were required to catalyze dimer formation (Figure 4.12c). Since the oxidant species were each synthesized from reagent hypochlorite (122), creating potential interhalogen products (123), HOBr was alternatively generated by

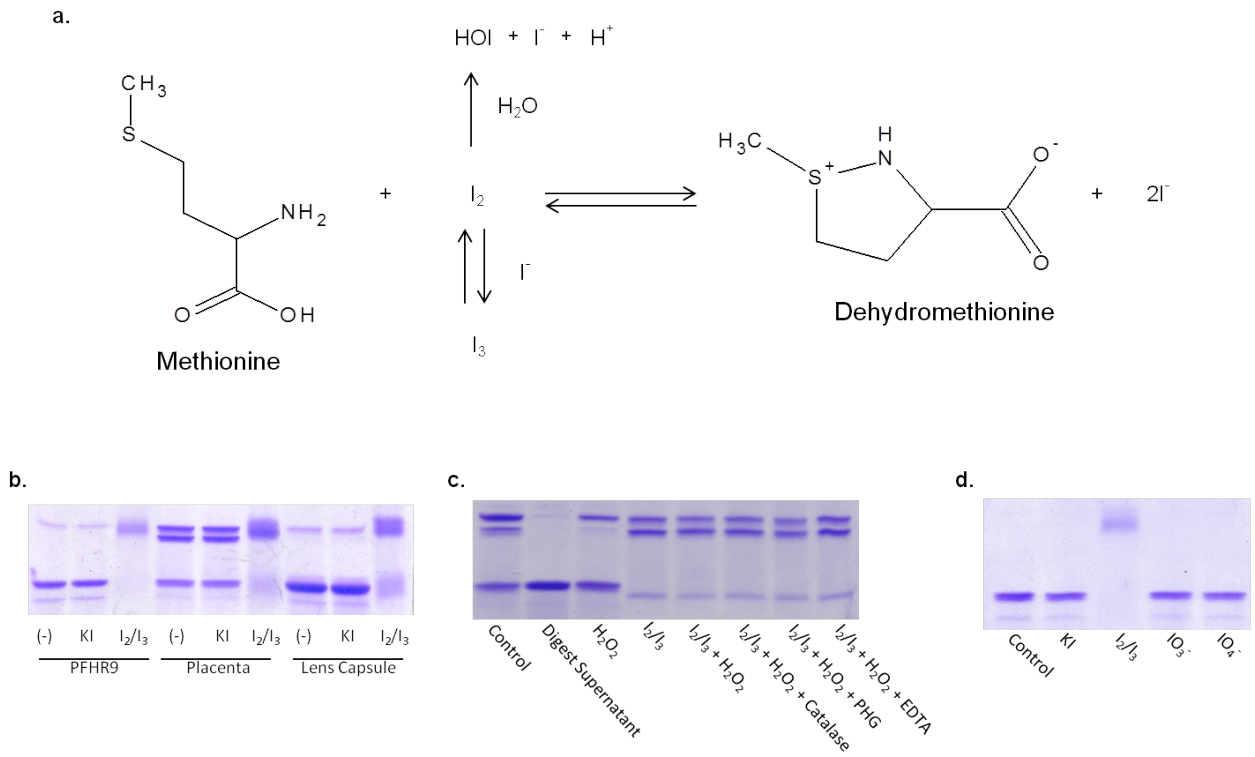

Figure 4.11: Oxidized Iodine Catalyzes the Chemical Formation of Sulfilimine Bonds. (**a**) Generalized reaction schematic of dehydromethione formation from methionine and molecular iodine, including alternative oxidized iodine species that are present in equilibria with I_2/I_3. (**b**) Molecular iodine was added to NC1 hexamers isolated from PFHR9 cells, placental basement membrane, and lens basement membrane yielding robust dimer formation from all three sources. (**c**) Using supernatant from PFHR9 collagenase digest containing NC1 hexamer and PXDN, I_2/I_3 catalysis of dimer formation was not sensitive to the supplemental addition of peroxide, catalase, PHG, or EDTA. (**d**) Dimer formation was not observed with the species IO_3^- or IO_4^-. Samples were digested with collagenase at 37˚C overnight, and visualized by SDS-PAGE using 12% gels under non-reducing conditions with Coomassie staining. Additional protocol details are contained in the Methods section.

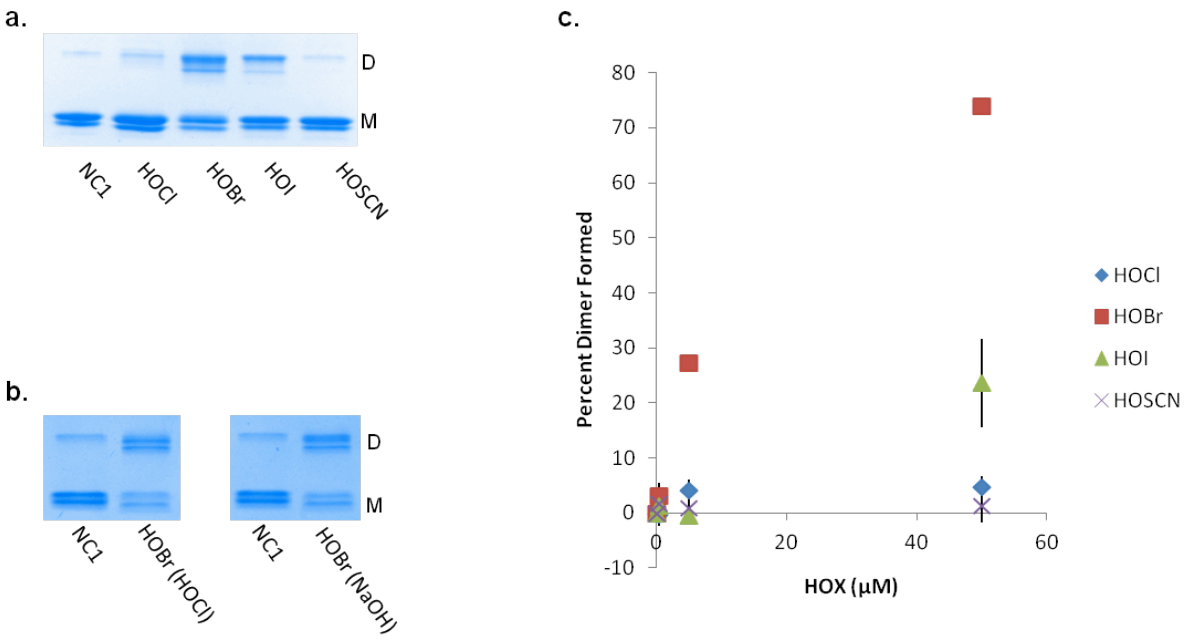

Figure 4.12: HOBr Forms NC1 Dimers. (**a**) Fifty micromolar of hypohalous oxidants were added to 5 µM uncrosslinked NC1 domains, and reacted for 5 minutes at 37˚C before quenching by adding L-methionine to 1 mM final concetration. HOBr, HOI, and HOSCN were each synthesized through a 1 minute reaction at room temperature with hypochlorite at pH >10 where the starting (pseudo)halide anion concentration was present in small excess, followed by dilution to the working concentration at pH 7.4. (**b**) Reagent HOBr was alternatively synthesized dissolving molecular bromine (solid) in of sodium hydroxide with the hydroxide concentration in molar excess of the final bromine concentration, and this product was termed "HOBr(NaOH)". HOBr generated from both synthetic pathways was reacted with uncrosslinked NC1 domains as in panel a. (**c**) Five micromolar of purified uncrosslinked NC1 domains was reacted for 5 minutes at 37˚C with the increasing amounts of hypohalous acids before quenching by adding L-Met. All samples were visualized by SDS-PAGE using 12% gels under non-reducing conditions with Coomassie staining. Densitometry was performed in ImageJ and analyzed in Excel. Additional protocol details are contained in the Methods section.

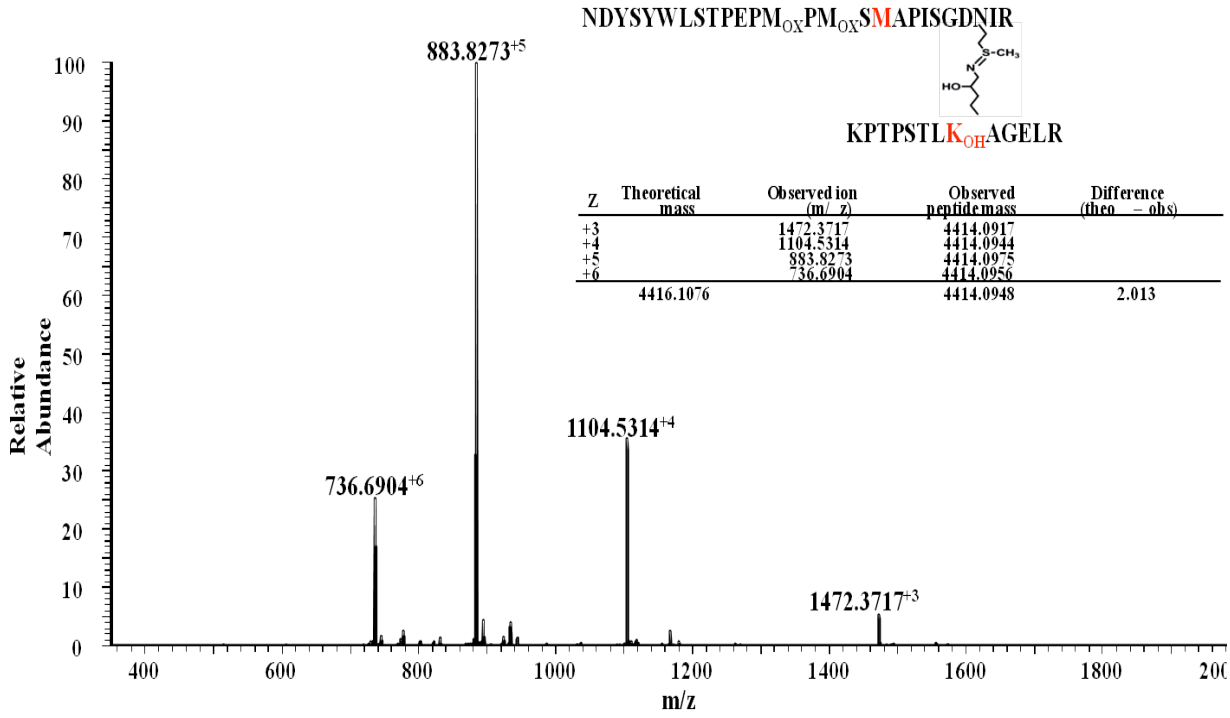

Figure 4.13: HOBr Catalyzes *In Vitro* Sulfilimine Bond Formation within NC1 Hexamers. Uncrosslinked NC1 hexamers were reacted with HOBr, with dimer formation monitored by SDS-PAGE. The reacted material was tryptically digested and analyzed by mass spectrometry to test whether sulfilimine crosslinks had been catalyzed. This representative spectrum shows +6, +5, +4, and +3 ions with an average mass of 4414.0958. The detected peptide mass is 2.013 amu less than the theoretical mass of the sum of the two polypeptide sequences, indicating that sulfilimine bonds are indeed present. M_{OX} represents methionine sulfoxide. Additional protocol details are contained in the Methods section. In collaboration with M. Rafi and R. Vanacore.

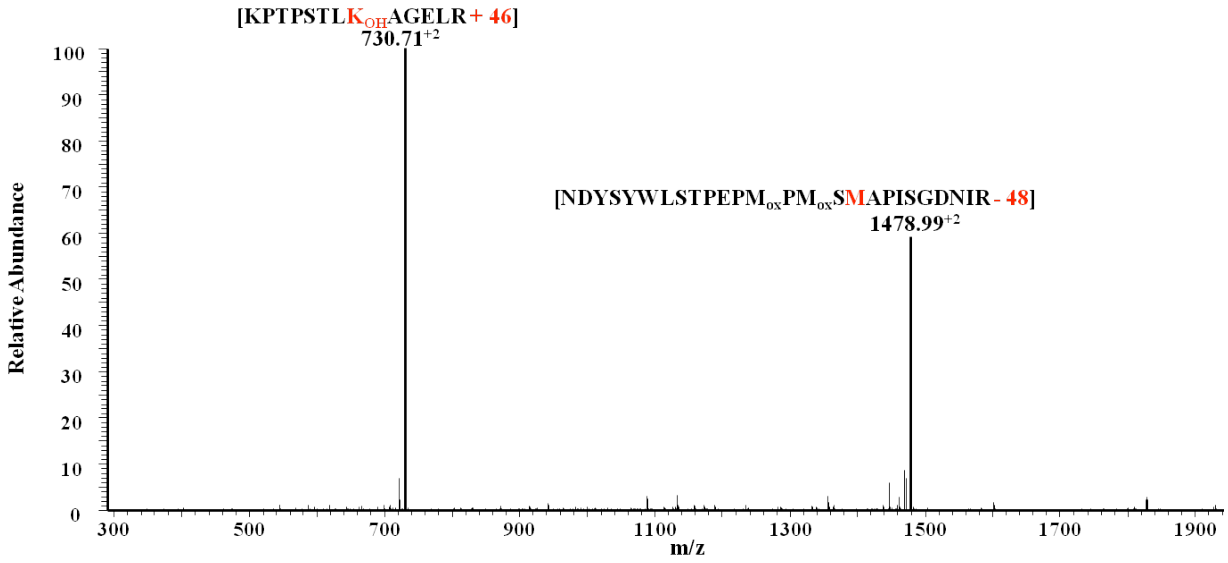

Figure 4.14: Mass Spectrometry Detection of Collision Induced Daughter Ions from HOBr-Catalyzed NC1 Sulfilimine Bonds. MS^2 analysis was performed on the m/z 883.8273 ion from HOBr-reacted NC1 hexamers. The peak was fragmented by CID into two main daughter ions, an m/z 730.71 ion as well as an m/z 1478.99 ion. The mass of the first ion corresponds to the hydroxylysine-containing peptide plus 46 amu, while the latter corresponds to the methionine containing peptide minus 48 amu. In turn, the 46 and 48 amu differences correspond to the expected products resulting from cleavage of the methionine side chain in a "Cope elimination" reaction (1), which is further evidence of sulfilimine bonds. M_{OX} stands for methionine sulfoxide. Additional protocol details are contained in the Methods section. In collaboration with M. Rafi and R. Vanacore.

adding molecular bromine to sodium hydroxide (124). Even in this more purified form, HOBr robustly formed dimers (Figure 4.12b). In sum, bromide is a sufficient halide source and HOBr is the most efficient hypohalous reagent for collagen IV sulfilimine bond formation.

Finally, confirmation that hypohalous acids produced sulfilimine crosslinks was obtained via mass spectrometry. HOBr- and HOCl reacted NC1 hexamers were digested with trypsin, and the resultant peptides were purified by gel filtration using a Superdex peptide column (GE Life Sciences, Piscataway, NJ). Peptides were analyzed by LC-FTMS for evidence of sulfilimine bond formation, using an LTQ Orbitrap mass spectrometer (Thermo Fischer Scientific; San Jose, CA). LC-FTMS spectra revealed +3, +4, +5, and +6 ions that corresponded to the sulfilimine crosslinked tryptic peptide (Figure 4.13), and this was further verified by identification of the daughter ions following collision induced dissociation (CID) MS^2 (Figure 4.14). Thus, NC1 sulfilmine biochemistry is chemically catalyzed by bromide.

Discussion

Bromide ions are required for collagen IV sulfilimine bond formation, being oxidized by PXDN into its catalytic form of HOBr. The magnitude of this finding is only truly appreciated by independently considering the requirement for this specific halogen as well as the biosynthetic activity of the oxidant. On the one hand, the element bromine has lacked any essential function within animals prior to this discovered sulfilmine-activity. Certainly, bromide activity is well documented in mammals though its function is either ambiguous (7) or associated with non-productive oxidation of proteins and lipids (122, 118). Furthermore, its biologic relevance is often overshadowed by the significantly greater serum chloride concentration and the chemical reactivity of thiocyanate. On the other hand, hypohalous acids are commonly described for their capacity as destructive oxidants; useful within the immunologic toolkit but pathologic when unregulated as seen in atherosclerosis. The anabolic activity of HOBr during sulfilimine catalysis is partially analogous to the activity of oxidized iodide during thyroid hormone

synthesis. Yet structural analysis of the products reveals an iodinated hormone that contrasts with the non-halogenated sulfilimine bond, strongly suggesting the utilization of distinct chemistry. In sufilimine bond formation, Br^- acts as a chemical catalyst and hypobromous acid the reactive intermediate.

Non-Bioequivalency of Halides in Matrix

The complexity of halide effects on matrix is exemplified by the dichotomous observations that ionic iodide inhibits the enzymatic reaction while HOI is a chemical catalyst of sulfilimine bond formation. Furthermore, HOI is the preferred reagent for dehydromethionine formation (Table 4.2) while HOBr is the superior catalyst of NC1 sulfilimine crosslinking. Thus, collagen sulfilimine chemistry is bound by constraints originating within the mechanistic profile of PXDN, chemical differences among halogens, and unique properties of the hexamer.

The enzyme is reported to generate HOBr as its major product, with HOCl and HOSCN in minor yields (4, 125), and the initial characterization of PXDN mentioned its ability to radio-iodinate extracellular proteins (94). Matrix reactions of sulfilimine crosslinking lend support to the abundant production of HOBr by PXDN, yet contradict the use of iodide as a halide cofactor. One explanation is that the kinetics of iodide oxidation by PXDN are insufficient for collagen sulfilimine crosslinking yet still detectable by the enhanced sensitivity of an autoradioactivity assay. Alternatively, it is also plausible that this discrepancy is based on differing activity profiles for the purified enzyme and its matrix-embedded form.

The variations among halogens and their effects on sulfilimine biochemistry can be seen in isolation within dehydromethionine literature. A particularly useful diagnostic for the efficiency of formation is the measurement of sulfoxide products (-S(O)=N- and -S(O_2)=N-), which compete with dehydromethionine as the reaction end point (126) and may function biologically in protecting against oxidative stress (127). By this metric, a literature review of hypohalous reactions with methionine show

that increasing electronegativity and atomic radii lead to enhanced sulfoxide levels with corresponding decreases in dehydromethionine and is also seen with haloamine reagents (Table 4.2). Oxidized iodide catalyzes the near exclusive formation of dehydromethionine, while the risk of sulfoxide synthesis is enhanced when HOCl is used in place of HOBr. In contrast to the linear relationship observed for dehydromethionine, the efficiency of collagen sulfilimine formation is biphasic across the halogen spectrum, peaking at bromide while declining with chloride or iodide.

An Essential Role for Bromide in Tissue Stability

The discovery that sulfilimine bond formation requires bromide gives fresh relevance to the biologic importance of the halide. In mammals, the anion performs many redundant functions alongside other halides such as chloride and thiocyanate ("pseudohalide"). Serum concentration of chloride overshadows that of bromide, though the immune peroxidase eosinophil peroxidase (EPO) does indeed utilize bromide as a cofactor (128), as does myeloperoxidase (MPO) to a lesser extent (129). In spite of its presence, however, any physiologic requirement for Br^- has been overshadowed to date by the competing chemistry of thiocyanate as well as functional overlap with HOCl in immunology.

Bromide is a major halide cofactor for mammalian EPO during immune responses, although thiocyanate is reportedly oxidized between 2.8- and 5.3-fold more rapidly than bromide (128, 130). As part of the immune response of activated eosinophils, EPO produces hypohalous and hypothiocyanous acids by oxidation of the corresponding "pseudo"-halide ions, and mice deficient in the enzyme display enhanced vulnerability to helminth infections (131). The involvement of bromide as an immunologic defense against helminths is only implied, however, and balanced by the enzymatic oxidation of thiocyanate.

The functional distinction between EPO-generated oxidants *in vivo* is further blurred by the extremely rapid reaction between thiocyanide ions and either HOBr or HOCl (118). Indeed, physiologic concentrations of SCN^- are sufficient to allow the possibility that a significant amount of the endogenously produced HOBr is converted to HOSCN (5, 121).

Physiologic bromination indeed occurs, despite the activities of competing halides, though it is difficult to define an essential function for the ion aside from sulfilimine bond formation. The endogenous neuropeptide B is a brominated ligand of the G protein-coupled receptors GPR7 & GPR8 (6), yet non-halogenated analogues possess similar *in vitro* and *in vivo* functional activity as the tissue-derived brominated peptides (7). 5-Bromouracil is a widely used mutagen (132, 123), demonstrating a pathological biologic function for the halogen at the genomic level. In asthmatic patients, EPO-Br activity has been implicated within the mechanism of disease as allergen-challenge leads to degranulated eosinophils and elevated levels of 3-bromotyrosine in brochoalveolar lavage fluids (8).

Aside from EPO, bromide is capable of being oxidized by other heme peroxidases (129, 133, 134) and its usage by MPO is particularly interesting within a physiological context. Enzymatic processing of bromide supersedes chloride, with second order rate constants of 1.1 (±0.1) $x10^6$ M^{-1} s^{-1} for bromide and 2.5 (±0.3) $x10^4$ M^{-1} s^{-1} for chloride (134). Measuring H_2O_2 consumption in 100 µM Br^- and 140 mM Cl^-, HOBr production rises from ca. 10% of MPO activity at pH 7.0 to ca. 40% at pH 7.8, demonstrating a clear pH dependence leading Senthilmohan and Kettle to conclude that "[a]bove pH 7.0, hypobromous acid is a major product" of MPO (129). Finally, a transhalogenation reaction has been postulated to further involve bromide whereby the MPO product OCl^- oxidizes Br^- to form the interhalogen BrCl and OBr^- (123).

Catalyst	Target Molecule	Dehydromethionine (%)	MetO (%)	Ref.
HOCl	Methionine	44	56	48
	Methionine	21 (3)	79 (3)	46
TauCl	Methionine	44	56	48
	Methionine	15 (3)	85 (3)	46
TauCl2	Methionine	43	57	48
HOBr (HOCl)	Methionine	74	26	48
	Methionine	46 (6)	54 (6)	46
HOBr (NaOH)	Methionine	78	22	48
TauBr	Methionine	77	23	48
	Methionine	64 (0)	36 (0)	46
TauBr2	Methionine	76	24	48
HOI	Methionine	100	0	46
I3	Methionine	97	3	48

Table 4.2: Efficiency of Dehydromethionine Formation with Respect to Halide Oxidant The efficiency of dehydromethionine formation is inversely proportional to the radii and electronegativity of the halogen, where oxidized iodine is most efficient while chloride is least among the three. Accordingly, risk of sulfoxide formation increases along with radii and electronegativity so that catalysis with chlorine species leads to the highest percentage of sulfoxides.

Unequivocally, bromide is essential for collagen sulfilimine bond formation via PXDN activity. The importance of this role may be observed in nematodes and *Drosophila* organisms possessing non-functional PXDN analogues that display unstable basement membranes and tissues (103, 4). Thus, bromide is remarkably distinguished among halides as catalyzing the formation of a fundamental component of tissue stability, bringing a form of closure to the question of its role within mammalian biology. Considering the subtle complexities of bromide usage by MPO, the requirement for bromide during collagen IV network formation becomes a precedent for revisiting prior assumptions of its redundancy as a halide within biology.

Bromide Oxidation by PXDN

Rationale for the relative abundance of HOBr production by PXDN may be derived from a structure-function analysis of MPO, focusing attention on the Met^{243} residue which forms a covalent sulfonium ion linkage with the heme pyrrole A ring (135). Mutation of corresponding residues present in other mammalian peroxidases strongly reduced chlorination activity (135), demonstrating its influence on the peroxidase halogenation cycle. Using an MPO-cyanide complex as an analogue of compound I, crystallographic studies of the complex with bound Br^- do not reveal any halide interactions of Met^{243}, though neighboring Glu^{242} and Arg^{239} both have Cγ atoms positioned 3.8 Å from Br^- (136). The sulfonium ion linkage between Met and pyrrole A results in a distortion of the heme planar orientation, and thus may influence halogenation via its effect on the redox properties of compound I (137). With regard to PXDN, the enzyme notably lacks Met at this position, providing justification for its poor chlorination ability (98).

Further consideration of the halogenation profile of PXDN with respect to bond formation in

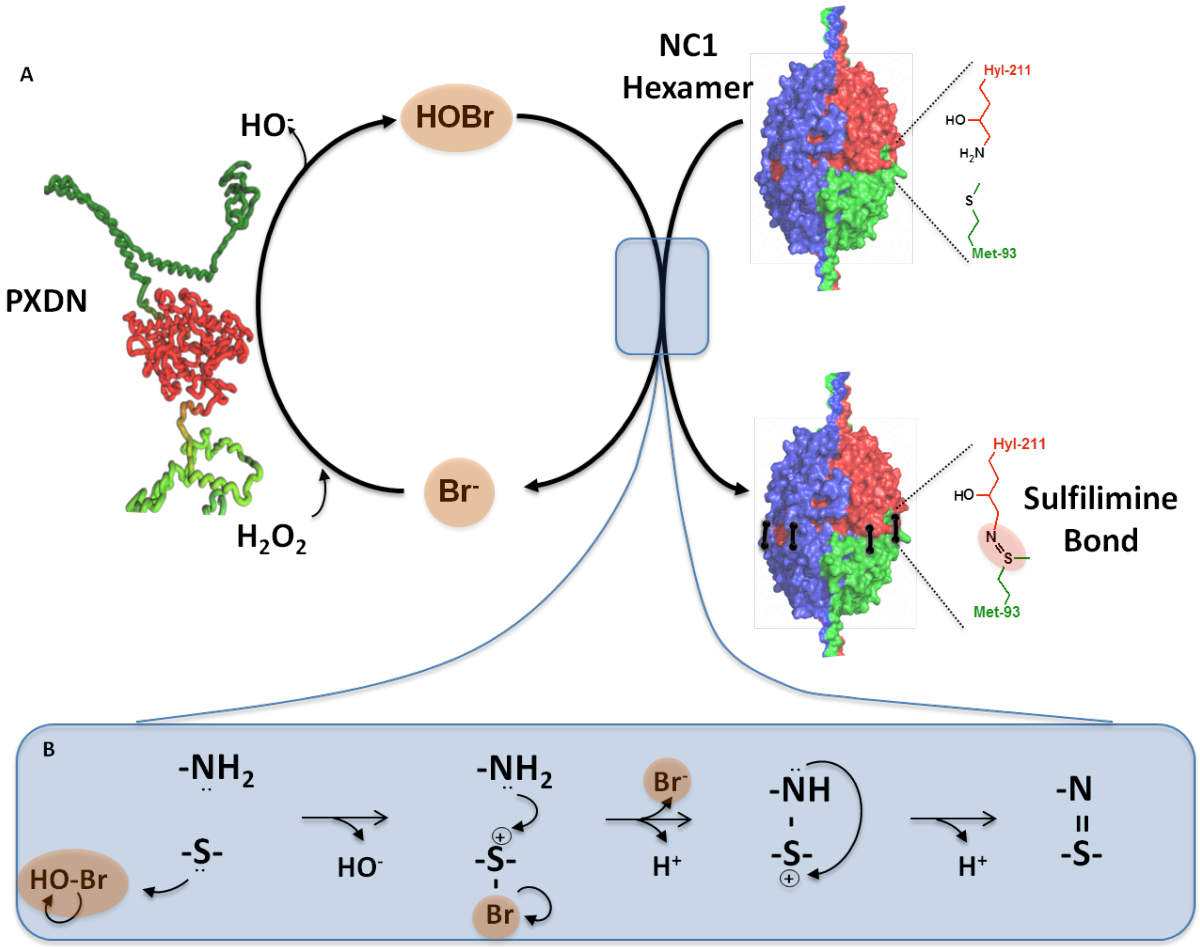

Figure 4.15: Proposed Mechanism of Sulfilimine Bond Formation via HOBr

matrix suggest the enzyme might be relatively inefficient at oxidizing ionic iodide. Oxidized iodide is very capable of catalyzing sulfilimine bond formation, yet repeated attempts have failed to demonstrate catalysis using iodide as a cofactor for PXDN. As a general rule, heme peroxidases can be defined by the most electronegative halide they oxidize while the lesser electronegative anions are more easily utilized (137, 138). Thus, for PXDN to perform bromination but not iodination would indeed be a notable characteristic.

Mechanism of Collagen Sulfilimine Bond Formation via HOBr

Considering the fundamental chemistry of thioethers and primary amines, both HOBr and HOCl possess similar patterns of reactivity in that thiols are the preferred functional target, yet the kinetics vary widely between the hypohalous reagents. With respect to the second order rate constants for reactivity with Met, HOCl proceeds at ca. $3x10^7$ M^{-1} s^{-1} and HOBr at $4x10^6$ M^{-1} s^{-1} (118). Primary amines interestingly favor reaction with HOBr, at $3.6x10^5$ M^{-1} s^{-1} with the ϵ-N of Lys compared to ca. $5x10^3$ M^{-1} s^{-1} for the same reaction with HOCl (118). Turning to collagen sulfilimine bond formation, it is unclear if the reaction mechanism encounters any steric hinderance by either the hexamer structure or the enzyme-substrate complex. In the absence of empirical evidence, the kinetic reactivity of HOBr suggest that collagen sulfilimine bond formation initiates with the bromination of Met^{93} creating a positively charged bromo-sulfonium ion. Sulfilimine bonds likely form through the subsequent neucleophilic attack by the Hyl^{211} residue, accompanied by an S_N2-like loss of bromide (Figure 4.15).

Difficulty is encountered in that a halogenated sulfonium ion would be at risk of forming a sulfoxide rather than sulfilimine. As an alternate synthetic route, bromination of Hyl^{211} might yield a bromamine that leads to a sulfilimine bond either by eliciting a neucelophilic attack by the thioether or possibly through a transhalogenation oxidation event with the sulfur (126). While the comparative

kinetics of HOBr with that of Met and Lys amino acids do not support this pathway, haloamine formation agrees with the rate law of dehydromethionine formation by iodine (126). Structural analysis of the orientation of Met^{93} and Hyl^{211} within the assembled hexamer may give insight to their relative reactivity with HOBr.

Tissue isolated collagen IV hexamers have not been observed with halogenated sulfilimine bonds. As a basic principle of organic chemistry, the leaving group capacity of halide ions increases along with longer atomic radii and decreasing electronegativity, possibly explaining the differential catalytic activity of HOBr relative to HOCl. Another possible factor is if the hexamer directs hypohalous reagents toward the Hyl^{211} residue, wherein the second-order rate constants would argue for catalysis by HOBr rather than HOCl. The experimental data with HOI is a bit more confounding given the formation of dehydromethionine in extremely high yield (48). It is probable that some inherent characteristic(s) of the NC1 hexamer are selective for HOBr, less responsive to HOI, and nearly exclude HOCl reactivity.

A Biosynthetic Function for HOBr

Hypohalous acids are widely known as destructive biologic oxidants, and particularly so within basement membranes (118, 139). They are strongly implied as key oxidants during atherosclerosis, where HOCl exposure causes oxidation of low-density lipoprotein to induce foam cell formation in macrophages that take up the protein (140-141), as well as oxidation of apolipoprotein A-1 in high-density lipoproteins (142). HOBr also oxidizes proteins and lipids (122, 118), and its production via heme peroxidases makes it an additional suspect atherosclerotic oxidant. MPO is strongly associated with atherosclerotic plaques (118), yet mice lacking the protein unexpectedly display increased atherosclerosis (143), quite likely due to dissimilarities between mice and men. As an embedded

basement membrane heme peroxidase, it is tempting to consider the capacity of PXDN to act etiologically in atherosclerosis through its production of oxidants.

While the strong reactivity of HOBr finds abundant potential as a destructive oxidant, the thermodynamic barrier to sulfilimine bond formation (44) provides a constructive opportunity for harnessing the same reactive potential towards anabolic activity. Though uncommon, certain other examples point to similar non-destructive usages of oxidized bromide. The bromination of NPB, while incompletely understood, is presumably non-harmful to the neuropeptide functioning (7). Brominated taurine (TauBr), formed via neutrophil release following initial inflammatory event, is an effective anti-inflammatory agent that upregulates heme oxygenase-1 to protect cells from oxidative damage (144). TauBr also exhibits antimicrobial properties suggesting that this halogenated compound may uniquely influence hosts towards homeostasis while targeting pathogens for destruction (145).

Finally, the synthesis of thyroid hormones via oxidized iodide bears similarity to HOBr formation of sulfilimines. The product of another heme peroxidase, thyroid peroxidase, uses oxidized iodide to halogenate the aromatic rings of tyrosine derivatives while the identity and activity of the hormones are based in part on the number of iodide substituents (146). This is indeed notable as an example of non-destructive halogen oxidative chemistry, though the analogy with sulfilimine bond formation breaks down beyond this point. Initial comparison notes the carbon chemistry involved with hormone synthesis while collagen IV crosslinking revolves around the sulfur and amine reactivity. Perhaps more fundamental, however, is the observation that halogenation is a defining feature of active thyroid hormones but only appears temporarily during collagen IV crosslinking. Hormone synthesis consumes iodide, but bromide catalyzes sulfilimine bond formation. Thus, bromide uniquely functions as a halide catalyst via the biosynthetic reactivity of HOBr.

Conclusion

PXDN formation of collagen IV sulfilimine bonds delineates an essential function for bromide and establishes a new paradigm for hypohalous acids in mammalian biology. The chemistry of this under-explored halide, while broadly similar with other halogens, is uniquely suited as a powerful biochemical tool for destructive and biosynthetic applications. Through its formation of sulfilimine bonds, bromide facilitates the sole covalent reinforcement of C-terminal collagen IV junctions, resulting in a stabilized extracellular foundation for tissue function.

Methods

Materials

All chemicals were purchased from Sigma-Aldrich (St. Louis, MO) unless noted otherwise. Chloride salt was obtained at ≥99.5% purity (Product S7653-1KG, Sigma-Aldrich, St. Louis, MO). As in Chapter III, PFHR9 cells were grown in complete DMEM (Product 15-013-CV, CellGro, Manassas, VA) in 5% CO_2 at 37˚C. After becoming confluent, the culture media was spiked with 1 mM KI to inhibit bond formation as well as with 50 µM ascorbic acid for post-translational modifications of collagen IV. Culture media was changed every 24-36 hours, and cells were grown for approximately 7-10 days after becoming confluent in order to allow sufficient matrix production.

The purification of PFHR9 matrix and NC1 hexamers was identical to the protocols in Chapter III. Briefly, matrix was scraped from tissue culture plates, sonicated in a detergent buffer, separated into 1 ml aliquots, washed sequentially in high salt and low salt buffers, and stored at 4˚C until use. Collagen IV NC1 domains were solubilized by enzymatic digestion of matrix with bacterial collagenase (Worthington Biochemical Corporation, Lakewood, NJ). For SDS-PAGE analysis of NC1 crosslinking, collagenase digest supernatant was used without further purification. To purify NC1 proteins, collagenase digest supernatant was passed over a DEAE-Cellulose column in 50 mM Tris-HCl (pH 7.5), and the flow-through material was separated on a Superdex™ 200 10/300GL gel filtration column (GE Healthcare Life Sciences; Piscataway, NJ) in 1x TBS. NC1 hexamers were identified and collected based on the A_{280} profile.

Cell Culture Screening of Halides

PFHR9 cells were grown in the presence of halide salts for up to 7 days post-confluency. As in Chapter III NC1 domains were first isolated via biochemical treatments and enzymatic digestion of PFHR9 matrix, then resolved into dimers and monomers by SDS-PAGE using 12% non-reducing gels, and

finally visualized with 0.1% Coomassie Blue R250 stain (National Diagnostics, Charlotte, NC). Destained gels were scanned using either a Molecular Imager® ChemiDoc™ XRS+ with Image Lab™ TM software (Bio-Rad Laboratories; Hercules, CA) and alternatively with an HP Scanjet 5590. Densitometry was conducted using ImageJ software (version 1.43u, National Institutes of Health, Bethesda, MD), and analyzed in Excel (Microsoft Office 2007).

In Vitro *Matrix Reactions*

Collagen IV matrix was produced from PFHR9 culture in the presence of 1 mM KI to prevent crosslinking. Following the biochemical isolation of matrix, aliquots were washed into either 1x PBS or TBS for experimental crosslinking reactions at 37˚C. For enhanced accuracy, the concentration of hydrogen peroxide was determined at 240 nm using an extinction coefficient of 43.6 $M^{-1}cm^{-1}$. All reactions were initiated upon addition of H_2O_2, stored at -20°C post-reaction, and digested with collagenase enzyme to solublize the NC1 domains. Crosslinking analysis was conducted by resolving dimers and monomers under non-reducing SDS-PAGE with 12% gels, Coomassie Blue R250 staining, and desitometry analysis with ImageJ v1.43u and Excel.

To examine whether halides are required for crosslinking in matrix, following matrix isolation, pellets were subsequently washed five times in 10 mM phosphate buffer (pH 7.4) to remove endogenous halides. When desired, the ionic strength of the reaction was controlled by either adding sodium gluconate to 140mM or potassium fluoride to 100mM.

For dual halide reactions containing bromide and chloride, one halide was titrated into the reaction while the other halide was held constant. To prepare the matrix for this type of experiments, following matrix isolation, samples were washed five times into 10 mM phosphate buffer (pH 7.4) containing the appropriate amount of the halide at constant concentration. Reaction was subsequently initiated by addition of the titrated halide and H_2O_2, with reaction and analysis being conducted as

above. In samples containing a constant level of 100 μM KBr, 100 mM KF was also included in the relevant buffer washes and in the 37˚C reaction in order to maintain ionic strength.

Ion Chromatography Inductively Coupled Plasma Mass Spectrometry (IC-ICP-MS)

Analysis was conducted by Applied Speciation and Consulting, LLC (Bothell, WA) and involved sample dilution into alkaline solution; isocratic separation by anion exchange chromatography; desolvation, atomization, and ionization of the eluant in a radio frequency plasma state; and mass spectrometric separation of the ions in a vacuum. Regular and frequent instrument calibration to known standards gave confidence that the IC-ICP-MS data reflected accurate bromide concentrations.

Purification of Chloride

Chloride was purified according to a published protocol (120). Briefly, concentrated solutions of reagent grade HCl and NaOH were separated within a diffusion chamber. Liquid HCl is more volatile than HBr, allowing separation of the halogens through vapor purification of the HCl. This vapor was then captured through a condensation reaction with the NaOH solution. The reaction was assessed by monitoring the pH of the hydroxide solution, where the end point was signified by reaching neutral pH. The diffusion chamber was supplied by Adams & Chittenden Scientific Glass (Berkeley, CA) and purity of all solutions was conducted by Applied Speciation and Consulting, LLC (Bothel, WA), as presented in the Results section. A.S. McCall and G. Bhave performed purification steps.

Preparation of Hypohalous Acids and Demonstration of In Vitro *Chemical Crosslinking*

Reagent hypochlorite (OCl^-) was mixed at 10 mM with an equal volume of 12mM potassium iodide, bromide, or thiocyanate salts, and allowed to react for one minute at pH >10. Following the reaction, the hypohalite solution was diluted into 1x PBS at pH 7.4 to protonate the hypohalite. Freshly

synthesized hypohalous acids were added to uncrosslinked NC1 hexamers, incubated at 37°C for 5 minutes, and quenched by adding L-Met to 1 mM (at least 20x greater Met over HOX). Crosslink formation was monitored by SDS-PAGE and Coomassie Blue R250 staining of the reaction samples, densitometry analysis in ImageJ, and quantification in Excel. Pure HOBr was alternatively synthesized by dissolving solid bomine in an excess of sodium hydroxide, and later used similar to hypochlorite-derived reagents. The efficiency of synthesis pathways was assessed by UV spectrophotometry.

Reagent I_2/I_3 was synthesized by dissolving solid iodine into an excess molar concentration sodium hydroxide. To screen for bond formation via oxidized iodide, PHFR9 NC1 domains were produced via treatment with PHG and reacted for 1 hour at 37°C with 1 mM of I_2/I_3, iodate (IO_3^-), or periodate (IO_4^-) in 1x TBS. Following the reaction, samples were analyzed by SDS-PAGE and Coomassie Blue R250 staining.

Mass Spectrometric Identification of Sulfilimine Bond Formation from HOBr Catalysis

Uncrosslinked NC1 hexamers were reacted at 37˚C with HOBr as described above. Sulfilimine bonds were identified in this reacted material similar to the protocol described in Chapter III and in the literature (4). Briefly, reacted hexamers were reduced with DTT and alkylated with iodoacetamide before enzymatic digestion with trypsin (sequencing grade, Promega; Madison, WI). Peptide fragments were separated by gel filtration on a Superdex peptide column (GE Healthcare Life Sciences; Piscataway, NJ), and fractions with peptides of ca. 5000 Da were selected for further purification by C18 reverse phase chromatography (Jupiter, 3 µm, 300 Å, Phenomenex) and MS/MS analysis on a LTQ Orbitrap instrument (Thermo Fischer Scientific; San Jose, CA) in the Vanderbilt Mass Spectrometry Core facility. Collision induced dissociation parameters included 2 m/z isolation width, 30 ms activation time, and 35% normalized collision energy. Mass spectra were analyzed with Xcalibur software (Thermo Fischer Scientific), GPMAW ver. 8.00sr1 (Lighthouse Data; Denmark), and Excel.

Chapter V

NC1 HEXAMER IS ASSEMBLED BY CHLORIDE

Introduction

As the primary constituent of basement membranes, protomeric collagen IV heterotrimers assemble into networks via head-to-head connections between their NC1 domains (C-termini) resulting in a hexameric structure, and crystallographic studies revealed six chloride ions were observed at the trimer-trimer interface (9). Here, direct evidence is presented that chloride is the central component during the electrostatic assembly of NC1 hexamers.

Results

Halides Stabilize Uncrosslinked NC1 Hexamers

Standard protocols for NC1 hexamer purification typically include gel filtration chromatography conducted in 50mM Tris-HCl (pH 7.5) buffer, with the protein complex reproducibly eluting as a single, well-defined peak when monitored by A_{280}. Harsh biochemical treatments can dissociate the hexamer, such as at acidic pH (<3.5), yielding a slower-migrating peak that corresponds to monomeric NC1 domains (16). In a subtle protocol adjustment utilizing the lowered buffer concentration of 20 mM Tris-HCl, uncrosslinked NC1 domains were unexpectedly observed in dissociated state by gel filtration. Noting that the change resulted in a reduction in buffer chloride from ca. 15 mM to 6 mM (pH 7.5), it was hypothesized that the internal chloride ions with the hexamer may have been disturbed. To test this, uncrosslinked PFHR9 hexamer was dialyzed into 50 mM Tris-acetic acid (pH 7.4) and observed by

gel filtration chromatography to indeed be dissociated as represented by a major monomeric NC1 peak, minor residual hexamer peak, and minor intermediate peak (Figure 5.1a)

This raised an intriguing possibility that halides may stabilize the quaternary hexamer structure (9). To verify this, PFHR9 hexamer was produced under KI conditions, dialyzed from Tris buffer into PBS and then into 10 mM phosphate buffer (pH 7.4). Gel filtration analysis demonstrated a near-identical A_{280} profile as the samples dissociated in Tris buffers (Figure 5.1b). PFHR9 hexamer inhibited via PHG treatment was similarly dissociated by placement into phosphate buffer without halides (Figure 5.1b).

Hexamer Assembly Requires Halides

Grasping the significance of halides for hexamer stability, the question was then raised whether this reaction might also be reversible, where the addition of halide promotes hexamer assembly. To test this possibility, uncrosslinked hexamer was first dialyzed into 50 mM Tris-Ac, with dissociation confirmed by gel filtration chromatography, and subsequently incubated with 100 mM NaCl for 24hr at 37°C. Gel filtration analysis confirmed the reappearance of the hexamer peak upon addition of halide (Figure 5.2).

Assessing the putative halide requirement during hexamer assembly, particular attention was given to whether the observed data did in fact reflect a defined chemical reaction rather than simply being the result of non-specific phenomena. Hexamer assembly was thus examined for its responsiveness to variations in the concentrations of halide and NC1 domains, without differentiating between the alpha subclasses of collagen IV. Initial testing assayed the reaction equilibrium for any responsiveness to changes in temperature or concentration of the reactants. At 100 mM NaCl and 1.5 mg/ml NC1, and hexamer assembly mostly occurred within 24 hours at 37°C (Figure 5.3a). Next, NC1 domains were titrated into 100 mM NaCl where the resultant amount of assembled hexamers increased with the protein concentration, when measured by the percent hexamer of the total NC1 (Figure 5.3b). In the converse experimental design where protein concentration was held constant at 2 mg/ml,

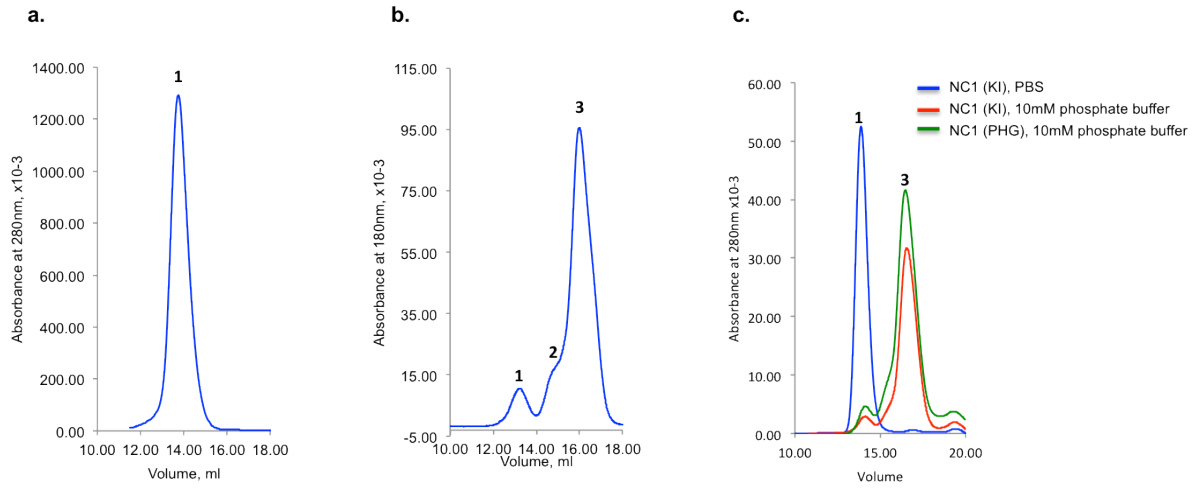

Figure 5.1: Halides Stabilize Uncrosslinked Hexamers. (**a**) Assembled NC1 hexamers elute as a single peak (peak 1) when observed by gel filtration in 15 mM Tris-HCl (S200). (**b**) Upon removal of halides through dialysis, the uncrosslinked hexamer peak is greatly reduced and accompanied by the emergence of slower migrating peaks (peaks 2 and 3) corresponding to components of the dissociated hexamer. (**c**) Halide dependent hexamer stability occurs in phosphate buffer. KI-inhibited hexamers are stabile in PBS (blue line) but dissociate in 10 mM phosphate buffer at pH 7.4 (red line), while PHG-inhibited hexamers are dissociated in 10mM phosphate buffer at pH 7.4 (green line). Peak identities correspond to hexamer (1), intermediate peak (2), and NC1 monomers (3). Additional protocol details are contained in the Methods section.

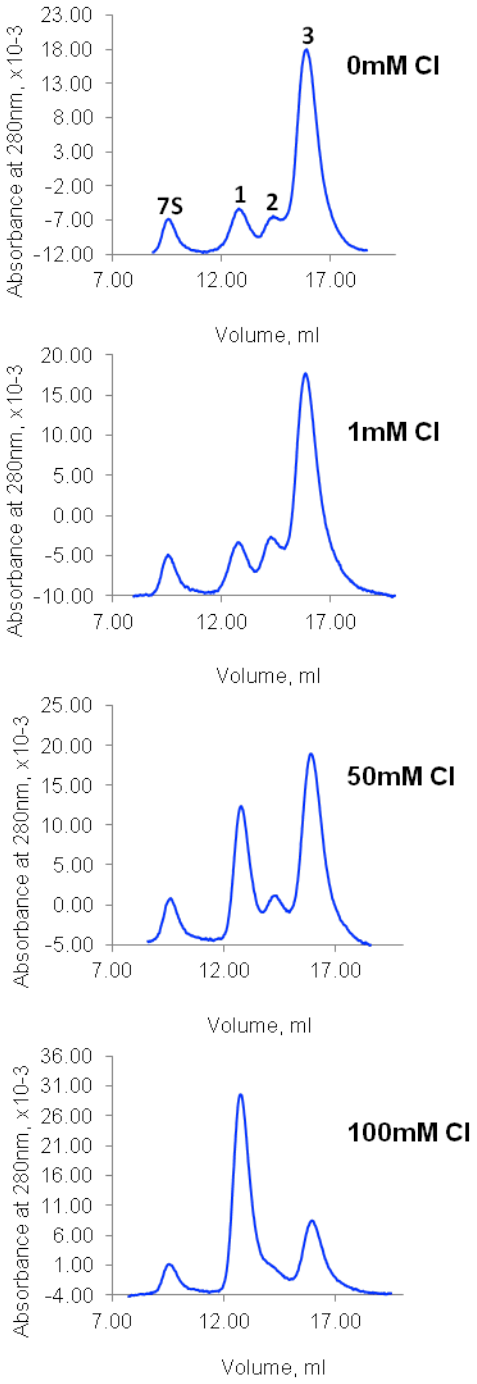

Figure 5.2: Hexamer Assembly Requires Halides. Gel filtration chromatographs of hexamer assembly caused by halide titration. Hexamer peak (peak 1) grows larger with increasing chloride concentration while peak 3 is reduced and peak 2 is lost. The 7S peak remains constant as internal control. Additional protocol details are contained in the Methods section.

increasing concentrations of chloride yielded greater hexamer assembly up to 100 mM NaCl (Figure 5.3c). Together, this suggests the assembly process is indeed a defined chemical reaction dependent on the protein and halide concentrations. The parameters of 2 mg/ml NC1, 100 mM Cl, and 24 hours at 37°C were utilized as constants for all assembly reactions unless noted otherwise.

Chloride Forms NC1 Hexamers

Since the varying electronegativities of halogen ions may differentially influence hexamer assembly, the reaction was examined with the sodium salts of chloride, bromide, and iodide between the concentrations 1-200 mM. One hundred milli-molar concentrations of either chloride or bromide catalyzed maximum hexamer formation, while the curve for iodide was shifted towards a higher halide concentration (Figure 5.4a). Considering the *in vivo* process, the three halides were examined at the physiologic concentrations of 100 mM Cl^-, 100 μM Br^-, and 1 μM I^-. The only appreciable amount of hexamer assembly occurred in the chloride sample (Figure 5.4b).

Potassium and calcium ions were also identified within the hexamer crystal structure (9) and their influence on assembly was examined. Dissociated NC1 domains assembled equally well in potassium and sodium solutions (Figure 5.4c), suggesting their binding sites may experience high degrees of solvent interactions. Calcium was examined first by dissociating hexamers in the presence of 1 mM EDTA, which yielded the expected dissociation profile plus an additional A_{280} peak that corresponded to EDTA in the buffer (Figure 5.5c). Chloride was subsequently added to 100mM with EDTA maintained in the buffer, leading to hexamer formation (Figure 5.5d). Finally, dissociated NC1 domains were pre-treated with 1mM EDTA, dialyzed back into 50 mM tris-Ac to remove the EDTA, and incubated with 1 mM CaOH to formally test the role of calcium in hexamer assembly, yet the NC1 domains remained dissociated after 24 hours (Figure 5.5e).

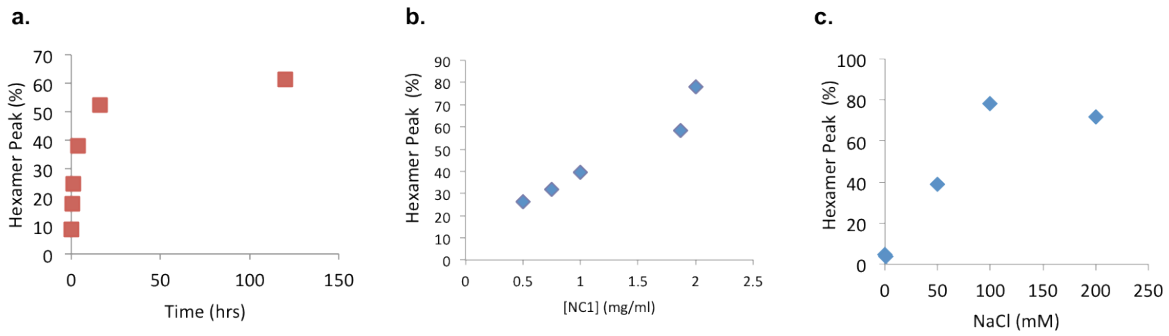

Figure 5.3: Hexamer Assembly Depends on Concentrations of NC1 and Chloride. Hexamer assembly was optimized in terms of kinetics and sensitivity to reagent concentrations. (**a**) A time course of hexamer assembly using 1.5 mg/ml NC1 and 100 mM NaCl, where most of the reaction occurred within 24 hours. (**b**) While maintaining 100 mM NaCl, protein was increased from 0.5 mg/ml to 2 mg/ml yielding higher percentage hexamer formation. (**c**) At 2 mg/ml NC1, sodium chloride concentration was increased up to 200 mM with corresponding increases in percent hexamer up to 100 mM NaCl. All reactions occurred at 37°C for 24 hours unless noted otherwise, and samples were pelleted at 4°C for ca. 15 minutes before analyzed by gel filtration chromatography (S200, GE Healthcare). Peak area under the curve was integrated with Unicorn software and the heaxameric peak expressed as a percent of the total NC1 peaks. Additional protocol details are contained in the Methods section.

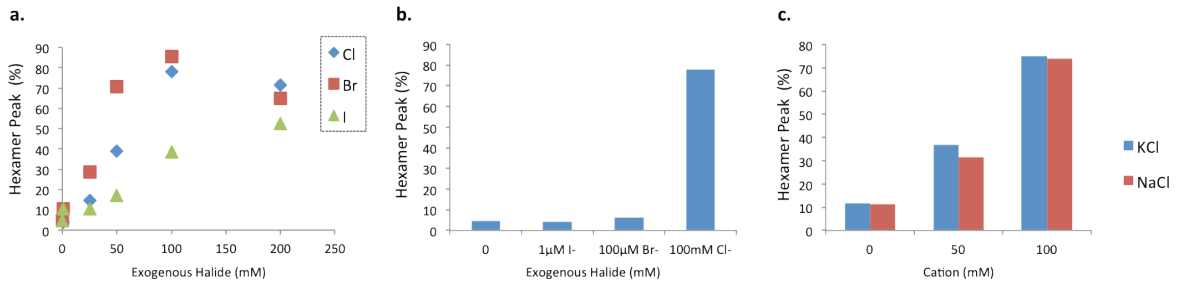

Figure 5.4: Physiologic Concentrations of Chloride are Critical for Hexamer Assembly (**a**) Hexamer assembly of NC1 domains occurs in response to increasing concentration of chloride, bromide, and iodide, (**b**) and at the approximate human serum concentration of chloride but not iodide or bromide. (**c**) Hexamer assembly occurred equally well in potassium and sodium salts. Peak area under the curve was integrated using Unicorn software and the heaxameric peak expressed as a percent of the total NC1 peaks. Additional protocol details are contained in the Methods section.

Structural Rationale for Chloride-Based Hexamer Assembly

Crystal structures of the hexamer reveal domain swapping between side-by-side monomers that stabilize trimers, as well as extensive non-covalent interactions throughout the hexamer (18, 9, 17). An initial overview of the hexamer (Figure 5.6a) presents an oblong structure where the long axis is perpendicularly severed by the trimer-trimer interface. Trimers are held together by domain swapping that occurs at the trimer-trimer interface as each NC1 monomer protrudes a β-hairpin motif (Figure 5.6c) that fits snug inside a corresponding grooved region termed the variable region 3 (VR3) on the adjacent monomer. Chloride and potassium ions are present along the trimer-trimer interface (Figure 5.6b) with one Ca^{2+} to each α2 NC1 domain.

Six halides are found in each hexamer, one per monomer, located within a specific binding site at the base of the domain swapping β-hairpin. The ion is nearly encircled by the protein backbone extending C-terminally from the β motif. This protein-halide interaction is likely mutually beneficial, with the halide being held in place through electrostatic interactions, and in turn providing support for an otherwise flexible region of the NC1 domain. The backbone amide of Arg^{77} is a participant in this halide coordination scheme, positioning the residue side chain into the trimer-trimer interface where it electrostatically interacts with Glu^{176} from the opposing trimer. Molecular dynamics simulations revealed that the halide is directly involved with an inter-trimer electrostatic bonding whereby Arg^{180} from the opposing trimer spans the interface and binds the ion via its positively charged guanidnium group (Figure 5.7). Ionic bonds between Arg^{77}-Glu^{176} and Arg^{180}-Cl form the crux of hexamer assembly.

Due to the proximity of chloride with regards to the β-hairpin, inter-trimer electrostatic bonds are not established between directly opposing monomers but rather attach in an offset fashion. Since the domain swapping motif of each monomer extends in a right-handed fashion, the chloride is positioned near the center of the NC1 domain that is directly adjacent to the β-hairpin, yet right-shifted relative to the Cl-binding NC1 domains (Figure 5.8).

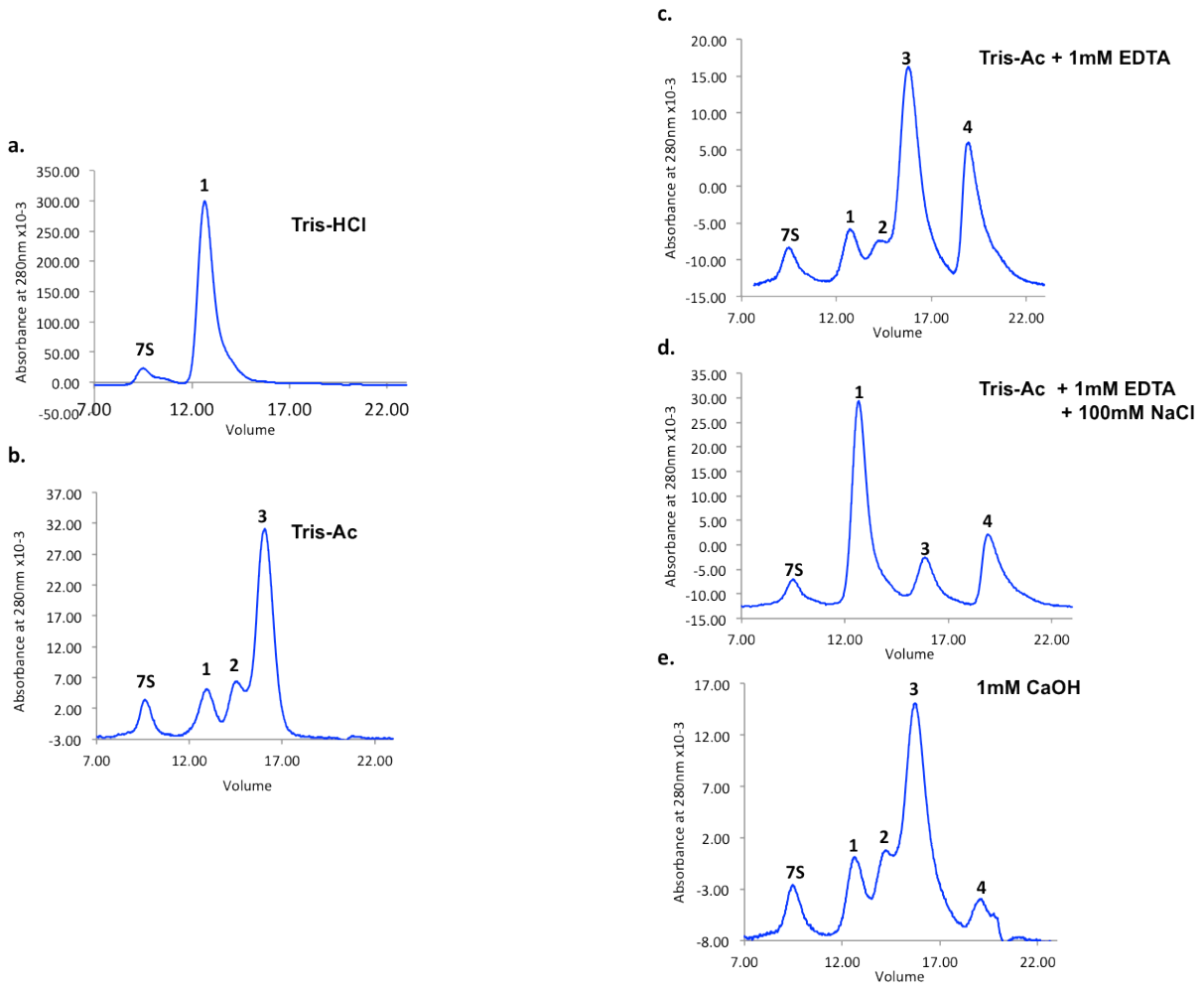

Figure 5.5: Calcium Is Not Required For Hexamer Assembly. (**a**-**b**) Uncrosslinked hexamer was stable in Tris-HCl (**a**) and dissociated in Tris-Ac (**b**) buffers at pH 7.4. (**c**) Addition of 1 mM EDTA to the dissociated NC1 resulted in the appearance of an additional slower migrating peak. (**d**) In the presence of EDTA, hexamer assembly proceeded after the addition of 100 mM NaCl. (**e**) After removing the EDTA, 1 mM CaOH was added to dissociated NC1 though assembly did not occur. Peaks correspond to 7S domain (7S), hexamer (1), intermediate peak (2), NC1 monomer (3), and overlapping peaks for EDTA and NC1 fragments (4). Additional protocol details are contained in the Methods section.

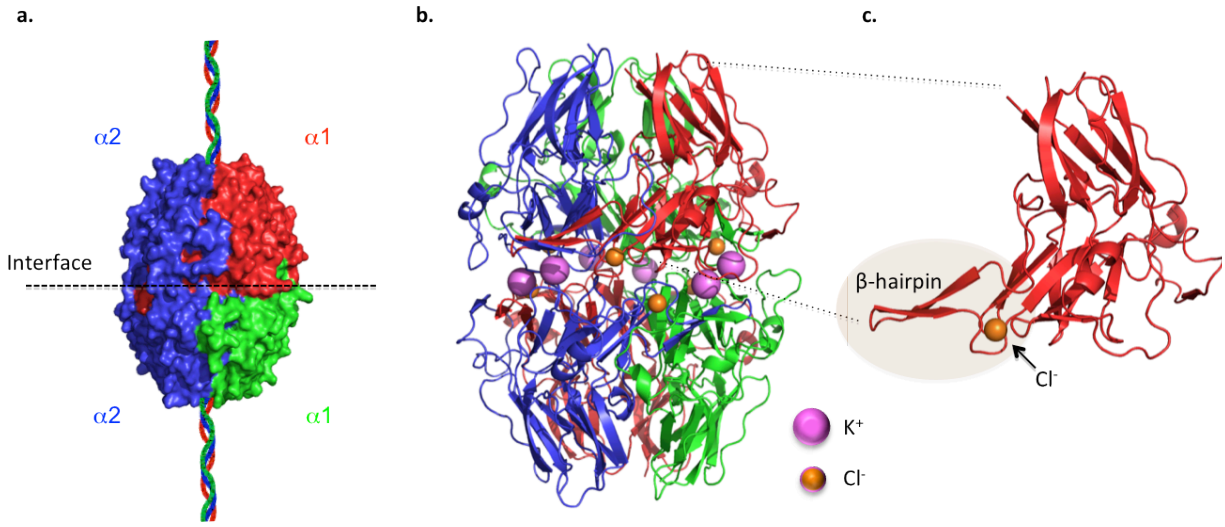

Figure 5.6: Chloride Ions Are Positioned At the Trimer-Trimer Interface. (**a**) NC1 hexamers appear as oblong quaternary structures that assembles through the interfacing of two trimers along a relatively flat junction. (**b**) The interface contains binding sites for six chloride ions as well as six potassium ions. (**c**) NC1 monomer shown, revealing chloride binding site located near β-hairpin fold. Additional protocol details are contained in the Methods section. Modeled with PYMOL software in collaboration with K. Brown.

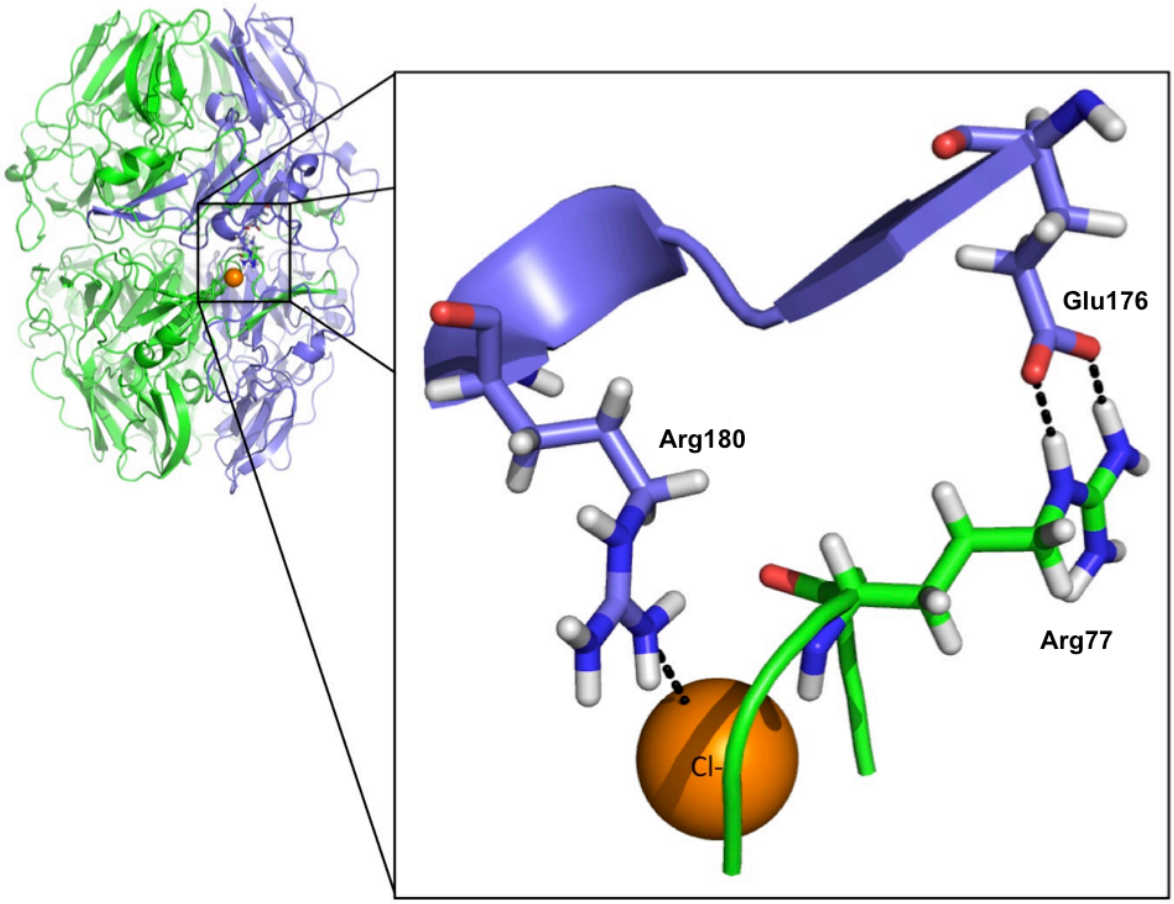

Figure 5.7: Chloride Facilitates Two Types of Ionic Bonding. Chloride binds via amide interactions with the backbone of Arg^{77} and adjacent amides. This orients the side chain primary and secondary amines of Arg^{77} so as to form ionic bonds with Glu176 from the opposing trimer. The hexamer is further stabilized by Arg^{180} that spans the interface to form a direct electrostatic interaction with the chloride ion. Additional protocol details are contained in the Methods section. Modeled with PYMOL software in collaboration with K. Brown.

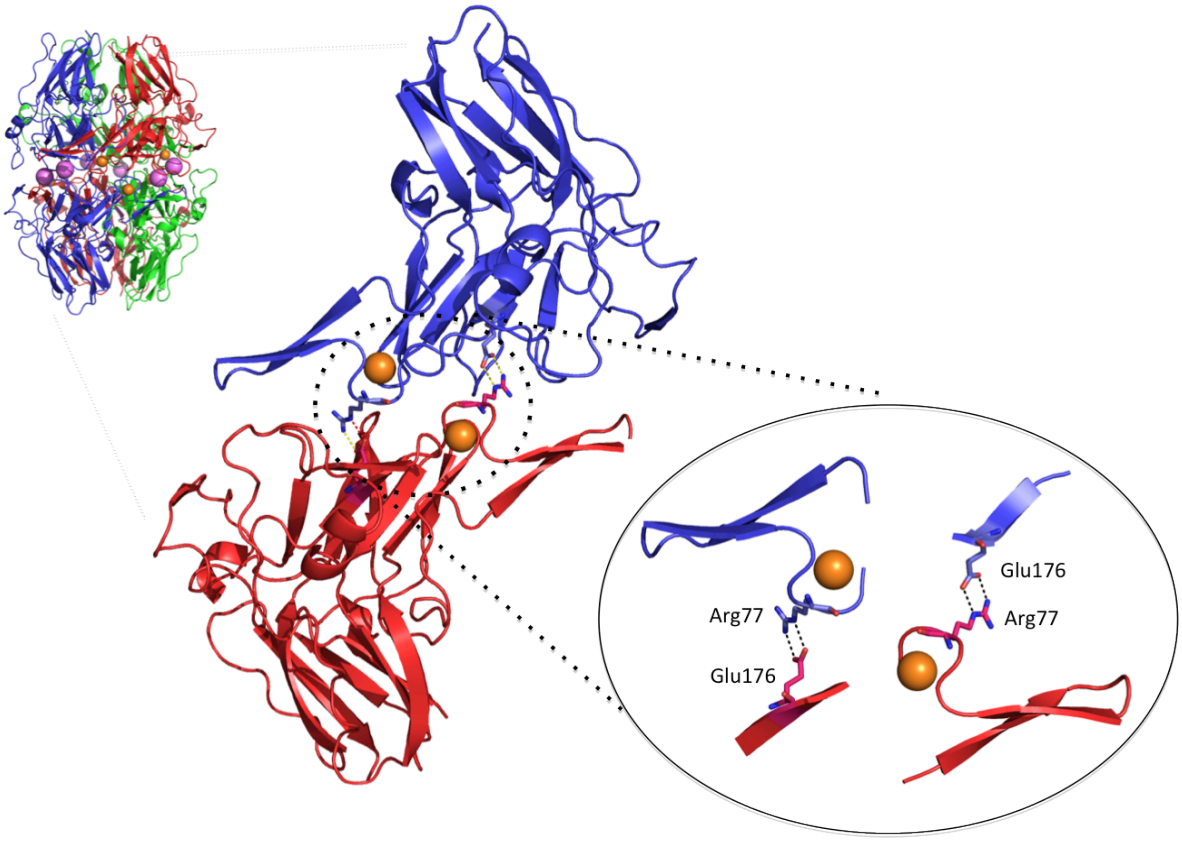

Figure 5.8: Chloride Coordinates Interaction Between Two Offset Monomers. Each NC1 monomer binds one chloride ion, yielding two ions per pair of interacting NC1 domains. Monomers overlap in an offset fashion near the β-hairpin folds. Additional protocol details are contained in the Methods section. Modeled with PYMOL software in collaboration with K. Brown.

Discussion

The discovery of chloride-induced hexamer assembly is an example of applying rigorous testing to a serendipitous observation. Halides have been well documented within the hexamer (18, 147, 9), but are here show to be the unexpected gatekeepers of the uncrosslinked quaternary structure. The halide concentrations required for *in vivo* hexamer assembly point strongly to chloride, which notably induces a conformational change that Ca^{2+} is unable to perform on its own. Drawing on prior structural understanding, this technical advance has fortuitously unlocked the mechanism of NC1 hexamer assembly.

Halides Stablize NC1 Hexamers

Formation of collagen IV networks relies on the coordinated roles of halide ions during hexamer assembly and the enzymatic catalysis of sulfilimine bonds (Figure 5.9). Both functions are unique within biology, not least of which are the protein-ion interactions required for hexamer formation and stability. The study of halide binding motifs is a developing specialty within structural biology, and while the binding events are commonly observed, the rational for such interactions still remains greatly unexplored. Zhou and colleagues (148) identified 782 such motifs in the PDB and calculated the thermodynamics of formation for each. As a whole, the motif is stabilizing with a ΔG_{TOT} of -15.16 ± 9.71 kcal/mol. Surprisingly, the more favorable energy change was experienced via non-electrostatic interactions at ΔG = -13.37 ± 4.83 kcal/mol as compared to the electrostatic changes of ΔG = -1.79 ± 6.86 kcal/mol. The low net electrostatic effect was largely due to the high desolvation energy barrier of 8.81 ± 4.97 kcal/mol that counteracted the energetically favorable electrostatic Coulomb interactions (-10.5 ± 9.97 kcal/mol). These numbers reflect a broad agglomeration of protein-halide interactions with a wide distribution of effects. Yet, it is difficult not to ponder the apparently high energy barrier incurred in order to remove chloride from solution during hexamer assembly. The ion is obviously stabilized by

electrostatic interactions with the backbone amide loop and the guanidinium ion of Arg^{180}, and hexamer assembly further involves the ionic bonding of Arg^{77}-Glu^{176}. Preservation of uncroslinked hexamer during gel filtration with halides present indicate that the structure is indeed stabilized via electrostatic forces, yet it presumably bears a thermodynamic penalty through the halide desolvation. One plausible mechanism for overcoming this barrier may be to absorb the desolvation energy input through one type of interaction, such as via multiple amide backbone interactions, while stabilizing ΔG values for the hexamer are gained through the remaining ionic bonds.

Crystal structures reveal a single Ca^{2+} ion per trimer bound to the α2 domain within the internal cavity of the α112 hexamer (9). Curiously, these sites displayed large electron density in PBM crystals and less so in LBM hexamer, indicating that NC1-calcium binding may be tissue-specific. These ions are well-known for their ability to induce conformational change in proteins containing the EF-hand motif (149-151), yet there are not detectably required for hexamer assembly. Though unidentified, calcium binding is likely functionally significant to NC1 physiology based on the data that the cation binding site and internal hexamer cavity are strongly negatively charged (9, 147) as well as the selectivity of the ion for α2 (9). Hypothetically, the ion may act as a stabilizing force for the monomer, though focused efforts will indeed be required to elucidate its true role.

NC1 Hexamer Assembly Mechanism

Underlying the various collagen IV isotypes and sulfilimine bonding patterns is the requirement that NC1 domains combine into heterotrimers that then assemble into the observed hexamer structure, a process that is strongly dependent of halides. Binding studies with the α112 hexamer suggest that the α2 domain initiates trimer assembly while sequence similarities among α2, α4, and α6 have shaped the hypothesis that these individual chains may direct the assembly of their respective protomers (17). Indeed, the NC1 domain acts as the nucleus of protomer formation and sequence variation within the

VR3 region imparts chain selectivity to direct the proper combination of collagen IV chains into the nascent protomer (17, 152). Given the proximity of the halide binding site to the β-hairpin motif, it is not unreasonable to presume that the chloride influences the conformation of the domain swapping region and is thereby a key participant of trimer assembly. Its positioning is indeed critical to hexamer assembly via the head-to-head interaction of timers.

The trimer-trimer interface is shaped by a diverse landscape, with the steric outline of one trimer fitting into the other like a puzzle. This naturally burdens the process of hexamer assembly so that approaching trimers are properly oriented. Notably, chloride-amide interactions within the backbone loop positions Arg^{77} such that the side chain juts into the interface cleft, potentially as a means of establishing the initial contact. Once in register, electrostatic interactions along the interface would expectedly place a certain amount of internal compression on the tightly-fitting steric interactions. This would obviously have benefits for hexamer assembly and would also likely provide a mechanism for resisting strain during dynamic movement by distributing any sheer stresses along the interface.

Conclusion

The assembly of NC1 hexamers is an elegant mechanism of ionic bonding. Halides are unexpectedly favored over the activity of calcium, desolvation energy costs are surmounted, and steric obstacles avoided during the process to yield a stable quaternary structure. In some matrices, such as lens basement membrane, electrostatic interactions stabilize the majority of hexamers. Yet in many collagen IV networks, as presented in the following chapter, hexamer assembly forms a substrate upon which sulfilimine bonds are established.

Methods

Materials

All chemicals were purchased from Sigma-Aldrich (St. Louis, MO) unless noted otherwise. The protocols for PFHR9 cell culture and isolation of collagen IV matrix were identical to that in Chapter III. Collagen IV matrix was produced in the presence of 1 mM KI to inhibit bond formation. After digestion of uncrosslinked matrix with collagenase enzyme, supernatant was passed over DEAE-Cellulose column in 50 mM Tris-HCl (pH 7.5). The flow through fractions contained collagen IV NC1 and 7S domains, and this material was used without further modification for all hexamer dissociation and assembly experiments.

Fast Protein Liquid Chromatography Analysis of NC1 Hexamers

As in Chapter III, gel filtration chromatography of NC1 hexamers was conducted with a Superdex™ 200 10/300GL gel filtration column (GE Healthcare Life Sciences; Piscataway, NJ) in 1x TBS. Chromatography was performed on ÄKTA Purifier P-900 HPLC (GE Healthcare Life Sciences; Piscataway, NJ) under fast protein liquid chromatography conditions near a 0.5 ml/min flow rate, with Unicorn software (GE Healthcare Life Sciences; Piscataway, NJ). NC1 hexamers were monitored by the A_{280} profile, with hexamer complexes eluting near 13 ml. Dissociation was observed by emergence of a slower migrating A_{280} peak near 18 ml, corresponding to NC1 monomers. The area under hexamer peak was integrated in Unicorn and analyzed in Excel as a percentage of the combined peaks, excluding 7S peak and the slower migrating buffer peak observed experiments containing EDTA.

Hexamer dissociation and assembly

Dissociation of uncrosslinked NC1 hexamers occurred by dialyzing the protein from 50mM Tris-HCl (pH 7.5) into a buffer with lower halide concentration such as 50 mM Tris-acetic acid (Tris-ac, pH 7.4)

or 20 mM Tris-HCl (pH 7.5). Dissociation occurred with 0.3-6 ml of 1mg/ml protein in 1 L of dialysis buffer, and dialysis was conducted 4°C with at least one buffer change over a two day period. For each batch of protein preparation, the efficiency of dissociation was assessed by gel filtration. Hexamer assembly reactions occurred at 37°C in 50 mM Tris-ac (pH 7.4) in 25 µl volumes. Reactions were initiated by the addition of halides, followed by a brief centrifugation, and then sample incubation at 37°C. After the reaction, samples were centrifuged at 14000 rpm and 5°C for 15 min, then loaded directly onto the Superdex™ 200 column for analysis.

Molecular Dynamic (MD) Simulations

Three-dimensional reconstruction of the NC1 hexamer was modeled on solved x-ray crystallography structures of the NC1 hexamer (9) (PDB 1T61). AMBER 12 was used to generate topology and coordinate files, via the xLEaP module (153) using ff99SB parameters (154, 155), monovalent ion parametes with literature support (156), and diavalent ions parameters from xLEaP. Solvation was based on an 8.0 Å TIP3P water model in a truncated octahedral box, and chloride ions added along a 1.0 Å Coulombic potential grid for charge neutralization. Periodic boundary conditions were defined for energy minimization and solvent equalization as described elsewhere (157). Pressure was held constant over 100 ns for production calculations, and backbond RMSD values were stabilized for equilibration. The particle mesh Ewald (PME) method was used to address electrostatic interactions (158). Where involving hydrogen atoms, bond lengths were constrained using the SHAKE algorithm (159). All minimization, equilibration, and production stages utilized a non-bonded cutoff of 9.0 Å, and a Langevin coupling algorithm was used to control temperature, involving a collision frequency of 0.5 ps^{-1} (160, 161). The CPPTRAJ module of AMBER was used for trajectory analysis. All MD simulations were conducted by K. Brown.

Structural modeling of NC1 hexamers

PYMOL software (162) was used to analyze MD data and for generating models of the NC1 domains. The PDB2PQR web service was used to define electrostatic parameters (163) and the Adaptive Poisson-Boltzmann Solver (APBS) was used to calculate and analyze the Poisson-Boltzmann electrostatic potentials (164). All modeling was conducted by K. Brown.

Chapter VI

SULFILIMINE BONDS STRUCTURALLY REINFORCE COLLAGEN IV NETWORKS

Introduction

Sulfilimine crosslinked NC1 hexamers are essential to the integrity of collagen IV networks, as inferred from genetic studies of collagen IV and PXDN (11-13, 4). These bonds provide the sole type of covalent biochemistry joining the protomers (4), yet the amount of sulfilimine crosslinking within matrices varies according to tissue type. Direct evidence is here presented for the structural function of sulfilimine bonds within hexamers, with repercussions for the stability of collagen IV networks.

The collagen IV sulfilimine bond has been implicated as an etiologic factor in Goodpasture's disease where uncrosslinked α345 NC1 hexamers are bound by pathologic auto-antibodies. Considering that damage of peroxidasin (PXDN) might inhibit crosslinking *in vivo*, we noted that the enzyme inhibitor phloroglucinol (PHG) is commercially used in dye production and various chemical syntheses, providing an environmental scenario for inhibition of bond formation via occupational exposure. Industrial hydrocarbon exposure has indeed been postulated as a disease risk factor (55). Thus, hypothesizing that sulfilimine bond formation may be inhibited by industrial compounds, a panel of candidate inhibitors bearing structural similarity to PHG was examined in matrix for their effect on dimer formation.

Results

Hexamer Assembly Precedes Sulfilimine Bond Formation

Considering the dual functions of chloride and bromide during hexamer assembly and crosslinking, respectively, the ordering of their activity was sought to be experimentally determined. *In vitro* HOBr crosslinking was thus conducted with uncrosslinked hexamer and dissociated NC1 domains.

Since the enzymatic reaction is dependent on the catalytic activity of HOBr, the *in vitro* assay provided a valid proxy for indentifying key requirements occurring upstream of PXDN activity. Dimerization occurred exclusively in hexamer populations (Figure 6.1), indicating that assembly of the quaternary structure is a prerequisite to PXDN sulfilimine bond formation.

Sulfilimine Bonds Reinforce the Hexamer Structure

Met^{93} and Hyl^{211} residues are located on flexible loops at the trimer-trimer interface periphery while the non-covalently interacting residues form a ring around the inner hexamer core (Figure 6.2). To better determine the functional significance of sulfilimine bonds, low-halide dissociation was performed on PHFR9 hexamers with either reduced or enhanced crosslinks, obtained via KI- and KBr-treatment in cell culture, respectively. Hexamer dissociation was inversely proportional to the degree of sulfilimine bonding, where reduced crosslinking resulted in the majority of NC1 domains being in the monomeric state while KBr-treatment yielded hexamers that were largely resistant to dissociation (Figure 6.3).

Support for this sulfilimine function was also observed in matrix. Uncrosslinked matrix pellets were washed into 10mM phosphate buffer (pH 7.4) with ionic strength being maintained with 140mM sodium gluconate rather than fluoride. After incubation and subsequent treatment with collagenase enzyme, SDS-PAGE analysis of the gluconate reactions revealed that while bromide indeed catalyzed bond formation at 100 µM, similar to results achieved in fluoride, all NC1 banding was lost in lower halide conditions while 7S loading control remained relatively constant (Figure 6.4). Further, NC1 monomers were absent in 100 µM Br^- while dimers were present, suggesting that the dissociated NC1 domains may have been subjected to proteolytic cleavage or another damaging event.

Loss of Lower Dimers Potential Risk Factor for Goodpasture's Disease

The permutations of sulfilimine bonding within hexamers were addressed from a theoretical

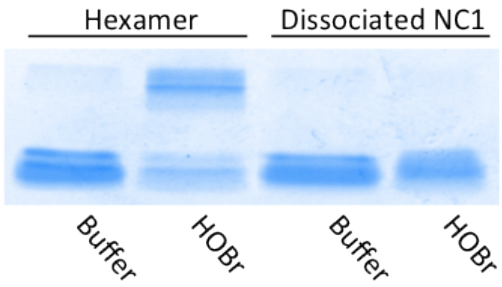

Figure 6.1: Hexamer Assembly is a Prerequisite for Sulfilimine Bond Formation via HOBr. HOBr (50 μM) was reacted with 5 μM of either assembled hexamers or dissociated NC1 domains. Reaction occurred for 5 minutes at 37°C before quenching with 1 mM of L-methionine. SDS-PAGE analysis revealed bond formation occurred only with the hexamer substrate. Additional protocol details are contained in the Methods section.

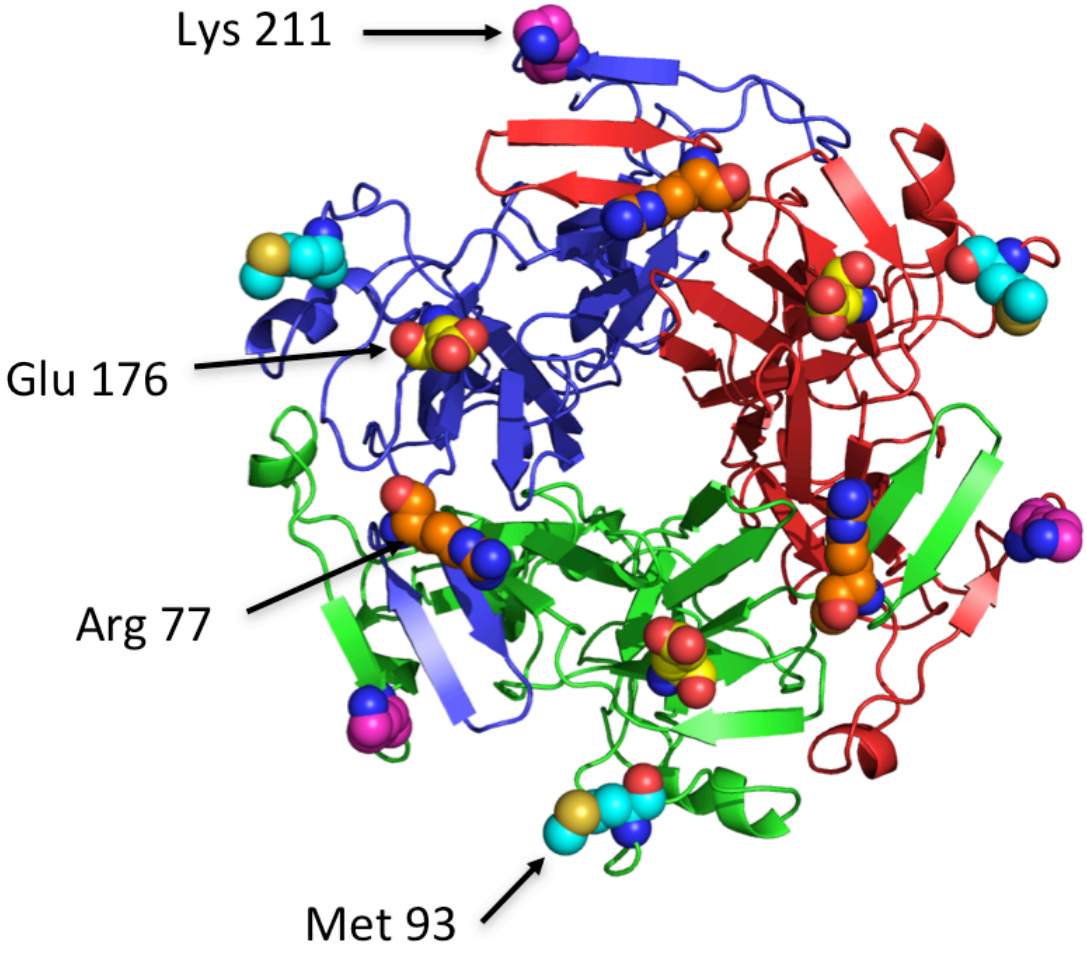

Figure 6.2: Distinct Distribution of Ionic and Covalent Bonds within Hexamers. Chloride-dependent ionic bonding between Glu^{176}-Arg^{77} is positioned as a ring around the inner hexamer cavity while covalent sulfilimine bonds between Met^{93} and Hyl^{211} are found around the hexamer exterior. Additional protocol details are contained in the Methods section. Modeled with PYMOL software in collaboration with K. Brown.

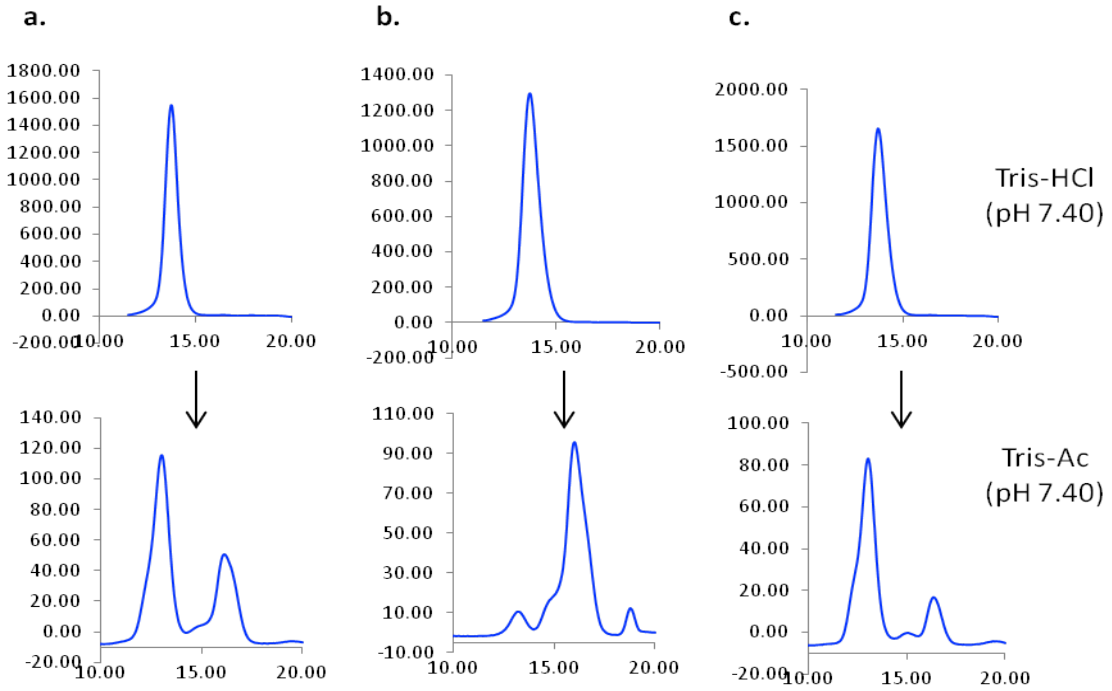

d.

	Pk.1	Pk.2	Pk.3
PFHR9	67.9%	0.0%	35.1
PFHR9 - KI	8.1%	0.0%	91.9%
PFHR9 - KBr	80.3%	2.8%	16.9%

Figure 6.3: Sulfilimine Bonds Reinforce Hexamer Structure. NC1 hexamers were dissociated by dialyzing from Tris-HCl (upper) into Tris-acetic acid (Tris-Ac, lower) buffer and analyzed by gel filtration chromatography. The amount of hexamers resistant to dissociation correlated with the degree of internal sulfilimine bonding shown by wild type PFHR9 hexamers (**a**), KI-treated hexamers lacking crosslinks (**b**), and KBr-treated hexamers with enhanced crosslinking (**c**). (**d**) Quantification of the dissociation studies with peak area under the curve was integrated with Unicorn software. Additional protocol details are contained in the Methods section.

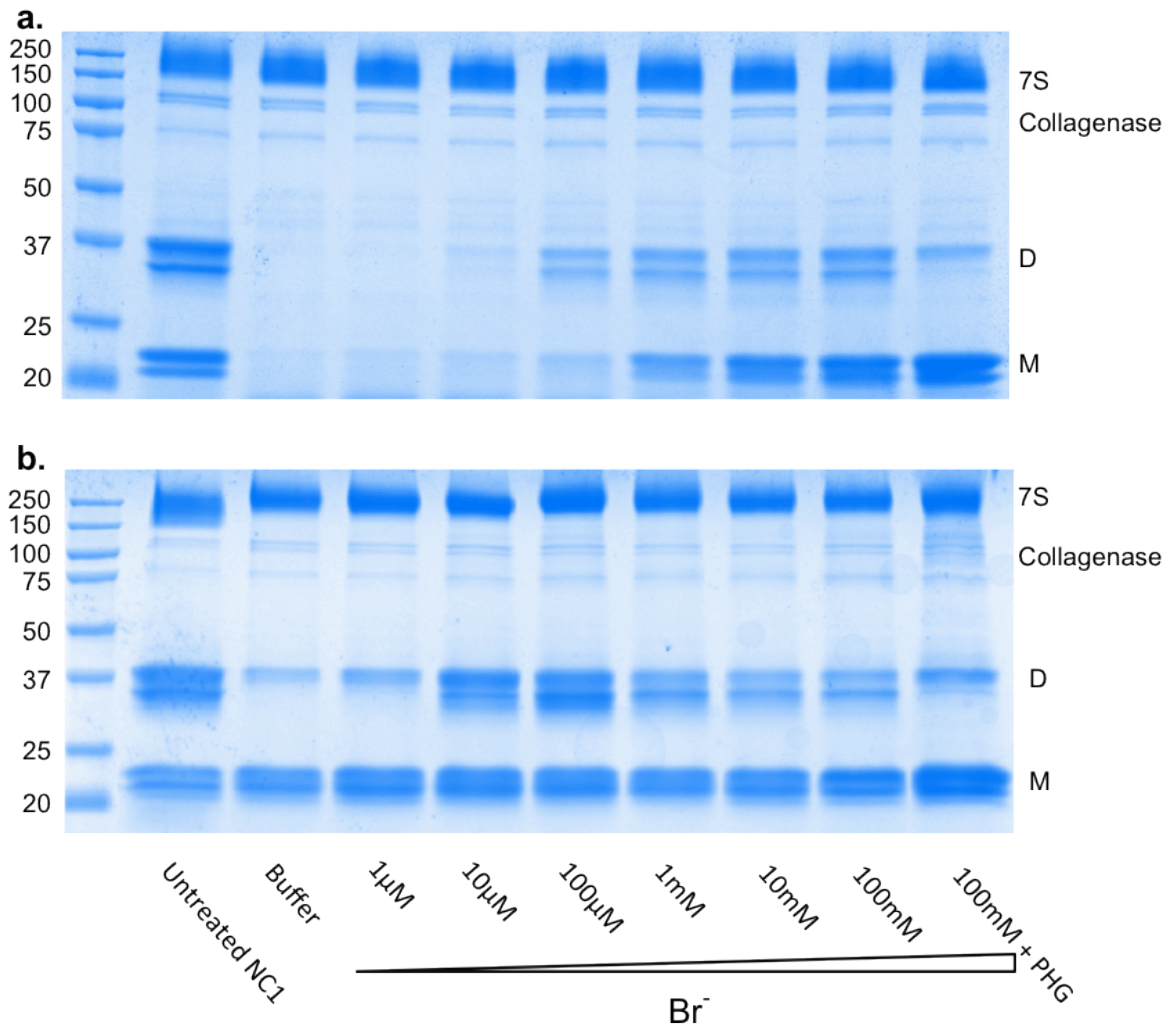

Figure 6.4: NC1 Domains Susceptible to Damage Within Matrix in Absence of Halides. (**a**) Controlling matrix ionic strength via 140 mM gluconate in 10mM phosphate buffer (pH 7.4) resulted in loss of NC1 banding below 100µM Br^-. (**b**) Utilization of 100 mM fluoride for ionic control prevented loss of protein. The reaction was run overnight at 37°C in 1 mM H_2O_2 and frozen to stop the reaction. Samples were digested with collagenase at 37˚C overnight, and visualized by SDS-PAGE using 12% gels under non-reducing conditions with Coomassie staining. Additional protocol details are contained in the Methods section.

standpoint. Considering the number of bonds per hexamer and per dimer, twenty-seven unique bonding patterns may exist (Figure 6.5). When sorted according to bonds per hexamer, the distribution shows a symmetric Gaussian curve with hexamers containing three sulfilimine bonds possessing the most bonding permutations. Hexamers with various degrees of crosslinking were examined according to the proportions of monomers, singly-crosslinked NC1 domains, and doubly-crosslinked NC1 domains (Table 6.1). This allowed the average number of sulfilimine bonds to be estimated from various sources of collagen IV, assuming that lower dimers are indeed an adequate proxy for NC1 dimers containing two sulfilimine bonds, as suggested by the data in Chapter IV. Hexamers isolated from untreated PFHR9 cells displayed 49% monomeric NC1 domains, 33% singly-crosslinked domains, and 18% doubly-crosslinked domain, which is similar to the predicted distribution of hexamers containing an average of two crosslinks (Figure 6.6b). This pattern differed from PBM, which has greater lower dimer than upper dimer banding, and from LBM, which is mostly monomeric (Figure 6.6c).

Finally, the amount of lower dimer in PFHR9 hexamer was similar to GBM. The susceptibility of GBM to Goodpasture autoantibody binding involves a reduced amount of sulfilimine crosslinked NC1 hexamers. Considering PXDN inhibition would likely appear most readily in doubly-crosslinked dimers, further understanding was sought regarding the lower dimer banding from GBM. Only 19% lower dimers were observed, so approximately 1-in-5 NC1 domains are reinforced by two sufiliimine bonds. Since hexamer each have six NC1 domains, this implies that there is one doubly-crosslinked NC1 dimer per 2 hexamers. By this, approximately half of the GBM hexamers possess a doubly-crosslinked dimer.

Identification of Environmental Inhibitors of Bond Formation

If sulfilimine biochemistry exerts protective effects on the hexamer structure, then limiting the degree of bonding by cleavage of sulfilimines or inhibition of formation might be destabilizing within tissues. This process might predispose an individual toward a disease state, and is indeed suspected

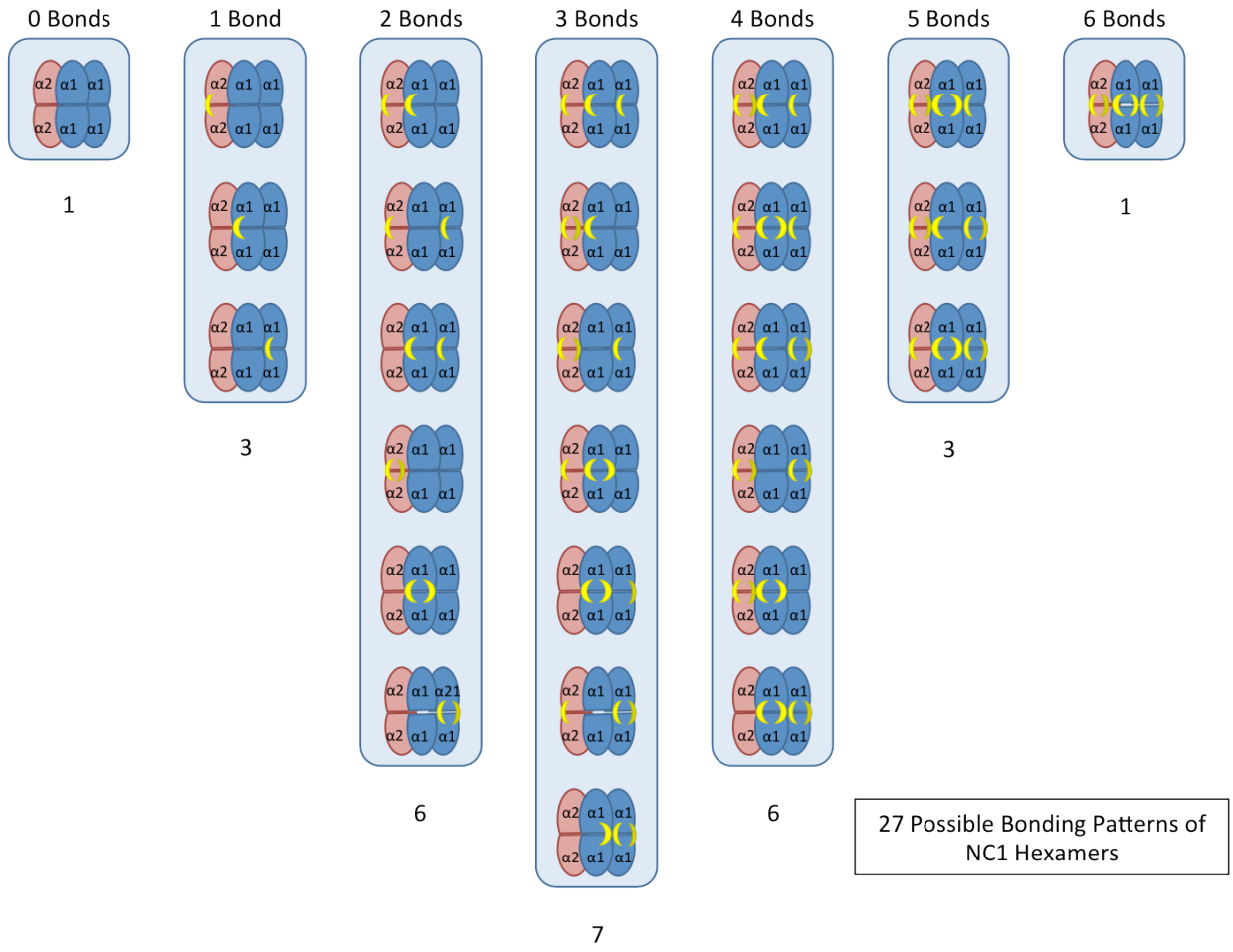

Figure 6.5: Potential Hexamer Sulfimine Bonding Combinations. Individual collagen IV NC1 hexamers may each contain up to 6 sulfilimine bonds, leading to 27 possible bonding patterns. These potential crosslinked forms are categorized into columns by total number of bonds per hexamer, with the number of forms in each category given below the columns. Since kinetic analysis of hexamer assembly revealed binding differences between the two α1 domains in trimers (17), this model of bonding assumes that each NC1 within a trimer represents a structurally distinct crosslinking site.

Bonds per Hexamer	Total NC1 Domains	Monomeric NC1		Single-Crosslinked NC1		Double-Crosslinked NC1	
		Amount	Percent	Amount	Percent	Amount	Percent
0	6	6	**100%**	0	**0%**	0	**0%**
1	18	12	**67%**	6	**33%**	0	**0%**
2	36	18	**50%**	12	**33%**	6	**17%**
3	42	12	**29%**	18	**43%**	12	**29%**
4	36	6	**17%**	12	**33%**	18	**50%**
5	18	0	**0%**	6	**33%**	12	**67%**
6	6	0	**0%**	0	**0%**	6	**100%**

Table 6.1: Predicted Distribution of Crosslinked and Monomeric NC1 Domains According to Hexamer Crosslinking. Table is populated with data derived from modeling of potential sulfilimine bonding combinations.

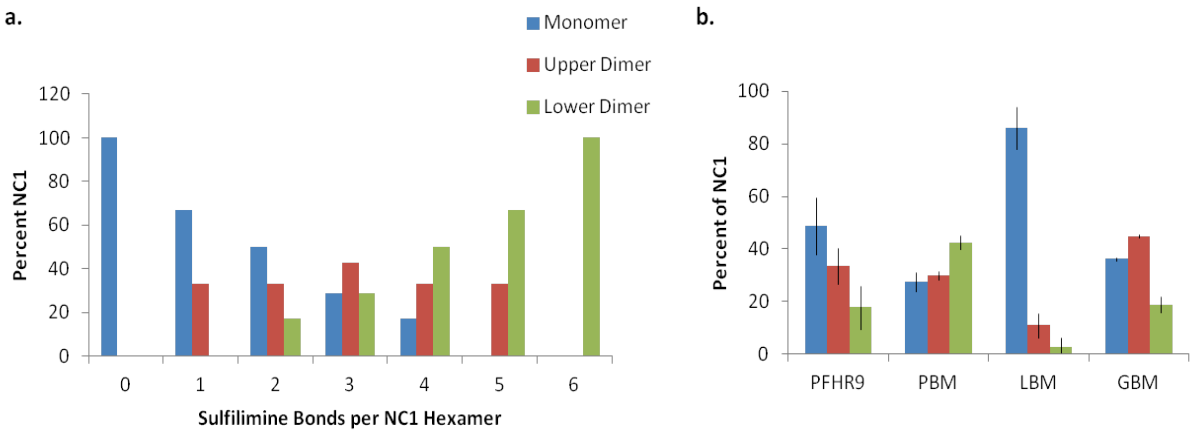

c.

2 Bonds Per Hexamer (theo)	PFHR9 (n=15)	PBM (n=13)	LBM (n=3)	GBM (n=3)
% Monomer	50%	49	28	86	36
% Upper Dimer	33%	34	30	11	45
% Lower Dimer	17%	18	43	3	19

Figure 6.6: Distribution of NC1 Banding by SDS-PAGE due to Crosslinking Status of Hexamer. (**a**) Graphic depiction of expected NC1 populations according to number of sulfilimine bonds per hexamer. (**b**) Quantification of monomer, upper dimer, and lower dimer bands from tissue and cell culture, as observed by SDS-PAGE using 12% gel under non-reducing conditions. (**c**) Densitometry was conducted with ImageJ and analyzed in Excel, while percentages of each NC1 population are given. Percentages are rounded to the nearest whole number, allowing the presence of small errors. Additional protocol details are contained in the Methods section.

Compound	Structure	Notes		Compound	Structure	Notes
Benzene		-Toxic -Organic chemistry synthetic pathways		Toluene		-Solvent -Paint thinner
Phenol		-Plastics manufacturing -Pharmaceutical & herbicide production		Aniline	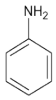	-Polyurethane & dye production -Rubber processing
Resorcinol	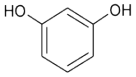	-Skin treatments -Production of dyes and plasticizers		P-toluidine	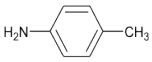	-Cigarette smoke -Dye production -Cyanoacrylate glue
Phloroglucinol	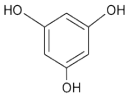	-Dye production -Pharmaceutical & explosives synthsis		M-toluidine	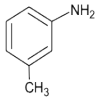	-Cigarette smoke -Dye production -Cyanoacrylate glue
Sulfanilamide	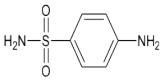	-Dye -Early antimicrobial agent		O-toluidine	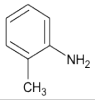	-Cigarette smoke -Dye production -Cyanoacrylate glue

Table 6.2: Panel of Candidate Inhibitors of Bond Formation.

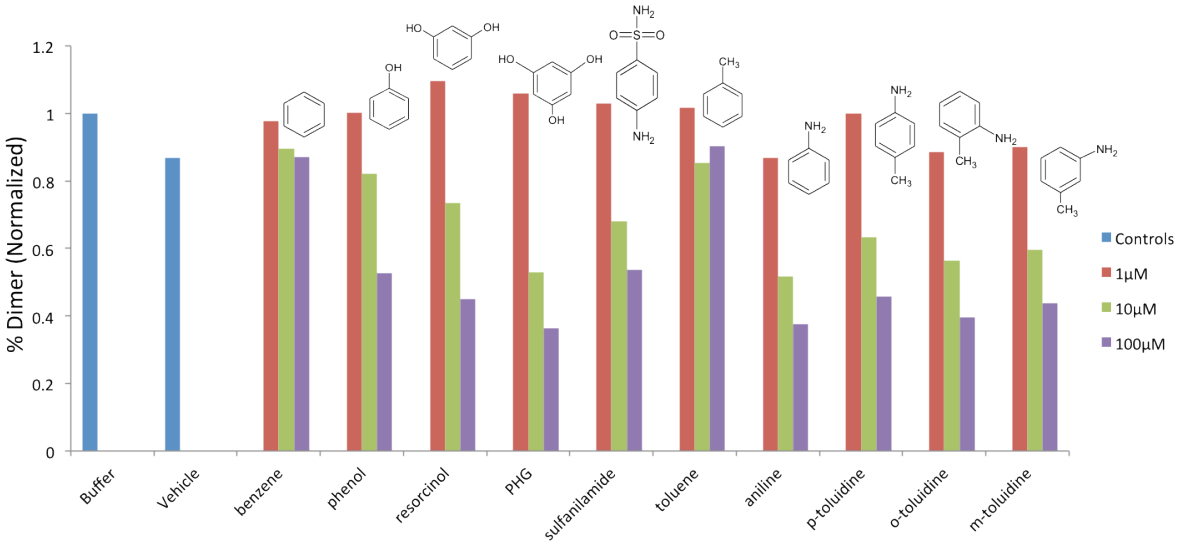

Figure 6.7: Inhibitor Screening in Matrix. Uncrosslinked matrix samples were reacted at 37°C in PBS for 24 hours before being placed at -20°C. Following the reaction, samples were digested with collagenase at 37˚C overnight, and visualized by SDS-PAGE using 12% gels under non-reducing conditions with Coomassie staining. Densitometry was performed with ImageJ and analyzed in Excel. Reagent compounds were solubilized in methanol, and vehicle reactions occurred in 1% methanol (final). Samples were incubated at 4˚C for 1.5 hours in the presence of the candidate inhibitor, before addition of H_2O_2 to 1mM (final) and placing sample at 37˚C. Additional protocol details are contained in the Methods section.

as an etiologic factor of Goodpasture's disease (2). Phenol-based compounds are known to inhibit peroxidases via their affinity for compound II (118). Some Goodpasture's cases have been anecdotally associated with industrial hydrocarbon exposure (55, 69, 70), though the low incidence of disease prevents large cohort studies. In light of this, the issue was approached mechanistically by hypothesizing that PXDN might be similarly inhibited by benzene derivates that are used industrially.

Using PHG (benzenetriol) as a reference, resourcinol (1,3-benzenediol) and phenol were included in the panel. Alternative substituents were examined including toluene (methylbenzene) and aniline (phenylamine). The toluidine series was included, containing methyl and amine substituents, as was sulfanilamide for its bulky substituent (Table 6.2). These compounds have industrial applications within various synthetic pathways such as in the production of rubber and dyes (165, 166), and many are also found in cigarettes (167). In matrix conditions containing 1x PBS and 1 mM H_2O_2 (Figure 6.7), all compounds containing hydrophilic substituents were able to inhibit bond formation at 100 µM, while PHG and aniline both approached 50% inhibition at 10 µM, and o- and m-toluidine showed slightly less inhibition (ca. 40% each) at similar concentration. 1 µM of aniline, o-toluidine, and m-toluidine all showed modest inhibition at 1 µM.

Discussion

Sulfilimine bonds provide structural integrity for NC1 hexamers, which is essential for general tissue stability and function. Yet in a localized sense, the physiologic needs of specific tissues and organs demand the tailored bioactivity of adjacent basement membranes in order to meet those requirements. Certainly this may be accomplished in part via the selective utilization of specific collagen IV chains and networks (α112 networks, α345 networks, or α556 protomers), while from a chemical perspective, sulfilimine bonds provide an additional potential mechanism for adjusting the mechanical properties of basement membranes. By themselves, sulfilimine bonds are sufficient to impart a high degree of

impenetrability to NC1 hexamers, and controlling the amount of suflilimine crosslinking might allow the basement membrane strength to be regulated.

Role of Sulfilimine Bonds Within Basement Membranes

Since collagen IV networks add stability to basement membranes, the hexamer itself is expected to be able to withstand high forces, including tensional and rotational stresses. The type of stress placed on the hexamer may result in distinct forms of strain at the trimer-trimer interface. Pulling by the collagenous domain will expectedly place tension on the hexamer, while helix twisting is likely translated into sheer stress at the interface. Electrostatic interactions along the hexamer interior likely allow the structure to resist rotational strain, as well as ensuring the proper alignment of subunits during assembly. In counterpart, the covalent sulfilimine bonds are located at the periphery of the interface, likely enabling any tensional forces to be distributed along the longitudinal axis from one protomer to the next, thereby allowing the collagen IV network to resist stretching.

Quite interesting is the varying degrees of sulfilmine bond formation found in tissue-specific patterns. Though there is a paucity of empirical evidence regarding the functional significance for these observations, an intellectual approach to the issue yields some particularly intriguing observations, albeit spectulative in nature. At one end of the spectrum are strongly crosslinked networks with copious amounts of doubly-crosslinked NC1 dimers as seen in GBM and PBM. Due to the stresses exerted by blood flow and the maternal priority of providing protection to the developing fetus, both the GBM and PBM likely benefit from collagen IV networks with high rigidity. This contrasts with the poorly crosslinked collagen IV networks of LBM. Ocular physiology is vastly different from both renal and placental physiology, particularly due to the conformational changes required for focusing during sight. Incoming light is refracted through the ocular lens, and eyes focus on near or far away objects by adjusting the shape of the lens via attached muscles. By inference, the lens capsule basement

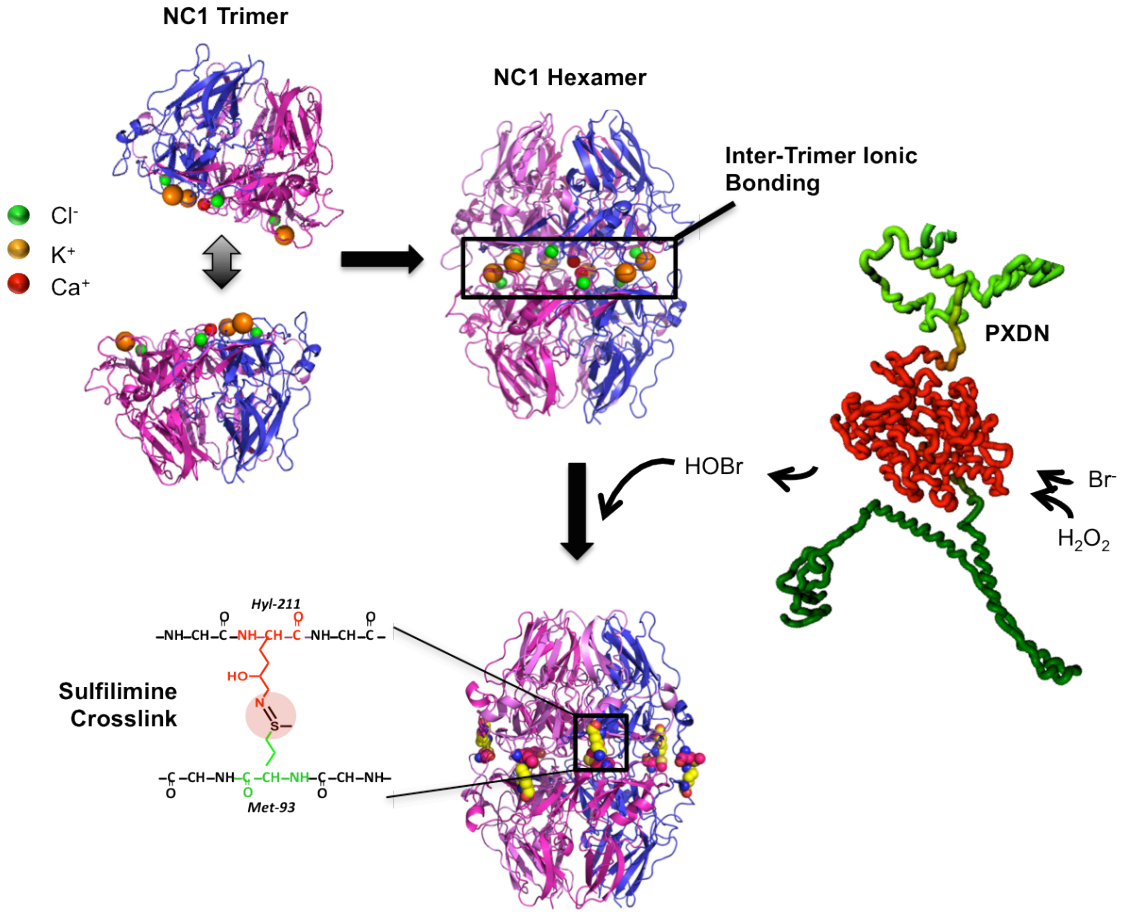

Figure 6.8: Working Model of NC1 Hexamer Assembly and Sulfilimine Bond Formation.

membrane might benefit from enhanced elasticity with rigidity present in moderation only. In the pathologies associated with *PXDN* mutations in humans (107), it is unclear whether the phenotype resulted from lack of sulfilimine bonds or was due to loss of an unrelated and unknown PXDN function.

Coincidentally, it is interesting to note that chloride is abundant near the highly-crosslinked placental and glomerular basement membranes (ca. 100 mM Cl in serum), contrasting with the weakly-crosslinked lens basement membrane that has a low chloride concentration (ca.3 mM) (168). While halide concentrations alone are not a sufficient proxy for estimating sulfilimine bonding, the associated amounts of chloride and crosslinks are indeed circumstantial and form a tempting basis from which to speculate about causality.

Hexamer Instability & Disease

Unquestionably, the degree of sulfilimine crosslinking fluctuates according to tissue location, likely as a means for adjusting to the particular physiologic needs of the locale. Yet disease may ensue in the absence of functioning crosslinks, mechanistically ocuring via damage to the bond, inhibition of formation, or their overabundance. The lack of bonds are strongly tied to the etiology of Goodpasture's while excessive crosslinking may be pertinent in some forms of fibrosis with expressed PXDN (169).

The sulfilimine bond is a structural element of hexamers, and is important to the binding of Goodpasture autoantibodies to NC1 hexamers. Categorically, Goodpasture's disease is considered a "conformorpathy" (50), and loss of the crosslink may allow the NC1 autoantigen to assume a pathological antigenic conformation. Localization of the disease to alveolar and glomerular basement membranes without spreading to alternative sites of α3 expression may support a putative role for an environmental etiologic component that damages the collagen IV network, where the agent is present in serum and/or is airborne. Damage of the sulfilimine bond or the inhibition of its formation may participate in the disease etiology, although other risk factors are likely involved as well.

Environmental compounds provide an avenue for potentially interfering with bond formation. Some phenol derivatives are known to have high affinity for compound II of peroxidases (118), thereby inhibiting enzymatic activity. PHG falls into this category, although its mechanism of PXDN inhibition is unknown. Among the panel of inhibitors tested, the concentration of o-toluidine in urine has been shown to be within a nanomolar to low micromolar range in workers following their work shifts at a rubber chemicals plant (153). Thus it is plausible that environmental compounds do indeed modulate the amounts of sulfiilimine crosslinking in tissue.

In an autoimmune response, antigen-presenting cells are responsible for the robust humoral response by activating auto-reactive B cells. This involves proteolytic processing of internalized antigen by the antigen-presenting cell and presentation of the auto-eptitope to B cells. Considering the sulfilimine influence on NC1 conformation, it is reasonable to presume that processing of the α3 NC1 auto-antigen might be dependent whether it is sulfilimine crosslinking (84). Uncrosslinked auto-antigens might lead to the presentation of disease-associated epitopes, causing B cells to mistake "self" for "foreign" peptides, and might thus participate in the etiology of Goodpasture's disease.

Conclusion

The assembly of collagen IV networks involves an intricate sequence of events and with notable functional components. The requirement for chloride delineates a novel role for the ion within network formation, and its activity is coordinated with that of bromide during sulfilimine bond catalysis. The activity of chloride ultimately leads to hexamer formation, which is a prerequisite event for sulfilimine bond formation. The PXDN-catalyzed sulfilimine bonding reinforces the hexamer, resulting in the covalent joining of adjacent collagen IV protomers.. The final networked product reflects the symphony of chemistry and biology whose coordinated activities provide a foundation for physiology. Perturbation of the crosslinked network creates dissonance within tissues, and can lead to pathologic outcomes.

Methods

Materials

All chemicals were purchased from Sigma-Aldrich (St. Louis, MO) unless noted otherwise. The protocols for PFHR9 cell culture and isolation of collagen IV matrix were identical to that in Chapter III. Collagen IV matrix was produced in the presence of 1 mM KI to inhibit bond formation or alternatively with 10 mM KBr to enhance crosslinking. After digestion of uncrosslinked matrix with collagenase enzyme, supernatant was passed over DEAE-Cellulose column in 50 mM Tris-HCl (pH 7.5). The flow through fractions were used as a source of collagen IV NC1 proteins, and also contained 7S domains that were co-purified.

NC1 Hexamer Dissociation

NC1 hexamers were dissociated via dialysis into low-halide buffer, identically to the methods in Chapter V. Briefly, hexamer samples at 1mg/ml in 50 M Tris-HCl (pH 7.5) were extensively dialyzed into 50 mM Tris-acetate (Tris-Ac, pH 7.4). Sample volumes of 0.3-6 ml were dialyzed into 1 L of buffer overnight at 4°C, followed by one buffer change into 1 L of fresh buffer. After dissociation, samples were centrifuged at 14000 rpm for 15 min at 5°C before assessment by gel filtration chromatography. A Superdex™ 200 10/300GL gel filtration column (GE Healthcare Life Sciences; Piscataway, NJ) attached to a ÄKTA Purifier P-900 HPLC (GE Healthcare Life Sciences; Piscataway, NJ) was used to perform gel filtration, and was operated with Unicorn software. Chromatography was conducted under fast protein liquid chromatography conditions as in Chapter V.

In vitro *HOBr Crosslinking Assay*

HOBr was synthesized from hypochlorite and reacted with 5 µM of either assembled hexamers or dissociated NC1 domains, using the same methods as in Chapter IV. Both NC1 populations were

produced in PHFR9 cell culture in the presence of 1 mM KI to inhibit crosslinking. NC1 domains were dissociated by extensive dialysis into 50 mM Tris-Ac at 4°C. After the reaction, the samples were assessed for crosslink formation by SDS-PAGE and Coomassie Blue R250 staining according to the protocols from Chapter IV for *in vitro* HOBr bond formation reactions.

Structural Modeling of NC1 Hexamers

PYMOL software (162) was used to generate models of the NC1 domains, using the same methodology as in Chapter V. All modeling was conducted by K. Brown.

Hexamer Crosslinking Analysis

Potential permutations of NC1 hexamer crosslinking were diagramed in PowerPoint (Microsoft Office 2007). The predicted distribution of monomeric, singly-crosslinked, and doubly-crosslinked NC1 domains was calculated from the permutation diagram. First, the individual permutations were grouped according to the total number of sulfilimine crosslinks per hexamer and the total number of NC1 domains was summed for each group. The number of NC1 domains participating in single- or double-crosslinking populations, as well as the number of monomeric NC1 domains, were identified. Finally, the size of each population per group was expressed as a percent of the total NC1 per group in Excel. Position of the bond within the hexamer was accounted for due to known differences in the binding kinetics between α1 and α2 domains with respect to the orientation of α2 NC1 during the interaction.

For application of the above crosslinking analysis, the NC1 banding patterns of PBM, LBM, GBM, and untreated PFHR9 matrices were analyzed in SDS-PAGE using 12% non-reducing gels. Interpretation of the dual dimer banding denoted upper dimer bands as containing one sulfilimine bond per dimer and lower bands possessing two bonds per dimer. After measuring the densitometry by ImageJ, the relative amounts of monomer, upper dimer, and lower dimer were determined in Excel.

Matrix Crosslinking Reactions

To assess whether halides can protect NC1 domains in matrix, potassium fluoride and sodium gluconate were added to uncrosslinked matrix that had been washed extensively in 10 mM phosphate buffer (pH 7.4) to remove endogenous halides. Bond formation in matrix was conducted identically to the protocols described in Chapter IV, where potassium bromide was titrated into matrix samples and the reaction initiated by addition of 1mM H_2O_2. Reaction was carried out at 37˚C for 12.5 hours before quenching by addition of PHG to 200 µM final and placing at -20˚C.

Uncrosslinked matrix was produced in PFHR9 culture via 1 mM KI treatment, and purified according to the protocol in Chapter III. Following the low salt buffer wash, samples were then washed into 1x PBS at 4°C. To screen for inhibition of crosslinking in matrix, samples were assayed for matrix crosslinking activity in the presence of the putative inhibitor candidates, as in Chapter IV. Prior to the reaction, samples were incubated with the candidates for 1.5 hours at 4˚C in 1x PBS, and the reaction was initiated by addition of H_2O_2 to 1 mM and placing samples at 37°C. All inhibitors were solubilized in methanol, and reactions occurred in the presence of up to 1% methanol. Final reaction volumes were 200 µM.

After all crosslinking assays, samples were stored at -20°C before overnight digestion with bacterial collagenase. Supernatants from digests were separated by SDS-PAGE in 12% gels under non-reducing conditions and Coomassie Blue R250 staining. Densitometry was measured and analyzed in ImageJ and Excel, respectively.

Chapter VII

FUTURE DIRECTIONS

Collagen IV sulfilmine bonds have unveiled a pandora's box of novel biologic mechanisms within basement membranes. The celebration of these discoveries spawns fresh questions that probe deeper into the basic science, seeking the advancement of knowledge and the bettering of mankind. This chapter outlines a non-exhaustive list of such questions and strategies for approach.

What is the mechanism for HOBr catalysis of sulfilimine bonds?

The fact that HOBr catalyzes sulfilimine bonds raises the question of whether there are mechanistic differences between the chemistry of HOBr-mediated destructive oxidation and biosynthesis. The NC1 hexamer itself seems to influence the reaction, as seen in its poor reactivity to HOI. Furthermore, it is quite ironic that the two functional groups joined through sulfilimine bonds are both readily reactive with HOBr (118). Delineating the initial target of HOBr via kinetic studies would certainly give additional insight to the mechanism of sulfilimine bond formation, but it may also illuminate key features that define anabolic functions of hypohalous acids.

Can sulfilimine bonds be used to direct cellular activity?

Sulfilmine bonds reinforce the NC1 hexamer, while genetic evidence implies the essential tissue function of these bonds (4). Further understanding of the underlying outside-in signaling may be facilitated by directly examining the relationship between collagen IV networks and cellular behavior. Sulfilmine crosslinking can indeed be modulated in culture with effects seen by SDS-PAGE and gel filtration, though atomic force measurements of the resultant stiffness of matrices would provide a

valuable quantitative framework. Furthermore, great insight may be gained by assessing the cellular response to variable amounts of sulfilimine bonds, such as through cell binding and migration assays.

How is PXDN activity modulated within basement membranes?

PXDN is an oxidant-generator within basement membranes that is vulnerable to pharmacologic inhibition, as seen through the data obtained in this work. Inhibition of enzymatic activity would reduce the amount of sulfilimine crosslinking within a basement membrane, while deregulation of the enzyme could cause oxidative stress. Environmental compounds are here shown to influence crosslinking *in vitro*, though their influences *in vivo* are not established within the context of basement membranes. A feasible approach might be to analyze the effects of phloroglucinol and analine *in vivo* with respect to sulfilimine bond formation within the vasculature.

APPENDIX A

LIST OF PUBLICATIONS

1. *Bhave, G., ***Cummings, C.F***., *Vanacore, R.M., Kumagai-Cresse, C., Ero-Tolliver, I.A., Rafi, M., Kang, J.S., Pedchenko, V., Fessler, L.I., Fessler, J.H., Hudson, B.G. 2012. Peroxidasin forms sulfilimine chemical bonds using hypohalous acids in tissue genesis. *Nat Chem Biol*. 8:784-790
   *Co-contributors

2. **Cummings, C.F.,** Bhave, G., McCall, A.S., Hudson, B.G. The element bromine is essential for tissues (*in preparation*)

3. Madu, H., Avance, J., Chetyrkin, S., Rose, K.L., Sanchez, O.A., Brown, K.L., **Cummings, C.F.,** Voziyan, P., Hudson, B. Halogenation contributes to protein damage in diabetes. (*in preparation*)

REFERENCES

1. Vanacore, R., Ham, A.L., Voehler, M., Sanders, C.R., Conrads, T.P., Veenstra, T.D., Sharpless, K.B., Dawson, P.E., Hudson, B.G. 2009. A sulfilimine bond in collagen IV. *Science.* 325:1230-1234

2. Vanacore, R., Pedchenko, V., Bhave, G., Hudson, B.G. 2001. Sulphilimine cross-links in Goodpasture's disease. *Clin. Exp. Immunol*. 164:4-6

3. Hudson, B.G., Tryggvason, K., Sundaramoorthy, M., Neilson, E.G. 2003. Alport's Syndrome, Goodpastures' Syndrome, and type IV collagen. *N. Eng. J. Med.* 348:2543-2556

4. Bhave, G., Cummings, C.F., Vanacore, R.M., Kumagai-Cresse, C., Ero-Tolliver, I.A., Rafi, M., Kang, J.S., Pedchenko, V., Fessler, L.I., Fessler, J.H., Hudson, B.G. 2012. Peroxidasin forms sulfilimine chemical bonds using hypohalous acids in tissue genesis. *Nat. Chem. Biol*. 8:784-790

5. Nagy, P., Beal, J.L., Ashby, M.T. 2006. Thiocyanate is an efficient endogenous scavenger of the phagocytic killing agent hypobromous acid. *Chem. Res. Toxicol*. 19:587-593

6. Fuji, R., Yoshida, H., Fukusumi, S., Habata, Y., Hosoya, M., Kawamata, Y., Yano, T., Hinuma, S., Kitada, C., Asami, T., Mori, M., Fujisawa, Y., Fujino, M. 2002. Identification of a neuropeptide modified with bromide as a endogenous ligand for GPR-7. *J Biol. Chem*. 277:34010-34016

7. Tanaka, H., Yoshida, T., Miyamoto, N., Motoike, T., Kurosu, H., Shibata, H., Yamanaka, A., Williams, S.C., Richardson, J.A., Tsujino, N., Garry, M.G., Lerner, M.R., King, D.S., O'Dowd, B.F., Sakurai, T., Yanagisawa, M. 2003. Characterization of a family of endogenous neuropeptide ligands for the G protein-coupled receptors GPR7 and GPR8. *Proc. Natl. Acad. Sci. U. S. A*. 100:6251-6256

8. Wu, W., Samoszuk, M.K., Comhair, S.A.A., Thomassen, M.J., Farver, C.F., Dweik, R.A., Kavuru, M.S., Erzurum, S.C., Hazen, S.L. 2000. Eosinophils generate brominating oxidants in allergen-induced asthma. *J. Clin. Invest*. 105:1455-1463

9. Vanacore, R.M., Shanmugasundararaj, S., Friedman, D.B., Bondar, O., Hudson, B.G., Sundaramoorthy, M. 2004. The α1.α2 network of collagen IV. Reinforced stabilization of the noncollagenase domain-1 by noncovalent forces and the absense of Met-Lys crosslinks. *J. Biol. Chem*. 279:44723-44730

10. Hynes, R.O. 2009. The extracellular matrix: not just pretty fibrils. *Science*. 326:1216-1219

11. Poschl, E., Schlotzer-Schrehardt, U., Brachvogel, B., Saito, K., Ninomiya, Y., Mayer, U. 2004. Collagen IV is essential for basement membrane stability but dispensable for initiation of its assembly during early development. *Development*. 131:1619-1628

12. Guptam M.C., Graham, P.L., Kramer, J.M. 1997. Characterization of α1(IV) collagen mutations in *Caenorhabditis elegans* and the effects of α1 and α2(IV) mutations on type IV collagen distribution. *J. Cell. Biol*. 137:1185-1196

13. Borchiellini, C., Coulon, J., Le Parcom, Y. 1996. The function of type IV collagen during *Drosophila* muscle development. *Mech. Dev*. 58:179-191

14. Templ, R., Bruckner, P., Fietzek, P. 1979. Characterization of pepsin fragments of basement membrane collagen obtained from a mouse tumor. *Eur. J. Biochem*. 95:255-263

15. Risteli, J., Bachinger, H.P., Engel, J., Furthmayr, H., Timpl, R. 1980. 7-S collagen: characterization of an unusual basement membrane structure. *Eur. J. Biochem*. 108:239-250

16. Boutaud, A., Borza, D.B., Bondar, O., Gunwar, S., Netzer, K.O., Singh, B., Ninomiya, Y., Sado, Y., Noelken, M.E., Hudson, B.G. 2000. Type IV collagen of the glomerular basement membrane: evidence that the chain specificity of network assembly is encoded by the noncollagenous NC1 domains. *J. Biol. Chem.* 275:30716-30724

17. Khoshnoodi, J., Sigmundsson, K., Cartailler, J.P., Bondar, O., Sundaramoorthy, M., Hudson, B.G. 2006. Mechanism of chain selection in the assembly of collagen IV: a prominent role for the α2 chain. *J. Biol. Chem*. 281:6058-6069

18. Sundaramoorthy, M., Meiyappan, M., Todd, P., Hudson, B.G. 2002. Crystal structure of NC1 domains: structural basis for type IV collagen assembly in basement membranes. *J. Biol. Chem*. 277:31142-31153

19. Timpl, R., Wiedemann, H., van Delden, V., Kuhn, K. 1981. A network model for the organization of type IV collagen molecules in basement membranes. *Eur. J. Biochem*. 120:203-211

20. Yurchenco, P.D. and H. Furthmayr. 1984. Self-assembly of basement membrane collagen. *Biochemistry*. 23:1839-1850

21. Gould, D.B., Phalan, F.C., Breedveld, G.J., van Mil, S.E., Smith, R.S., Schimenti, J.C., Aguglia, U., van der Knaap, M.S., Heutink, P., John, S.W.M. 2005. Mutations in *Col4a1* cause perinatal cerebral hemorrhage and porencephaly. *Science*. 308:1167-1171

22. Gould, D.B., Phalan, F.C., Saskia, B.A., van Mil, Sundber, J.P., Vahedi, K., Massin, P., Bousser, M.G., Heutink, P., Miner, J.H., Tournier-Lasserve, E., John, S.W.M. 2006. Role of COL4A1 in small-vessel disease and hemorrhagic stroke. *N. Eng. J. Med.* 354:1489-1496

23. Fox, M.A., Sanes, J.R., Borza, D.B., Eswarakumar, V.P., Fasser, R., Hudson, B.G., John, S.W.M., Ninomiya, Y., Pedchenko, V., Pfaff, S.L., Rheault, M.N., Sado, Y., Segal, Y., Werle, M.J., Umemori, H. 2007. Distinct target-derived signals organize formation, maturation, and maintenance of motor nerve terminals. *Cell*. 129:179-193

24. Koper, A., Schenck, A., Prokop, A. 2012. Analysis of adhesion molecules and basement membrane contributions to synaptic adhesion at the *Drosophila* embryonic NMJ. *PLoS One.* 7(4):e36339

25. Pastor-Pareja, C.J. and T. Xu, 2011. Shaping cells and organs in *Drosophila* by opposing roles of fat body-secreted collagen IV and perlecan. *Dev. Cell*. 21:245-256

26. Koshnoodi, J., Pedchenko, V., Hudson, B.G. 2008. Mammalian collagen IV. *Microsc. Res. Tech*. 71:357-370

27. Kramer, J.M. 2005. *WormBook*. Ed. The *C. elegans* Research Community, WormBook

28. Oka, Y., Naito, I., Manabe, K., Sado, Y., Ninomiya, Y., Mizuno, M., Tsuji, T. 2002. Distribution of collagen type IV alpha1-6 chains in human normal colorectum and colorectal cancer demonstrated by immunofluorescense staining using chain-specific epitope-define monoclonal antibodies. *J. Gastroenterol. Hepatol*. 17:980-986

29. Hynes, R.O. 2007. Cell-matrix adhesion in vascular developmet. *J. Throm. Haemost*. Suppl 1:32-40

30. Wang, X., Harris, R.E., Bayston, L.J., Ashe, H.L. 2008. Type IV collagens regulate BMP signaling in *Drosophila*. *Nature*. 455:72-77

31. Sawala, A., Sutcliffe, C., Ashe, H.L. 2012. Multistep molecular mechanism for Bone morephogenetic protein extracellular transport in the *Drosophila* embryo. *Proc. Nat. Acad. Sci. U. S. A.* 109:11222-11227

32. Ashe, H.L. 2008. Type IV collagens and DPP. *Landes Bioscience*. 2:313-315

33. Bunt, S., Hooley, C., Hu, N., Scahill, C., Weavers, H., Skaer, H. 2010. Hemocyte-secreted type IV collagen enhances BMP signaling to guide renal tubule morphogenesis in *Drosophila*. *Dev. Cell*. 19:296-306

34. Shieh, A.C. 2011. Biomechanical forces shape the tumor microenvironment. *Ann. Biomed. Eng*. 39:1379-1389

35. Pathak, A., and S. Kumar. 2012. Inependent regulation of tumor cell migration by matrix stiffness and confinement. *Proc. Nat. Acad. Sci. U. S. A*. 109:10334-10339

36. Petitclerc, E., Boutaud, A., Prestayko, A., Xu, J., Sado, Y., Ninomiya, Y., Sarras, M.P., Hudson, B.G., Brooks, P.C. 2000. New functions for non-collagenous domains of human collagen type IV: novel integrin ligands inhibiting angiogenesis and tumor growth *in vivo*. *J. Biol. Chem*. 275:8051-8061

37. Cretu, A. and P.C. Brooks. 2007. Impact of the non-celular tumor microenvironment on metastasis: potential therapeutic and imaging opportunities. *J. Cell. Physiol*. 213:391-402

38. Rowe, R.G and S.J. Weiss. 2008. Breaching the basement membrane: who, when and how?. *Tends Cell. Biol*. 18:560-574

39. Burnier, J.V., Wang, N., Michel, R.P., Hassanain, M., Li, S., Lu, Y., Metrakos, P., Antecka, E., Burnier, M.N., Ponton, A., Gallinger, S., Brodt, P. 2011. Type IV collagen-initiated signals provide survival and grwth cues required for liver metastasis. *Oncogene*. 30:3766-3783

40. Gilcrist, T.L. and C.J. Moody. 1976. The chemistry of sulfilimines. *Chem. Rev*. 77:409-435

41. Koval, I.V. 1990. Progress in the chemistry of sulfilimines. *Russ. Chem. Rev*. 59:1409-1430 (translated from *Uspekhi Khimii*)

42. Pichierri, F. 2010. Theoretical characterization of the sulfilimine bond: double or single?. *Chem Phys Lett*. 487:315-319

43. Glass, R.S. and J.R. Duchek. 1976. The structure of dehydromethionine: an azasulfonium salt. *J. Am. Chem. Soc*.98:965-969

44. Oncak, M., Berka, K., Slavicek, P. 2011. Novel covalent bond in proteins: calculations on model systems question the bond stability. *ChemPhysChem*. 12:3449-3457

45. Lavine, T.F. 1943. An iodometric determination of methionine. *J. Biol. Chem*. 151:281-297

46. Peskin, A.V., Turner, R., Maghzal, G.J., Winterbourn, C.C., Kettle, A.J. 2009. Oxidation of methionine to dehydrmethionine by reactive halogen species generated by neutrophils. *Biochemistry*, 48:10175-10182

47. Fu, X., Mueller, D.M., Heinecke, J.W. 2002. Generation of intramolecular and intermolecular sulfenamides, sulfinamides, and sulfonamides by hypochlorous acid: a potential pathway for oxidative cross-linking of low-density lipproein by myeloperoxidase. *Biochemistry*. 41:1293-1301

48. Beal, J.L., Foster, S.B., Ashby, M.T. 2009. Hypochlorous acid reacts with the N-terminal methionines of proteins to give dehydromethionine, a potential biomarker for neutrophil-induced oxidative stress. *Biochemistry.* 48:11142-11148

49. Raftery, M.J., Yang, Z., Valenzuela, S.M., Geczy, C.L. 2001. Novel intra- and inter-molecular sulfinamide bonds in S100A8 produced by hypochlorite oxidation. *J. Biol. Chem*. 276:33393-33401

50. Pedchenko, V., Bondar, O., Fogo, A.B., Vanacore, R., Voziyan, P., Kitching, R., Wieslander, J., Kashtan, C., Borza, D.B., Neilsn, E.G., Wilson, C.B., Hudson, B.G. 2010. Molecular architecture of the Goodpasture autoantigen in anti-GBM nephritis. *N. Eng. J. Med*. 363:343-354

51. Borza, D.B., Bondar, O., Colon, S., Todd, P., Sado, Y., Neilson, E.G., Hudson, B.G. 2005. Goodpasture autoantibodies unmask cryptic epitopes by selectively dissociating autoantigen complexes lacking structural reinforcement: novel mechanisms for immune privilege and autoimmune pathogenesis. *J. Biol. Chem*. 280:27147-27154

52. Vanacore, R.M., Ham, A.J.L., Cartailler, J.P., Sundaramoorthy, M., Tod, P., Pedchenko, V., Sado, Y, Borza, D.B., Hudson, B.G. 2008. A role for collagen IV cross-links in conferring immune privilege to the Goodpasture autoantigen: structural basis for the crypticity of B cell epitopes. *J. Biol. Chem*. 283:22737-22748

53. Phelps, R.G., Jones, V. Turner, A.N., Rees, A.J. 2000. Properties of HLA class II molecules divergently associated with Goodpasture's disease. *Intl. Immunol.* 12:1135-1143

54. Zhou, X.J., Lv, J.C., Zhao, M.H., Zhang, H. 2010. Advances in the genetics of anti-glomerular basement membrane disease. *Am. J. Nephrol.* 32:483-490

55. Bombassei, G. J. and A.A Kaplan. 1992. The association between hydrocarbn exposure and anti-glomerular basement membrane antibody-mediated disease (Goodpasture's Syndrome). *Am. J. Ind. Med*. 21:141-153

56. Goodpasture, E.W. 1919. The significance of certain pulmonary lesions in relation to the etiology of influenza. *Am. J. Med. Sci.* 158:863-870

57. Stanton, M.C. and J.D. Tange. 1958. Godpasture's syndrome (pulmonary hemorrhage associated with glomerulonephritis). *Aust. Ann. Med*. 7:132-144

58. Ooi, J.D., Holdsworth, S.R., Kitching, A.R. 2008. Advances in the pathogenesis f Goodpasture's disease: from epitopes to autoantibodies to effector T cells. *J. Autoimmunity*. 31:295-300

59. Kluth, D.C. and A.J. Rees. 1999. Anti-glomerular basement membrane disease. *J. Am. Soc. Nephrol.* 10:2446-2453

60. Saus, J., Wieslander, J., Langeveld, J.P.M., Quinones, S., Hudson, B.G. 1988. Identification of the Goodpasture antigen as the α3(IV) chain of collagen IV. *J. Biol. Chem*. 263:13374-13380

61. Lerner, R.A., Glassock, R.J., Dixon. F.J. 1967. The role of anti-glomerular basement membrane antibody in the pthogenesis of human glomerulonephritis. *J. Exp. Med*. 126:989-1004

62. Kitagawa, W., Imai, H., Komatsuda, A., Maki, N., Wakui, H., Hiki, Y., Sugiyama, S. 2008. The HLA-DRB1*1501 allele is prevalent among Japanese patients with anti-glomerular basement membrane antibody-mediated disease. *Nephrol. Dial. Transplant*. 10:3126-3129

63. Handunnetthi, L., Ramagopalan, S.V., Ebers, G.C. 2010. Multiple sclerosis, vitamin D, and HLA-DRB1*15 *Neurology*. 74:1905-1910

64. Furukawa, F. and M. Muto. 2009. Ethnic differences in immunogenetic features and photosensitivity of cutaneous lupus erythematosus. *Arch. Dermatol. Res*. 301:111-115

65. Luo, H., Chen, M., Yang, R., Xu, P.C., Zhou, X.J., Zhao, M.H. 2011. The association of HLA-DQB1, -DQA1, and –DPB1 alleles with anti-glomerular basement membrane (GBM) disease in Chinese patients. *BMC Nephrol*. 12:21

66. Phelps, R.G., Turner, A.N., Rees, A.J. 1996. Direct identification of naturally processed autoantigen-derived peptides bound to HLA-DR15. *J. Biol. Chem*. 271:18549-18553

67. Zhou, X.J., Lv, J.C., Bu, D.F., Yu, L., Yang, Y.R., Zhao, J., Cui, Z., Yang, R., Zhao, M.H., Zhang, H. 2009. Copy number variation of *FCGR3A* rather thatn *FCGR3B* and *FCGR2B* is associated with susceptibility to anti-GBM disease. *Int. Immunol*. 22:45-51

68. Nakamura, A., Yuasa, Y., Ujike, A., Ono, M., Nukiwa, Y., Ravetch, J.V., Takai, Y. 2000. Fcγ IIB-deficient mice develop Goodpasture's Syndrome upon immunization with type IV collagen: a

novel murine model for autoimmne glomerular basement membrane disease. *J. Exp. Med*. 191:899-905

69. Stevenson, A., Yaqoob, M., Mason, H., Pai, P., Bell, G.M. 1995. Biochemical markers of basement membrane disturbances and occupational exposure to hydrocarbonds and mixed solvents. *Q. J. Med*. 88:23-28

70. Donaghy, M. and A.J. Rees. 1983. Cigarette smoking and lung haemorrhage in glomerulonephritis caused by autoantibodies to glomerlar basement membrane. *Lancet.* 2:1392-1392

71. Cui, Z., Wang, H.Y., Zhou, M.H. 2006. Natural autoantibodies against glomerular basement membrane exist in normal human sera. *Kidney Intl*. 69:894-899

72. Cui, Z., Zhar, M.H., Segelmark, M., Hellmark, T. 2010. Natural autoantibodies to myeloperoxidase, peroteinase 3, and the glomerular basement membrane are present in normal individuals. *Kidney Intl*. 78:590-597

73. Zou, J., Hannier, S., Cairns, L.S., Barker, R.N., Rees, A.J., Turner, A.N., Phelps, R.G. 2008. Healthy individuals have Goodpasture autoantigen-reactive T cells. *J. Am. Soc. Nephol*. 19:396-404

74. Elkon, K. and P. Casali. 2008. Nature and functions of autoantibodies. *Nat. Chem. Pract. Rheum.* 4:491-498

75. Avrameas, S. 1991. Natural autoantibodies: from 'horror autotoxicus' to gnothi seauton' *Immunol. Today*. 12:154-159

76. Anderson, C.J., Neas, B.R., Pan, Z. Taylor-Albert, E., Reichlin, M., Stafford, H.A. 1998. The presence of masked antiribosomal P autoantiboides in healthy children. *Arthritis. Rheum*. 41:33-40

77. Dwyer, D.S., Bradley, R.J., Urquhart, C.K., Kearney, J.F. 1983. Naturally occurring anti-idiotypic antibodies in myasthenia gravis patients. *Nature*. 301:611-614

78. Graybar, P. 1983. Autoantibodies and the physiological role of immunoglobulins. *Immunol. Today,* 4:337-339

79. Zhao, J., Yan, Y., Cui, Z., Yang, R., Zhao, M.H. 2009. The immunoglobulin G subclass distribution of anti-GBM autoantibodies against rHα3(IV)NC1 is associated with disease severity. *Hum. Immunol.* 70:425-429

80. Cui, Z., Zhao, M.H., Singh, A.K., Wang, H.Y. 2007. Antiglomerular basement membrane disease with normal renal function. *Kidney Intl*. 72:1403-1408

81. Cairns, L.S., Phelps, R.G., Bowie, L., Hall, A.M., Saweirs, W.W., Rees, A.J., Barker, R.N. 2003. The fine specificity and cytokine profile of T-helper cells responsive to the alpha3 chain of type IV collagen in Goodpasture's disease. *J. Am. Soc. Nephrol*. 14:2801-1012

82. Zou, J., Henderson, L., Thomas, V., Swan, P., Turner, A.N., Phelps, R.G. 2007. Presentation of the Goodpasture autoantigen requires proteolytic unlocking steps that destroy prominent T cell epitopes. *J. Am. Soc. Nephrol.* 18:771-779

83. Simitsek, P.D>, Campbell, D.G., Lanzavecchia, A., Fairweather, N., Watts, C. 1995. Modulation of antigen processing by bound antibodies can boost or suppress class II major histocompatibility complex presentation of different T cell determinants. *J. Exp. Med*. 181:1957-1963

84. Dai, Y, Carayanniotis, K.A., Elliades, P., Lymberi, P., Shepherd, P., Kong Y.C., Carayanniotis, G., 1999. Enhancing or suppressive effects of antibodies on processing of a pathogenic T cell epitope in thyroglobulin. *J. Immunol*. 162:6987-6992

85. Lin, R.H., Mamula, M.J., Hardin, J.A., Janeway, C.A. 1991. Induction of autoreactive B cells allows priming of autoreactive T cells. *J. Exp. Med.* 173:1433-1439

86. Yan, J., Harvey, B.P., Gee, R.J., Shlomchik, M.J., Mamula, M.J. 2006. B cells drive early T cell autoimmunity in vivio prior to dendritic cell-mediated autoantigen presentation. *J. Immunol.* 177:4481-4487

87. Chan, O. and M.J. Schlomchik, 1998. A new role for B cells in systemic autoimmunity: B cells promote spontaneous T cell activation in MRL-lpr/lpr mice. *J. Immunol.* 160:51-59

88. Yan, J. and M.J. Mamula. 2002. B and T cell tolerance and autoimmunity in autoantibody transgenic mice. *Int. Immunol.* 14:963-971

89. Serreze, D.V., Chapman, H.D., Varnum, D.S., Hanson, M.S., Reifsnyder, P.C., Richard, S.D., Fleming, S.A., Leiter, E.H., Shultz, L.D. 1996. B lymphocytes are essential for the initiation of T cell-mediated autoimmune diabetes: analysis of a new “speed congenic” stock of NOX.Ig mu null mice. *J. Exp. Med.* 184:2049-2053

90. Serreze, D.V., Fleming S.A., Chapman, H.D., Richard, S.D., Leiter, E.H., Tisch, R.M. 1998. B lymphocytes are critical antigen-presenting cells for the initation of T cell-mediated autoimmune diabetes in nonobese diabetic mice. *J. Immunol.* 161:3912-3918

91. Wong, F.S., Wen, L., Tang, M., Ramanathan, M., Visintin, I., Daugherty, J., Hannum, L.G., Janeway, C.A., Shlomcik, M.J. 2004. Investigation of the role of B-cells in type 1 diabetese in the NOD mouse. *Diabetes.* 2581-2587

92. Eyre, D.R. and J.J. Wu. 2005. Collagen cross-links. *Top. Curr. Chem*. 247:207-229

93. Chung, A.E., Estes, L.E., Shinozuka, H., Braginsi, J., Lorz, C., Chung, C.A. 1977. Morphological and biochemical observations n cells derived from the *in vitro* differentiation of the embryonal carcinoma cell line PCC4-F *Cancer Res.* 37:2072-2081

94. Bachinger, H.P., Fessler, L.I., Fessler, J.H. 1982. Mouse procollagen IV. Characterization and supramolecular association. *J. Biol. Chem*. 257:9796-9803

95. Nelson, R.E., Fessler, L.I., Takagi, Y., Blumber, B., Keene, D.R., Olson, P.F., Parker, C.G., Fessler, J.H. 1994. Peroxidasin: a novel enzyme-matrix protein of *Drosophila* development. *EMBO J*. 13:3438-3437

96. Eng, P.H., Cardona, G.R., Fang, S.L., Previti, M. Alex, S., Carrasco, N., Chin, W.W., Braverman, L.E. 1999. Escape from the acute Wolff-Chaikoff effect is associated with a decrease in thyroid sodium/iodide symporter messenger ribonucleic acid and protein. *Endocrinology*. 140:3404-3410

97. Cheng, G., Salerna, J.C., Cao, Z., Pagano, P.J., Lambeth, J.D. 2008. Identification and characterization of VPO1, a new animal heme-containing peroxidase. *Free Radical Biol. Med*, 45:1682-1694

98. Hutchins, J.T., Dean, R.J., Mitchell, M.S., Uchiyama, C., Kan-Mitchell, J. 1991. Novel gene sequences expressed by huan elanoma cells identified by molecular subtraction. *Cancer Res*. 51:1418-1425

99. Soudi, M., Zamocky, M., Jakopitsch, C., Furtmuller, P.G., Obinger, C. 2012 Molecular evolution, structure, and function of peroxidasin. *Chem. Biodiversity*. 9:1776-1792

100. Chen, G., Li, H., Cao, Z., Qiu, X., McCormic, S., Thannickal, V.J., Nauseef, W.M. 2011. Vascular peroxidase-1 is rapidly secreted, circulates in plasma, and supports dityrosine cross-linking reactions. *Free Radical Biol. Med*. 51:1445-1453

101. Weiler, S.R., Taylor, S.M., Deans, R.J., Kan-Mitchell, J., Mitchell, M.S., Trent, J.M. 1994. Assignment of a human elanoma associated gene MG50 (D2S448) to chromosome 2p25.3 by fluorescence *in situ* hybridization. *Genomics*. 1994. 22:243-244

102. Gotenstein, J.R., Swale, R.E., Fududa, T., Wu, Z., Giurumescu,C.A., Goncharov, A., Jin, Y., Chisholm, A.D. 2010. The *C. elegans* peroxidasin PXN-2 is essential for embryonic morphogenesis and inhibits adult axon regeneration. *Development*. 137:3603-3613

103. Fujisawa, T., Huang, Y., Sebald, W., Zhang, J.L. 2009. The binding of von Willebrand factor type C domains of Chordin family proteins to BMP-2 and Tsg is mediated by their SD1 subdomain. *Biochem. Biophys. Res. Commun*. 385:215-219

104. Zhang, J.L., Qiu, L.Y., Kotzsch, A., Weidauer, S., Patterson, L., Hammerschmidt, M., Sebald, W., Mueller, T.D. 2008. Crystal structure analysis reveals how the chordin famil member crosssveinless 2 blocks BMP-2 receptor binding. *Dev. Cell*. 14:739-750

105. Bella, J., Hindle, K.L., McEwan, P.A., Lovell, S.C. 2008. The leucine-rich repeat structure. *Cell. Mol. Life. Sci*. 65:2307-2333

106. Khan, K., Rudkin, A., Parry, D.A., Burdon, K.P., McKibbin, M., Logan, C.V., Abdelhamed, Z.I.A., Muecke, J.S., Fernandez-Fuentes, N., Laurie, K.J., Shires, M., Fogarty, R., Carr, I.M., Poulter, J.A., Morgan, J.E., Mohamed, M.D., Jafri, H., Raashid, Y., Meng, N., Piseth, H., Toomes, C., Casson, R.J., Taylor, G.R., Hammerton, M., Sheridan, R., Johnson, C.A., Inglehearn, C.F., Craig,

J.E., Ali, M. 2011. Homozygous mutation in *PXDN* cause congenital cataract, corneal opacity, and developmental glaucoma. *Am. J. Hum. Gen.* 89:464-473

107. Nischal, K.K. 2007. Congenital corneal opacities – a surgical approach to nomenclature and classification. *Eye*. 21:1326-1337

108. Tindall, A.J., Pownall, M.E., Morris, I.D., Isaacs, H.V. 2005. Xenopus tropicalis peroxidasin gene is expressed within the developing neural tube and pronephric kidney. *Develop. Dynamics*. 2005. 232:377-384

109. Olofsson, B. and D.T. Page. 2005. Condensation of the central nervous system in embryonic Drosophila is inhibited by blocking hemocyte migration or neural activity. *Develop. Biol*. 279:233-243

110. Homma, S., Shimada, T., Hikake, T., Yaginuma, H. 2009. Expression pattern of LRR and Ig domain-containing protein (LRRIG protein) in the early mouse embryo. *Gene Expression Patterns*. 9:1-26

111. Mitchell, M.S., Kan-Mitchell, J., Mineve, B., Edman, C., Deans, R.J. 2000. A novel melanoma gene (MG50) encoding the interleukin 1 receptor antagonist and six epitopes recognized by human cytolytic T lymphocytes. *Cancer Res*. 60:6448-6456

112. Liu, y., Carson-Walter, E.B., Cooper, A., Winans, B.N., Johnson, M.D., Walter, K.A. 2010 Vascular gene expression patterns are conserved in primary and metastatic brain tumors. *J. Neurooncol*. 99:13-24

113. Tauber, S., Jais, A., Jeitler, M., Haider, S., Husa, J., Lindroos, J., Knofler, M., Mayerhofer, M., Pehamberger, H., Wagner, O., Bilban, M. 2010. Transcriptome analysis of human cancer reveals a functional role of heme oxygenase-1 in tumor cell adhesion. *Mol. Cancer*. 9:200

114. Shi, R., Hu, C., Yuan, Q., Yang, T., Peng, J., Li, Y., Bai, Y., Cao, Z., Cheng, G., Zhang, G. 2011 Involvement of vascular peroxidase 1 in angiotensin II-induced vascular smooth muscle cell proliferation. *Cardiovasc. Res*. 91:27-36

115. Bai, Y.P., Hu, C.P., Yuan, Q., Peng, J., Shi, R.Z., Yang, T.L., Cao, Z.H., Li, Y.J., Cheng, G., Zhang, G.G. 2011. Role of VPO1, a newly identified heme-containing peroxidase, in ox-LDL induced endothelial cell apoptosis. *Free Radical Biol. Med*. 51:1492-1500

116. Zhang, Y.S., He, L., Liu, B., Li, N.S., Luo, X.J., Hu, C.P., Ma, Q.L., Zhang, G.G., Li, Y.J., Peng, J. 2012. A novel pathway of NADPH oxidase/vascular peroxidase 1 in mediating oxidative injury following ischemiareperfusion. *Basic. Res. Cardiol*. 107:266

117. Hoikoshi, N., Cong, J., Kley, N., Shenk, T. 1999. Isolation of differentially expressed cDNAs from p53-dependent apoptotic cells: activation of the human homologue of the *Drosophila* peroxidasin gene. *Biochem. Biophys. Res. Commun*. 261:864-869

118. Davies, M.J., Hawkins, C.L., Pattison, D.I., Rees, M.D. 2008. Mammalian heme peroxidases: from molecular mechanisms to health implications. *Antioxid. Redox Signaling.* 10:1199-1234

119. Markou, K., Georgopoulos, N., Kyriazopoulou, V., Vagenakis, A.G. 2001. Iodine-induced hypothyroidism. *Thyroid*. 11:501-510

120. Joy, E.F., Bonn, J.D., Barnard, A.J. 1973. Photometric determination of trace bromide in alkali metal chlorides. *Anal. Chem*. 45:856-860

121. Ashby, M.T., Carlson, A.C., Scott, M.J. 2004. Redox buffering of hypochlorous acid by thiocyanate in physiologic fluids. *J. Am. Chem. Soc*. 126:15976-15977

122. Pattison, D.I. and M.J. Davies. 2004. Kinetic analysis of the reactions of hypobromous acid with protein components: implications for cellular damage and use of 3-bromotyrosine as a marker of oxidative stress. *Biochemistry*. 43:4799-4809

123. Henderson, J.P., Williams, M.V., Mueller, D.M., McCormick, M.L., Heinechke, J.W. 2001. Production of brominating intermediates by myeloperoxidase. A transhalogenation pathway for generating mutagenic nucleobases during inflammation. *J. Biol. Chem*, 276:7867-7875

124. Toth, Z. and I. Fabian. 2004. Oxidation of chlorine(III) by hypobromous acid: kinetics and mechanism. *Inorg. Chem*. 43:2717-2723

125. Li, H., Cao, Z., Zhang, G., Thannickal, V.J., Cheng, G. 2012. Vascular peroxidase 1 catalyzes the formation of hypohalous acids: Characterization of its substrate specificity and enzymatic properties. *Free Rad. Biol. Med*. 53:1954-1959

126. Gensch, K.H. and T. Higuchi. 1967. Kinetic investigation of reversible reaction between methionine and iodine. Improved iodometric determination of methionine. *J. Pharm. Sci*. 56:177-184.

127. Luo, S. and R.L. Levine. 2009. Methionine in proteins defends against oxidative stress. *FASEB J*. 23:464-472.

128. van Dalen, C.J. and A.J. Kettle. 2001. Substrates and products of eosinophil peroxidase. *Biochem. J*. 358:233-239

129. Senthilmohan, R. and A.J. Kettle. 2006. Bromination and chlorination reactions of myeloperoxidase at physiological concentrations of bromide and chloride. *Arch. Biochem. Biophys*. 445:235-244

130. Furtmuller, P.G., Burner, U., Regelsberger, G., Obinger, C. 2000. Spectral and kinetic studies on the formation of eosinophil peroxidase compound I and its reaction with halides and thiocyanate. *Biochemistry*. 39:15578-15584

131. Specht, S., Saeftel, M., Arndt, M., Endl, E., Dubben, B., Lee, N.A., Lee, J.J., Hoerauf, A. 2006. Lack of eosinophil peroxidase or major basic protein impairs defense against murine filarial infection. *Infect. Immun*. 74:5236-5243

132. Kaufman, E.R. 1984. Replication of DNA containing 5-bromouracil can be mutagenic in Syrian hamster cells. *Mol. Cell. Biol*. 4:2449-2454

133. Furtmuller, P.G., Jantschko, W., Regelsberger, G., Jakopitsch, C., Arnhold, J., Obinger, C. 2002. Reaction of lactoperoxidase compound I with halides and thiocyanate. *Biochemistry*. 41: 11895-11900

134. Furtmuller, P.G., Burner, U., Obinger, C. 1998. Reaction of myeloperoxidase compound I with chloride, bromide, iodide, and thiocyanate. *Biochemistry*. 37:17923-17930

135. Kooter, I.M., Moguilevsky, N., Bollen, A., van der Veen, L.A., Otto, C., Dekker, H.L., Wever, R. 1999. The sulfonium ion linkage in myeloperoxidase. Direct spectroscopic detection by isotopic labeling and effect of mutation. *J. Biol. Chem*. 274:26794-26802

136. Blair-Johnson, M., Fiedler, T., Fenna, R. 2001. Human myeloperoxidase: structure of a cyanide complex and its interaction with bromide and thiocyanate substrates at 1.9 Å resolution. *Biochemistry*. 40:13990-13997

137. Furtmuller, P.G., Zederbauer, M., Jantschko, W., Helm, J., Bogner, M., Jakopitsch, C., Obinger, C. 2006. Active site structure and catalytic mechanisms of human peroxidases. *Arch. Biochem. Biophys*. 445:199-213

138. Butler, A. and M. Sandy. 2009. Mechanistic considerations of halogenating enzymes. *Nature*. 460:848-854

139. Rees, M.D., Kennett, E.C., Whitelock, J.M., Davies, M.J. 2008. Oxidative damage to extracellular matrix and its role in human pathologies. *Free Rad. Biol. Med*. 44:1973-2001

140. Hazell, L.J. and R. Stocker. 1993. Oxidation of low-density lipoprotein with hypochlorite causes transformation of lipoprotein into a high-uptake form for macrophages. *Biochem. J*. 290:165-172

141. Moore, K.J. and I. Tabas. 2011. Macrophages in the pathogenesis of atherosclerosis. *Cell*. 145:341-355

142. Peng, D., Wu, Z., Brubaker, G., Zheng, L., Settle, M., Gross, E., Kinter, M., Hazen, S.L., Smith, J.D. 2005. Tyrosine modification is not required for myeloperoxidase-induced loss of apolipoprotein A-1 functional activities. *J. Biol. Chem*. 208: 33775-33784

143. Brennan, M.L., Anderson, M.M., Shih, D.M., Qu, X.D., Wang, X., Mehta, A.C., Lim, L.L., Shi, W., Hazen, S.L., Jacob, J.S., Crowley, J.R., Heinecke, J.W., Lusis, A.J. 2001. Increased atherosclerosis in myeloperoxidase-deficient mice. *J. Clin. Invest*. 107:419-430

144. Olszanecki, R. and J. Marcinkiewicz. 2004. Taurine chloramine and taurine bromamine induce heme oxygenase-1 in resting and LPS-stimulated J774.2 macrophages. *Amino Acids*. 27:29-35

145. Marcinkiewicz, J. 2010. Taurine bromamine (TauBr)—its role in immunity and new perspectives for clinical use. *J. Biomed. Sci*. 17:S1-S3.

146. Ruf, J. and P, Carayon. 2006. Structural and functional aspects of thyroid peroxidase. *Arch. Biochem. Biophys*. 445:269-277

147. Than, M.E., Henrich, S., Huber, R., Ries, A., Mann, H., Kuhn, H., Timpl, R., Bourenkov, G.P., Bartunik, H.D., Bode, W. 2002. The 1.9-Å crystal structure of the noncollagenous (NC1) domain of human placenta collagen IV shows stabilization via a novel type of covalent Met-Lys cross-link. *Proc. Nat. Acad. Sci. U. S. A*. 99:6607-6612

148. Zhou, P., Tian, F., Zou, J., Ren, Y., Liu, X., Shang, Z. 2010. Do halide motifs stabilize protein architecture?. *J Phys. Chem*. 114:15673-15686

149. Grabarek, Z. 2006. Structural basis for diversity of the EF-hand calcium-binding proteins. *J. Mol. Biol*. 359:509-525

150. Gifford, J.L., Walsh, M.P., Vogel, H.J. 2007. Structures and metal-ion-binding properties of the Ca^{2+}-binding helix-loop-helix EF-hand motifs. *Biochem. J*. 405:199-221

151. Grabarek, Z. 2001. Insights into modulation of calcium signaling by magnesium in calmodulin, topponin C, and related EF-hand protein. *Biochim. Biophys. Acta*. 1813:913-921

152. Khoshnoodi, J., Cartailler, J.P., Alvares, K., Veis, A., Hudson, B.G. 2006. Molecular recognition in the assembly of collagens: terminal noncollagenous domains are key recognition modules in the formation of triple helical protomers. *J. Biol. Chem*. 281:38117-38121

153. Case, D. A., Cheatham, T. E., 3rd, Darden, T., Gohlke, H., Luo, R., Merz, K. M., Jr., Onufriev, A., Simmerling, C., Wang, B., and Woods, R. J. 2005. The Amber biomolecular simulation programs, *J. Comput. Chem.* 26, 1668-1688.

154. Cornell, W. D., Cieplak, P., Bayly, C. I., Gould, I. R., Merz, K. M., Ferguson, D. M., Spellmeyer, D. C., Fox, T., Caldwell, J. W., and Kollman, P. A. 1996. A Second Generation Force Field for the Simulation of Proteins, Nucleic Acids, and Organic Molecules J. Am. Chem. Soc. 1995, 117, 5179,àí5197, *J. Am. Chem. Soc.* 118, 2309-2309.

155. Hornak, V., Abel, R., Okur, A., Strockbine, B., Roitberg, A., and Simmerling, C. 2006. Comparison of multiple Amber force fields and development of improved protein backbone parameters, *Proteins: Struct., Funct., Bioinf.* 65, 712-725.

156. Joung, I. S., and Cheatham, T. E., 3rd. 2008. Determination of alkali and halide monovalent ion parameters for use in explicitly solvated biomolecular simulations, *J. Phys. Chem. B.* 112, 9020-9041.

157. Cerutti, D. S., Le Trong, I., Stenkamp, R. E., and Lybrand, T. P. 2009. Dynamics of the streptavidin-biotin complex in solution and in its crystal lattice: distinct behavior revealed by molecular simulations, *J. Phys. Chem. B.* 113, 6971-6985.

158. Essmann, U., Perera, L., Berkowitz, M. L., Darden, T., Lee, H., and Pedersen, L. G. 1995. A smooth particle mesh Ewald method, *J. Chem. Phys.* 103, 8577-8593.

159. Ryckaert, J.-P., Ciccotti, G., and Berendsen, H. J. C. 1977. Numerical integration of the cartesian equations of motion of a system with constraints: molecular dynamics of n-alkanes, *J. Comput. Phys.* 23, 327-341

160. Larini, L., Mannella, R., and Leporini, D. 2007. Langevin stabilization of molecular-dynamics simulations of polymers by means of quasisymplectic algorithms, *J. Chem. Phys.* 126, 104101.

161. Wu, X. W., and Brooks, B. R. 2003. Self-guided Langevin dynamics simulation method, *Chem. Phys. Lett.* 381, 512-518.

162. The PyMOL Molecular Graphics System, 1.5.0.2 ed., Schrodinger, LLC.

163. Dolinsky, T. J., Nielsen, J. E., McCammon, J. A., and Baker, N. A. 2004. PDB2PQR: an automated pipeline for the setup of Poisson-Boltzmann electrostatics calculations, *Nucleic Acids Res.* 32, W665-667.

164. Baker, N. A., Sept, D., Joseph, S., Holst, M. J., and McCammon, J. A. 2001. Electrostatics of nanosystems: application to microtubules and the ribosome, *Proc. Natl. Acad. Sci. U. S. A.* 98, 10037-10041.

165. Ward, E.M., Sabbioni, G., DeBord, D.G., Teass, A.W., Brown, K.K., Talaska, G.G., Roberts, D.R., Ruder, A.M., Streicher. R.P. 1996. Monitoring of aromatic amine exposure in workers at a chemical plant with a known bladder cancer excess. *J. Nat. Cancer Inst*. 88:1046-1052

166. Meth-Cohn, O., and M. Smith. 1994. What did W.H. Perkin actually make when he oxidized aniline to obtain mauveine?. *J. Chem. Soc. Perkin Trans.* 1. 1:5-7

167. Hada, N., Totsuka, Y., Enya, T., Tsurumaki, K., Nakazawa, M., Kawahara, N., Murakami, Y., Yokoyama, Y., Sugimura, T., Wakabayashi, K. 2001. Structures of mutagens produced by the co-mutagen norharman with *o*- and *m*-toluidine isomers. *Mutat. Res.* 493:115-126

168. Paterson, C.A. and B.A. Eck. 1971. Chloride concentration and exchance in rabbit lens. *Exp Eye Res*. 11:207-213

169. Peterfi, Z., Donko, A., Orient, A., Sum, A., Prokai, A., Molnar, B., Vereb, Z., Rajnavolgyi, R., Kovacs, K.J., Muller, V., Szabo, A.J., Geiszt, M. 2009. Peroxidasin is secreted and incorporated into the extracellular matrix of myofibroblasts and fibrotic kidney. *Am. J. Pathol.* 175:725-735